MDOT RC-1527

Condition Assessment and Methods of Abatement of Prestressed Concrete Box-Beam Deterioration

Phase II

Final Report
Volume I

Western Michigan University

Michigan Tech

Research

Center for Structural Durability
A Michigan DOT Center of Excellence

Intentionally left blank

Technical Report Documentation Page

1. Report No. **Research Report RC-1527**	2. Government Accession No.	3. MDOT Project Manager **Steve Kahl, P.E.**
4. Title and Subtitle **Condition Assessment and Methods of Abatement of Prestressed Concrete Box-Beam Deterioration – Phase II**		5. Report Date **April 13, 2009**
7. Author(s) **WMU: Dr. Haluk Aktan, Dr. Upul Attanayake, and Mr. Evren Ulku** **MTU: Dr. Theresa Ahlborn and Dr. Yogini Deshpande**		6. Performing Organization Code **WMU and MTU**
9. Performing Organization Name and Address **A joint effort between**		8. Performing Org Report No.
Western Michigan University **1903 W. Michigan Ave,** **Kalamazoo, MI 49008**	**Michigan Technological University** **1400 Townsend Drive** **Houghton MI 49931**	
12. Sponsoring Agency Name and Address **Michigan Department of Transportation** **Construction and Technology Division** **PO Box 30049, Lansing MI 48909**		Work Unit No. 11. Contract Number : 11(a). Authorization Number:
15. Supplementary Notes		13. Type of Report and Period Covered **Final Report, 2006-2008** 14. Sponsoring Agency Code

16. Abstract

Side-by-side box-beam bridge constitutes approximately 17 percent of bridges built or replaced annually on public roads and there is a renewed thrust to use this bridge type for rapid construction under the Highway for LIFE program. Further, failure of a fascia girder of Lakeview Drive bridge in Pennsylvania on December 27, 2005 and with a large number of aging bridges in the U.S., highway agencies are concerned about the safety of similar bridges. This project was developed to evaluate the capacity of distressed box-beam through load testing; investigate the impact of distress types identified during phase I of this project on flexure and shear capacities of a beam in a structural system; identify proper materials and methods for long lasting repairs to improve the structural integrity of distressed box-beam bridges; and by performing simulations of the construction process using finite element (FE) models investigate stresses developed in components during each stage of construction and under operation, develop recommendations for changes or modifications to the design procedures, construction process, material specifications, and to the maintenance and repair techniques of side-by-side box-beam bridge deck.

Six tasks were performed in this project ranging from literature review, instrumentation and load testing of a severely deteriorated fascia beam, laboratory investigation of fresh and hardened (durability) properties of shear key grout and repair materials, evaluation of mechanical properties of shear key grout and repair materials, construction process simulation, and evaluation of flexural and shear capacities of distressed beams considering structural system behavior.

Recommendations of this project include selection of repair and shear key material, development of comprehensive inspection procedures to assure bridge safety and implementation of the rational design procedure given in the report for improved durability.

17. Key Words: **Box-Beam Bridge, Concrete, Deterioration, Finite Element, Transverse Posttension, Rational Design**		18. Distribution Statement **No restrictions. This document is available to the public through the Michigan Department of Transportation.**	
19. Security Classification (report) **Unclassified**	20. Security Classification (Page) **Unclassified**	21. No of Pages **273**	22. Price

Intentionally left blank

CONDITION ASSESSMENT AND METHODS OF ABATEMENT OF PRESTRESSED CONCRETE BOX-BEAM DETERIORATION

Phase II

Project Manager: Mr. Steve Kahl, P.E.

Submitted to

MDOT

Submitted by

Western Michigan University
Department of Civil & Construction Engineering
College of Engineering and Applied Sciences
Kalamazoo, MI 49008
Fax: (269) – 276 – 3211

Dr. Haluk Aktan, P.E.
Professor & Chair
(269) – 276 – 3206
haluk.aktan@wmich.edu

Dr. Upul Attanayake
Assistant Professor
(269) – 276 – 3217
upul.attanayake@wmich.edu

Mr. Evren Ulku
Graduate Research Assistant
(313) – 577 – 3785
evren@eng.wayne.edu

Michigan Technological University
Dept. of Civil & Environmental Engineering
1400 Townsend Drive
Houghton, MI 49931
Fax: (906) – 487 – 1620

Dr. Theresa M. Ahlborn, P.E
Associate Professor
(906) – 487 – 2625
tess@mtu.edu

Dr. Yogini Deshpande
Post Doctoral Researcher
(906) – 487 – 1474
yogini@mtu.edu

Intentionally left blank

DISCLAIMER

The content of this report reflects the views of the authors, who are responsible for the facts and accuracy of the information presented herein. This document is disseminated under the sponsorship of the Michigan Department of Transportation in the interest of information exchange. The Michigan Department of Transportation assumes no liability for the content of this report or its use thereof.

Intentionally left blank

ACKNOWLEDGEMENTS

This project is funded by the Michigan Department of Transportation. The authors would like to acknowledge the support and effort of Mr. Steve Kahl for initiating this research. The authors also wish to acknowledge the continuing assistance of the Research Advisory Panel (RAP) members in contributing to the advancement of this study.

Intentionally left blank

EXECUTIVE SUMMARY

INTRODUCTION

Side-by-side box-beam bridge, described as adjacent box-beam bridge, constitutes approximately 17 percent of bridges built or replaced annually on public roads (www.trb.org). The bridge is constructed by placing box-beams adjacent to each other, grouting shear keys, applying transverse posttension, and placing on top either a three inch riding wear surface or a six-inch concrete deck with composite action. The bare top of the box-beam is sometimes used as the riding surface. Adjacent box-beam bridge is the preferred choice for short to medium span bridges, up to 110 feet. Additionally, there is a renewed thrust to use this bridge type for rapid construction under the Highway for LIFE (Longer-lasting highway infrastructure using Innovations to accomplish the Fast construction of Efficient and safe highway and bridges) program (www.fhwa.dot.gov and www.trb.org).

Box-beam design procedure in Michigan and in many other states as well as in many other countries was documented during phase I of this project. In addition, 15 in-service bridges were inspected, distress types and states were documented and the performance was evaluated. Longitudinal deck cracking reflecting from the shear-keys was identified as the leading cause of other distresses. Several distress types were identified as critical to the box-beam capacity. Load rating was performed for various levels of the identified distress types following load factor method described in 2003 Michigan Bridge Analysis Guide.

The objectives for Phase II of this project were identified as follows:

1. Evaluate capacity of a distressed box-beam through load testing,
2. Identify proper materials and methods for long lasting repairs which improve the structural integrity of distressed box-beam bridges,
3. Simulate construction process using finite element (FE) models investigating stresses developed in components during each stage of construction,
4. Investigate impact of distress types identified during phase I of this project on flexure and shear capacities of a beam using 3D full bridge models,
5. Develop changes or modifications to the design procedure, construction process, and to the maintenance and repair techniques of side-by-side box-beam bridge deck.

To satisfy the objectives, this project was organized with six main tasks: (1) literature review; (2) capacity evaluation through load testing; (3) laboratory investigation of fresh and hardened (durability) properties of shear key grout and repair materials; (4) mechanical property evaluation of shear key and repair materials; (5) construction process simulation; and (6) flexural and shear capacity evaluation of distressed beams considering structural system behavior.

LITERATURE REVIEW

A through literature review including capacity evaluation and load testing of distressed bridges/components, materials used for shear keys and repair, durability of shear key and repair materials, properties of cementitious materials that have a potential to be used for shear keys, and design parameters for transverse design of box-beam bridge superstructure was performed. Literature regarding the capacity evaluation of box-beams through load testing indicates that fatigue should not be a concern for uncracked beams. It was recommended to avoid frequent loading on bridges that causes bottom fiber stress in excess of $6\sqrt{f_c'}$ (psi) or strand stress greater than $0.06f_{pu}$. Transverse connection, established with grout joints (shear key), posttension, and cast-in-place concrete deck governs the load distribution. Diaphragms generate rigid zones in the box-beam bridge superstructure and works as the primary load transfer mechanism. According to the results of a study on the bearing capacity and compressive strength of mortar joints between precast columns, when grout material modulus is lower than the parent material, joint load transfer efficiency increases with reduced joint width. However, uniform thickness of the joint is of paramount importance to maintain uniform stress distribution. Mechanical properties of grout material at the time of posttension govern the stress distribution along the joint and sealing performance. Customized shear key grout mixes can be developed for specified mechanical property requirements achieved at the time of transverse posttensioning.

LOAD TESTING

The second task was to remove a severely deteriorated fascia beam, instrument, and perform load testing for evaluating the capacity of the beam. A 50-year old box-beam with severe longitudinal cracking at the beam soffit was removed from the bridge (S11-38101) that carries Hawkins road over I-94. Beam capacity was calculated using strain data and load rating was performed. Analysis of load test data indicated that the beam capacity was still more than the design capacity. However, there is a safety concern because beam was designed for smaller load (H-15) than the currently required loads. The remaining prestress was calculated from camber measurements and the strain gauge data; however it was found that using camber overestimates remaining prestress by 40-50 percent. It is essential to implement an inspection procedure that is capable of identifying the concealed corrosion, evaluating condition of transverse posttension strands, characterizing material properties, and quantifying the load transfer.

LABORATORY INVESTIGATION OF SELECTING PROPER REPAIR AND GROUT MATERIALS

The third task included conducting a survey of commonly used repair materials and shear key grouts for prestressed box beam bridges and laboratory evaluation of selected materials. The intended result of the laboratory evaluation was development of required material characteristics from the perspective of dimensional stability and durability of prestressed box beam bridges.

Three shear key grouts were selected for laboratory evaluation. Of these, two were cement based grouts whose mixture proportion was based on MDOT specifications, whereas the third shear key grout was SET 45, a commercially available rapid setting phosphate cement based grout. Laboratory evaluation of shear key grouts consisted of fresh properties including slump and air content and hardened properties including compressive and bond strength testing and free shrinkage. Durability of shear key grouts was evaluated by measuring the resistance to freezing and thawing cycles and sorptivity. It was observed that the cement based grouts had compressive strength of lower than 5000 psi at the end of 28 days whereas all the shear key grouts exhibited lower slant shear bond strength values. All the shear key grouts exhibited good durability properties.

Four commonly used polymer based repair materials were selected to evaluate their performance in terms of dimensional stability and durability. The properties evaluated were slump, air content, rate of gain of compressive strength, bond strength, shrinkage and cracking susceptibility, resistance to freezing and thawing cycles, coefficient of thermal expansion, chloride permeability and sorptivity. It was observed that the repair materials investigated in this study have a wide range of values for all the properties for which the materials were evaluated, and selection of a repair material for field use must consider prioritization of critical performance properties.

MECHANICAL PROPERTIES OF SHEAR KEY GROUT AND REPAIR MATERIALS

The fourth task was to evaluate mechanical properties of shear key grout and repair materials. Mechanical properties of some of the repair materials and manufactured grout materials (e.g., set gout and set-45) are documented in manufacturers' technical data sheets. Mechanical properties of Type R-2 grout, which is commonly used in Michigan box-beam bridges to form the shear-keys, are not documented in literature. Compressive strength test of grout material was performed. Ultrasonic pulse velocity (UPV) test was performed to determine the dynamic elasticity modulus and the Poisson's ratio of the material. The dynamic modulus is generally greater than the static modulus determined in accordance with ASTM C469. However, for the grout materials, the measured dynamic modulus was lower than the static modulus determined following the ASTM C469 procedure. Further testing to establish the uniaxial stress-strain properties showed a hysteretic strain hardening behavior not typical of concrete. The elastic modulus consequently changes dramatically within the load cycle. The static modulus test (ASTM C469) is not able to capture this behavior and provides a nominal modulus value. Other repair materials also showed a similar behavior and further investigations were suggested. Further, grout materials tested during the project are not capable of satisfying the strength level required by AASHTO Standard or LRFD at the time of posttension.

CONSTRUCTION PROCESS SIMULATION

The fifth task was to simulate construction procedure verifying the design assumptions and identifying the stresses developed within various components. In addition to simulating the construction process stages, box-beam bridge transverse connection design and material parameters were also investigated using sub-assemblage models. The parameters investigated are: grout mechanical properties, posttension force magnitude and location, number of diaphragms, and the bridge width. The sub-assemblage models with 50 ft long 27×36-in. box beams connected with shear keys and posttension at diaphragm locations were analyzed under concentrated load, dead load, and transverse posttension. Sub-assemblage models were developed with three and four box-beams. Analysis results showed that load transfer is primarily followed through the stiffer sections of the bridge superstructure (i.e., through the diaphragms). AASHTO LRFD (2004) Section 5.14.1.2.8 recommendations regarding transverse normal interface stress distribution are vague. It is not clear whether the minimum stress of 250 psi at joints should be obtained either at shear keys along the entire beam length or diaphragm locations. A comprehensive redesign of diaphragm topology as well as well spacing may be required to obtain uniform stress distribution along the length of shear keys.

Following the latest MDOT design and construction procedures, every step of side-by-side box-beam construction process was simulated. Full bridge models were subjected to loads that may be expected to develop during construction and service life of the bridge. Stresses developed in beams, shear keys, and the deck were documented at each step of simulations. According to the results, barrier loading creates tensile stresses on the 6-in. deck and thermal gradient loading is the primary source generating critical stresses within the deck and certain portions of shear key

A rational analysis and design model (macromechanical model) based on mechanics of materials and macromechanics concepts was presented. Using macromechanical model, changes to construction procedures such as applying posttension in two stages were suggested and evaluated with construction process simulation. It was identified that macromechanical model can predict the posttension requirements to eliminate tensile stresses that occur under gravity loading. With the proposed construction process, applying posttension after deck placement greatly helps reducing tensile stresses in the deck that occur under positive and negative thermal gradient loading. Transverse tensile deck stresses that occur under live load can be completely be removed except at some isolated regions close to fascias.

FLEXURAL AND SHEAR CAPACITY OF DISTRESSED BOX-BEAMS

The sixth task was to evaluate flexural and shear capacity of distressed beams considering structural system behavior. Full bridge models used for construction process simulation were also used in the case of capacity evaluation. Three major beam distress types; spall, spall and single broken strand, and spall and two broken strands were incorporated into the models by gradually reducing the elasticity modulus on regions where distress was defined. All the distresses were along the corner of beam bottom flange for calculating flexure and shear critical capacities. Analysis results showed that, for the selected span length of 50 ft., the flexural capacity was reduced only when the distresses were at the midspan. Spall alone was not a major cause of capacity reduction. Beam capacity reduction was significant if broken tendons were present. In addition to beam distresses, impact of shear key grout loss and broken posttension strands on beam capacity was investigated. Partial loss of grout did not affect the capacity of the beam, however dead and live load demands on the fascia beam changed due to reduced stiffness. It was shown that posttension did not influence the load distribution provided that shear keys were intact. However, it contributed to the beam capacity and provides redundancy to the systems especially when weak bond exists between the grout and beams.

RECOMMENDATIONS

The following key recommendations are based on the findings from the project tasks of literature review, load testing of a salvaged box-beam, testing of grout and repair material properties, and the development of subsequent finite element modeling and simulations:

1. Among the fresh properties of utmost importance is workability in case of polymer based repair materials. Repair materials which do not need excessive force for proper placement and consolidation should be selected.

2. Repair materials with shrinkage values comparable to the substrate concrete should be selected. In this study all the repair materials did not necessarily exhibit the required behavior and, hence, it is essential to select a repair material based on its intended use. It is necessary to evaluate the shrinkage behavior of a selected repair material prior to application on site.

3. To protect exposed steel from corrosion, repair materials evaluated in this study can be adopted for use because all of them exhibited high resistance to chloride ion transport as well as low sorption values.

4. When selecting a shear key grout it is essential to determine the early age compressive strength as well as its early age shrinkage properties based on the load applied to it. A more detailed understanding of shear key grout from a material standpoint as well as the total design of the shear key itself is recommended.

5. Adequate load transfer and achieving a watertight connection along the transverse joint cannot be achieved with the currently specified grout with nonlinear hysteretic behavior. Revisions to grout material specifications are recommended.

6. In-service bridge beam load capacity assessment should be based on material characterization, load transfer evaluation along the shear keys, and estimation or assessment of concealed corrosion.

7. The recommended load analysis procedure and the associated design criteria requiring a two-stage posttension process should be implemented for improved durability performance of side-by-side box-beam bridges.

Intentionally left blank

Contents

Intentionally left blank

TABLE OF TABLES

TABLE OF FIGURES

Intentionally left blank

1 INTRODUCTION

1.1 BACKGROUND

The side-by-side box-beam bridge, described as an adjacent box-beam bridge, constitutes approximately 17 percent of bridges built or replaced annually on public roads (www.trb.org). The bridge is constructed by placing box-beams adjacent to each other, grouting shear keys, applying transverse posttension, and placing on top either a three-inch riding wear surface or a six-inch concrete deck with composite action. The bare top of the box-beam is sometimes used as the riding surface. The adjacent box-beam bridge is the preferred choice for short to medium span bridges, up to 110 feet. The favorable aspects are: ease of construction, favorable span-to-depth ratios, aesthetic appeal, and high torsional stiffness of the box-beams (El-Remaily et al. 1996; Lall et al. 1998; Miller et al. 1999). Additionally, there is a renewed thrust to use this bridge type for rapid construction under the Highway for LIFE (Longer-lasting highway infrastructure using Innovations to accomplish the Fast construction of Efficient and safe highway and bridges) program (www.fhwa.dot.gov and www.trb.org).

There is a large stock of existing side-by-side box-beam bridges in the U.S.; for example, in Michigan, the numbers exceed 2000. Evolving box-beam design procedures in Michigan and in many other states as well as in many other countries was documented during phase I of this project. In addition, 15 in-service bridges were inspected, distress types and states were documented, and bridge performance was evaluated. From the phase I study, longitudinal deck cracking reflecting from the shear-keys was identified as the leading cause of other distresses. Also, several distress types were identified as critical to the box-beam capacity. Load rating was performed for various levels of the identified distress types following the load factor method described in the 2003 Michigan Bridge Analysis Guide (Aktan et al. 2005).

1.2 PROJECT OBJECTIVES AND TASKS

The overall project objectives are to:

- Evaluate the experimental capacity of a distressed box-beam through load testing of a salvaged beam;
- Identify proper materials and methods for repairs, to improve the structural integrity of distressed box-beam bridges;

- Investigate stresses developed in components during each stage of construction and under operation by performing simulations of the construction process using finite element (FE) models;
- Investigate the impact of distress types identified during phase I of this project on flexure and shear capacities of a beam considering structural system behavior;
- Develop recommendations for changes or modifications to the design procedures, construction process, load ratings, and maintenance and repair techniques of side-by-side box-beam bridges.

The project tasks are as follows: (1) literature review on capacity evaluation and load testing of distressed bridges/girders, materials used for shear keys and repair, durability of shear key and repair materials, properties of cementitious materials that have a potential to be used for shear keys, and design parameters for transverse design of box-beam bridge superstructure; (2) capacity evaluation of a distressed box-beam removed from an in-service bridge through load testing; (3) laboratory investigation of fresh and hardened (durability) properties of shear key grout and repair materials; (4) mechanical property evaluation of shear key and repair materials; (5) construction process simulation; and (6) flexural and shear capacity evaluation of distressed beams considering structural system behavior.

Research findings are documented in two volumes with 12 chapters. The contents of the two volumes of the report are described below:

Volume I:
A Literature review is presented in chapter 2 comprising capacity evaluation and load testing of distressed bridges/girders, materials used for shear keys and repair, durability of shear key and repair materials, properties of cementitious materials that have a potential to be used for shear keys, and design parameters for transverse design of box-beam bridge superstructure.

Chapter 3 includes the condition description of the decommissioned box-beam, beam removal process, instrumentation and load configuration, capacity evaluation using load test data, and load rating of the beam using load factor method.

The experimental procedure for durability studies is presented in chapter 4.

Experimental test results of durability studies and analysis of data are presented in chapter 5.

Mechanical properties of shear key grout and beam repair materials are documented in chapter 6.

Volume II:

Side-by-side box-beam transverse design parameters are investigated using sub-assemblage models of box-beams. Model parameters and analysis results are presented in chapter 7.

Chapter 8 contains the model parameters, simulation steps, and the results of construction process simulation. Based on MDOT design and construction procedures, every step of the side-by-side box-beam construction process is simulated using advanced pre/post processing capabilities of HyperMesh and FE analysis capabilities of ABAQUS. Stresses developed in beams, shear keys, and the deck are obtained and documented in this chapter.

Phase I of this project showed that in Michigan and elsewhere the transverse connection design of a side-by-side box-beam bridge is based on empirical procedures. This is due to the lack of rational analysis models that allow the load demand calculation at the longitudinal joints between precast box-beams. Chapter 9 presents a rational analysis and design model for transverse connection design and a proposed construction procedure. Further, the stresses developed in beams, shear keys, and the deck during the recommended construction procedure are investigated, in chapter 9, using advanced FE modeling and analysis techniques.

Chapter 10 presents modeling and analysis of a box-beam superstructure with distressed beams evaluating the influences of distresses on beam capacity and the bridge capacity when the beam is part of the structural system.

Chapter 11 presents the comprehensive results and recommendations.

Chapter 12 discusses the recommendations for further work on this topic towards the implementation of the project findings.

Intentionally left blank

2 STATE-OF-THE-ART LITERATURE REVIEW

2.1 OBJECTIVE AND APPROACH

The objective of the literature review is to identify, review, and synthesize information related to capacity evaluation and load testing of distressed bridges/beams, materials used for shear keys and repair, and properties of cementitious materials that have a potential to be used for shear keys. In addition, a few articles that are relevant to the finite element analysis performed during the second phase of the project are reviewed and summarized in this chapter. The literature review complements the comprehensive literature review related to side-by-side box-beam bridge design and performance conducted during phase I of this project.

2.2 CAPACITY EVALUATION OF DISTRESSED GIRDERS

Failure of a fascia girder on the Lakeview Drive bridge in Pennsylvania on December 27, 2005 prompted the capacity evaluation of the remaining girders to understand the impact of various damage scenarios on the girder capacity. Harries (2006) performed visual inspection, load testing, and analytical and numerical investigations evaluating the load capacity of girders removed from the Lake View Drive bridge. This study shows the importance of quantifying the extent of strand corrosion and other distress. When visual inspection is the only source of information, it is recommended to consider 50% additional strand corrosion than what is observed. Further, it is recommended to measure the camber and estimate the remaining prestress. Unless there is adequate information to verify the functional shear keys and transverse tie rods in existing bridges, the load rating should be performed assuming no load distribution (Harries 2006). When strands are broken, a conservative recommendation is to neglect the entire strand for capacity evaluation or use engineering judgment since redevelopment of strands is uncertain.

Civjan et al. (1998) developed a mechanism to estimate the remaining prestress of exposed strands (Figure 2-1). His estimates are useful for evaluating the remaining prestress of existing bridges for accurate estimation of load carrying capacity.

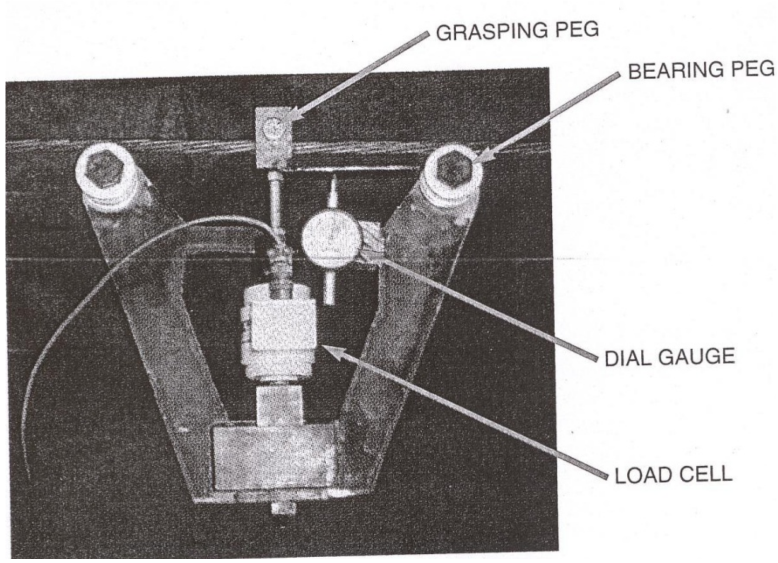

Figure 2-1. Instrument for measuring remaining prestress of exposed strands

Rao and Frantz (1996) performed fatigue tests on 27-years old prestressed concrete box-beams. The beams were 27×36-in. sections. Their span length was 56 ft. One of the beams had two one-foot long cracks at the strand levels while the other beam showed only a few rust stain patches. It was concluded that fatigue should not be a concern for uncracked beams. Cracked beams with nominal bottom fiber stress of $6(f_c^{'})^{1/2}$ were subjected to more than 1,500,000 cycles of loading without any evidence of fatigue problems. When the load was increased to generate bottom fiber stress of $9(f_c^{'})^{1/2}$, strands ruptured after 145,000 cycles. It is recommended that fatigue would be a concern for beams under frequent loading that causes bottom fiber stress in excess of $6(f_c^{'})^{1/2}$ or strand stress greater than $0.06f_{pu}$.

Miller and Parekh (1994) performed a destructive test on a 12-year old 36-in. wide and 33-in. deep prestressed concrete beam. The beam was designed in 1980 and was removed from the bridge in 1992. Beam contained 18 strands but inspection revealed only 15 effective strands. The beam was in good condition with only concrete spall along one edge. The beam was designed for 5500 psi concrete, and at the time of load testing, the compressive strength of the concrete was established to be 8000 psi. Capacity was also evaluated by analytical methods incorporating loss of concrete and strands. Test results were in agreement with the analytical results. It was concluded that the asymmetry of the cross-section due to loss of strands and concrete at the corner influenced the post-cracking and failure behavior.

2.3 REPAIR MATERIALS

Repair of reinforced concrete structures or prestressed concrete structures is not a “band-aid” process; but in actuality is a complex engineering task. It is a process presenting unique challenges which are different from those associated with new concrete construction. A repair system must successfully integrate new materials with old materials, forming a composite system capable of enduring exposure to service loads, exterior and interior environments of the structure and time (Vaysburd 2006).

This Phase II project has been constituted to evaluate in detail the repair materials commonly adopted for repair of adjacent prestressed concrete box beam bridges in Michigan. Investigation results of the MDOT Box-Beam Phase-I project identified several levels of deterioration in fifteen side-by-side prestressed concrete box-beam bridges currently in service (Ahlborn et al. December 2005). The detailed field inspection of the fifteen bridges of various ages indicated a general trend of deterioration in terms of longitudinal and transverse cracking on the decks, substantial of cracking along beam lengths and presence of moisture in beams. A large number of beams in many bridges exhibited concrete spalling and extensive corrosion of steel strands likely due to the presence of moisture and ingress of de-icing chlorides from deck cracks. The field investigations indicated that the shear keys in all bridges built after 1985 were cracked along the length in many cases. Many bridges also exhibited large amount of spalling of the grout in the shear keys.

For a successful repair of a structure, it is essential that the root cause of the deterioration be studied in detail and a solution be developed to stop further damage to the structure. The summary of inspections related to the bridge deck in the Phase-I report identifies extensive longitudinal and transverse cracks in deck concrete. The cracks could have developed due to drying shrinkage, untimely saw cutting of construction joints, improper curing, presence of cold joints and cracks in expansion joints. To ensure long-term performance of the bridge, it is essential to carry out the mitigation of deck deterioration as per proven methods. MDOT has other research projects (completed and ongoing) that address deck deterioration. This Phase II study focused on repair of the beam elements, including shear keys, and assumed that deck deterioration has been mitigated. Additional information on deck repair can be found in the literature (Deshpande 2006; Young and Kreider 2006).

2.3.1 Characteristic Requirements of Repair Materials for Prestressed Concrete Box-beam Deterioration

The selection of repair materials is a predictive effort in order to maximize future performance of the structure by ensuring long-term durability. Typically, the selection of patch repair materials is based on availability, workability requirements, and economical criteria. According to Kosednar and Mailvaganam (2005) selection of a repair material must be based on the knowledge of the physical and chemical properties, function imposed on it and environmental conditions. Every repair job is unique and, especially in the case of this study, the loadings, structural concrete being repaired, environmental conditions and extent of damage vary considerably. Concrete repairs usually fail because of inappropriate selection of the repair material (Vaysburd 2006). There are many commercially available repair materials and there are considerable variations in their chemical composition, mechanical and durability characteristics (Deshpande 2006; Parameswaran 2004). The main factors which cause premature failure of repairs include freezing and thawing, aggressive chemical exposure, mechanical abrasion, loss of bond between existing concrete and repair material, and dimensional incompatibilities between repair material and the existing concrete. While some of the problems associated with premature deterioration of repairs are because of structural failures, most of the problems are related to durability. When a repair material is chosen, care should be taken such that the properties of the repair material match those of the existing concrete to achieve long-term performance of the repair system.

The characteristics of a repair material for long-term performance of repaired concrete under service conditions are illustrated in Figure 2-2.

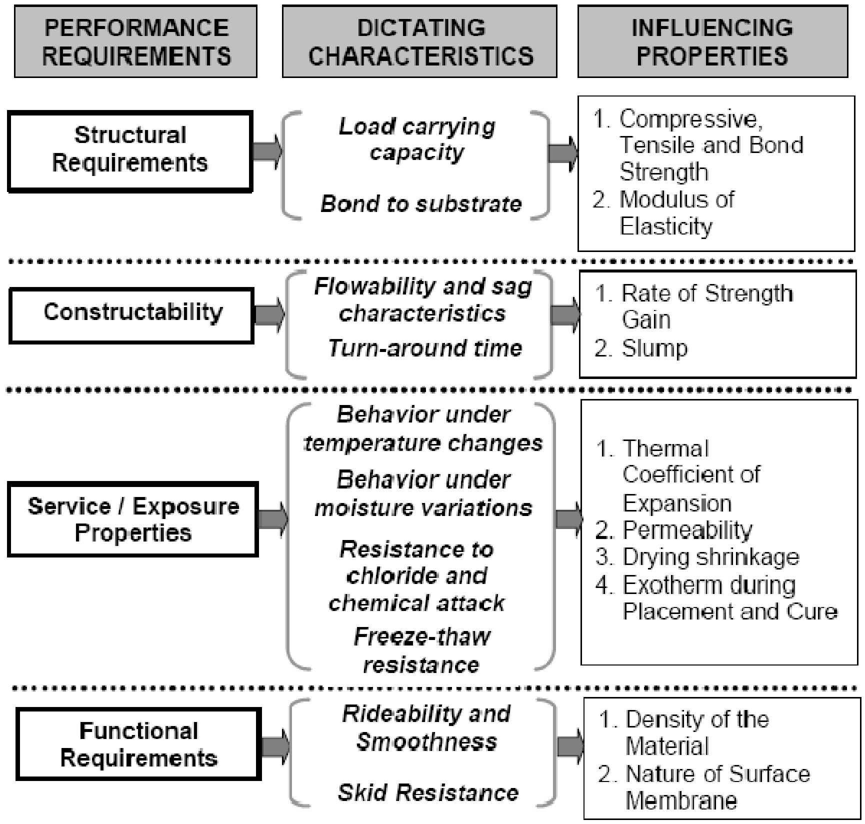

Figure 2-2. Characteristics of an ideal repair material (Parameswaran 2004)

In general the repair material should have the following properties:

1. The repair mortar should have adequate workability so that it can be easily placed, consolidated and finished.
2. The repair mortar must be able to meet the structural requirements of the intended existing structure so as to have sufficient or comparable compressive, tensile and bond strengths. It is also essential that the repair material have a similar stiffness i.e. elastic modulus, than the substrate concrete.
3. The long term durability of the repaired concrete is of great importance for increase in the service life of the repaired structure. The performance of the repair concrete under temperature and moisture changes, freeze-thaw cycles and exposure to deicing salts is very critical. These aspects predominantly affect the bond characteristics and the bond strength between the repair mortar (RM) and concrete substrate (RC).

Emberson and Mays (1990) have provided the summary of the properties required of a patching material for structural compatibility with the existing concrete (refer to Table 2-1).

Table 2-1. General Requirements of Patch Material for Structural Compatibility (Emberson and Mays 1990)

Property	Relationship of repair mortar (R) to concrete substrate (C)
Strength in compression, tension and flexure	RM ≥ RC
Modulus in compression, tension and flexure	RM ≈ RC
Poisson's ratio	Dependent on modulus and type of repair
Coefficient of thermal expansion	RM ≈ RC
Adhesion in tension and shear	RM ≥ RC
Curing and long-term shrinkage	RM ≤ RC
Strain capacity	RM ≥ RC
Creep	Dependent on whether creep causes desirable or undesirable effects
Fatigue performance	RM ≥ RC

In terms of design requirements, strengths (compressive, tension and flexure) of repair mortar/concrete should be greater than or similar to that of the parent concrete. Higher strength values are necessary especially for tensile and flexural strength due to service loads. Mangat and Flaherty (2000) through an extensive field investigation showed that repairs applied with relatively stiff materials, $E_R > E_C$, display efficient structural interaction with the structure. It was observed that high stiffness repairs were effective: i) in redistributing shrinkage strain to the substrate thereby reducing restrained shrinkage tension and ii) strain transfer to the repair patch in the long term due to external load transfer from the substrate structure. The investigation of low stiffness repair materials ($E_R < E_C$) indicated that they are much more likely to undergo tensile cracking due to restrained shrinkage and displayed no long term structural interaction. In addition, low stiffness repairs were ineffective in redistributing strain.

Loading conditions also affect the stability of the structure when materials of different elastic moduli are expected to carry the load. When load is perpendicular to the bond line the difference in load conditions does not cause problems, whereas if the load is parallel to the bond line the material with lower elastic modulus deforms and transfers a larger part of the load to the material with higher elastic modulus leading to fracture of this material (Kosednar and Mailvaganam, 2005).

Any concrete in general has a tendency to shrink on drying. If the concrete is allowed to dry freely, no cracking is observed whereas if the concrete is restrained from changing its dimension owing to shrinkage then cracking occurs as a result of development of high shrinkage stresses. Similarly, repair mortar/concrete is applied concrete substrate has a tendency to crack on drying. The substrate concrete acts as a restraint at the base or the periphery in case of repair concrete leading to potential damage to the dimensional stability of the total repaired element. The restrain provided by the substrate concrete results in development of different types of stress components and the interaction of which leads to failure in the repaired concrete. The potential failure modes include vertical cracking due to direct tension, horizontal cracking due to transverse or peeling tensile stresses, and delamination due to interface shear stresses as shown in Figure 2-2 (Baluch et al. 2002). Thus, the material properties to be considered to ensure reduced cracking of repaired concrete are tensile strength, shrinkage, relaxation and elastic modulus.

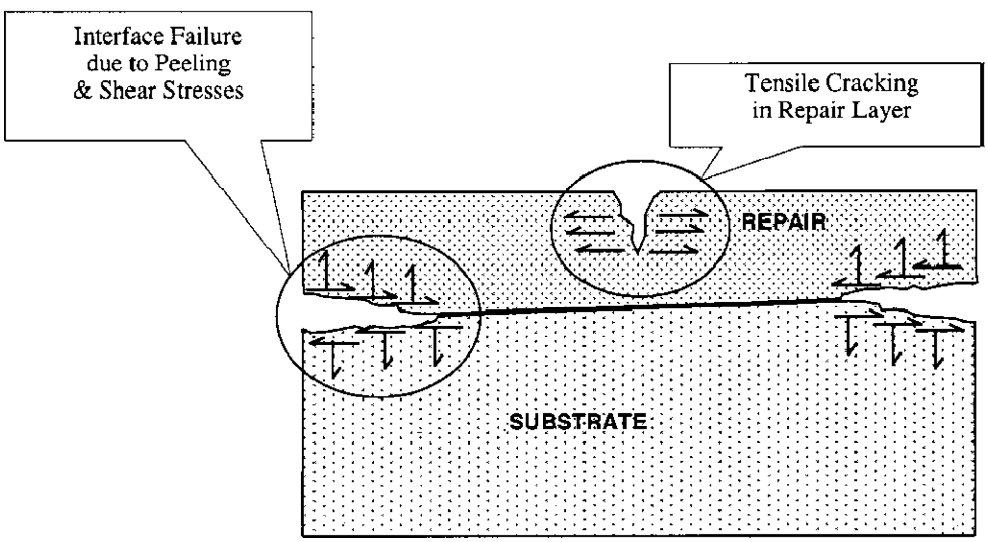

Figure 2-3. Modes of failure in patch repair (Baluch et al. 2002)

Another important property that can potentially increase cracking is coefficient of thermal expansion (CTE). It is important to closely match the CTE of the repair mortar/concrete with the substrate concrete. A composite system of two materials with different CTEs can cause volumetric unstability when subjected to temperature changes. Typically, variation in CTE results in debonding of the repair concrete at the interface.

Structural and volumetric stability of repaired concrete is a crucial factor for long-term durability and serviceability of repaired concrete. Surface failure, resulting in cracking or peeling, increases the probability of substrate concrete being damaged by harmful salts and water.

2.3.2 Polymer / Epoxy Based Repair Material

A survey of the repair materials for overhead and vertical repairs was conducted and included manufacturers such as BASF, Sika and Dayton Superior. The survey and communication with the manufacturers indicated that most repair materials used for overhead applications are typically latex based polymer modified mortars.

Polymer modified cement repair materials are typically adopted for overhead and vertical repairs due to need for stiff mortars which do not require longer curing times unlike cement based repair material. Polymer based repair materials are formulated to provide properties tailored to the requirement of a specific application and take in account wet-state properties, surface penetration and hardened properties such as strength and permeability. According to ACI 548 (2005) the improvements from adding polymer modifiers to concrete include increased bond strength, freezing-and thawing resistance, abrasion resistance, flexural and tensile strengths, and reduced permeability. Polymer addition also increases resistance to penetration by water and dissolved salts, and reduced need for sustained moist curing.

The concept of polymer-hydraulic cement system is almost a century old and was first patented in 1923 (Ohama 1995b). There are various types of polymers that are used with hydraulic cements (ACI 2005). Among these, the most popularly used in the construction industry are elastomeric, thermoplastic and thermosetting types. Addition of each type of latex polymer imparts different properties when used as an additive or modifier. The most commonly used polymers for modification of cementitious mixtures are copolymers (S-A), styrene-butadiene copolymers (S-B), vinyl acetate copolymers (VAC), and vinyl acetate homopolymers (PVA) (ACI 2005; Ohama 1995a). According to the review done for ACI 548 (2005), "the selection of a particular polymer for a PMC depends on the specific properties required for the application. The optimum polymer is the least-expensive one that gives the required properties. Although the prices of polymers vary widely, in general, the cost of polymers depends on the price of their monomers and polymer prices from highest to lowest are PAE > S-A > S-B > VAE > PVA."

2.3.3 Mechanism of Polymerization

The most common method of combining concrete with a polymer is to add polymer latex during mixing. The combination is called latex-modified concrete. Latex is an emulsion, a stabilized suspension of colloidal polymer beads. Polymers are usually used as admixtures; they are supplied as milky white dispersions in water. When a polymer is added to a cementitious mixture the polymerization is underpinned by two major mechanisms: cement hydration and polymer coalescence. In a polymer based cementitious system, typically cement hydration occurs first followed by setting and hardening of the mixture similar to non polymer based cementitious mixture. In case of polymer modified mixtures, the polymer particles start to concentrate in the void spaced created as the mixture starts to set. With continuous water removal by cement hydration, evaporation, or both, the polymer particles coalesce into a polymer film that is interwoven in the hydrated cement resulting in a mixture that coats the aggregate particles and lines the interstitial voids (refer to Figure 2-4). Flocculation of polymer particles takes place as water is removed by evaporation.

Typically, latex particles are greater than 100 nm in diameter and hence cannot penetrate the small capillaries in the cement paste that may be as small as 1 nm. Therefore, it is in the larger capillaries and voids that the latex can be most effective.

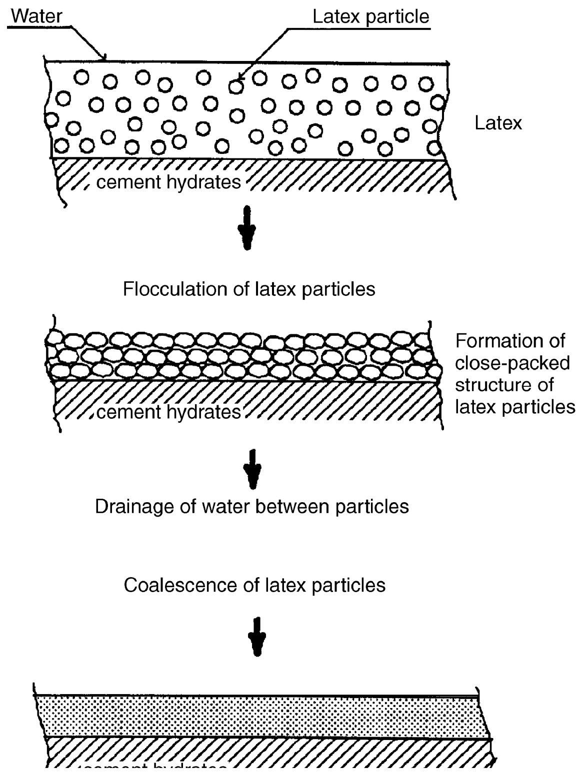

Figure 2-4. Simplified model of formation of polymer film on cement hydration (ACI 2005)

2.3.4 Fresh Polymer Repair Concrete Properties

Each type of polymer imparts different fresh and hardened properties to the polymer modified concrete. The properties of the fresh and hardened mortar and concrete are affected by a multiplicity of factors such as polymer type, polymer-cement ratio, water-cement ratio, air content, and curing conditions.

Figure 2-5 and Figure 2-6 show the effect of unit water content and polymer cement ratio on the consistency of latex modified mortars and concretes respectively (Ohama 1995a). The flow of the latex modified mortars increase as both, the water cement ratio and the polymer cement ratio increase.

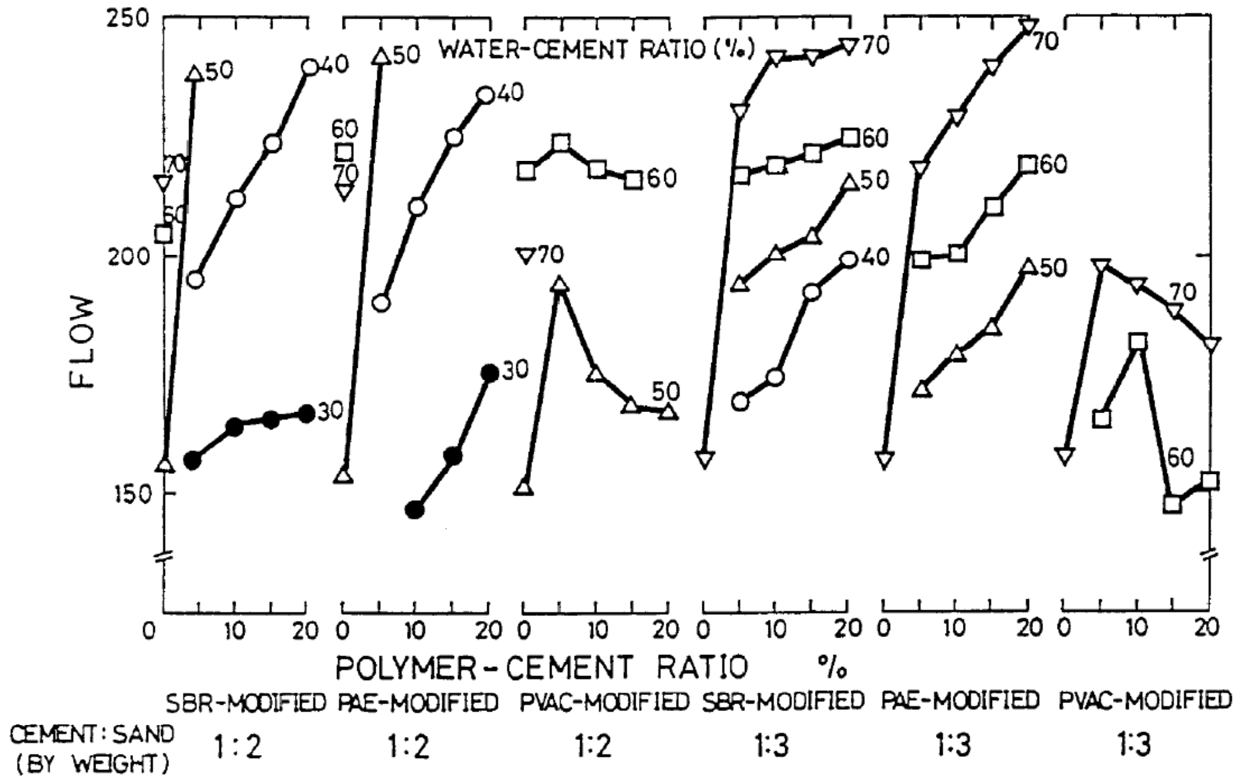

Figure 2-5. Effects of water-cement ratio and polymer-cement ratio on flow of latex modified mortars (Ohama 1995a)

The slump of the latex-modified concretes tends to increase with rising unit water content (or water-cement ratio) and polymer-cement ratio, and at each unit water content, a rise in the polymer-cement ratio causes an increase in the slump. This tendency is more significant at smaller sand-aggregate ratios and at large unit cement contents (Ohama 1995a).

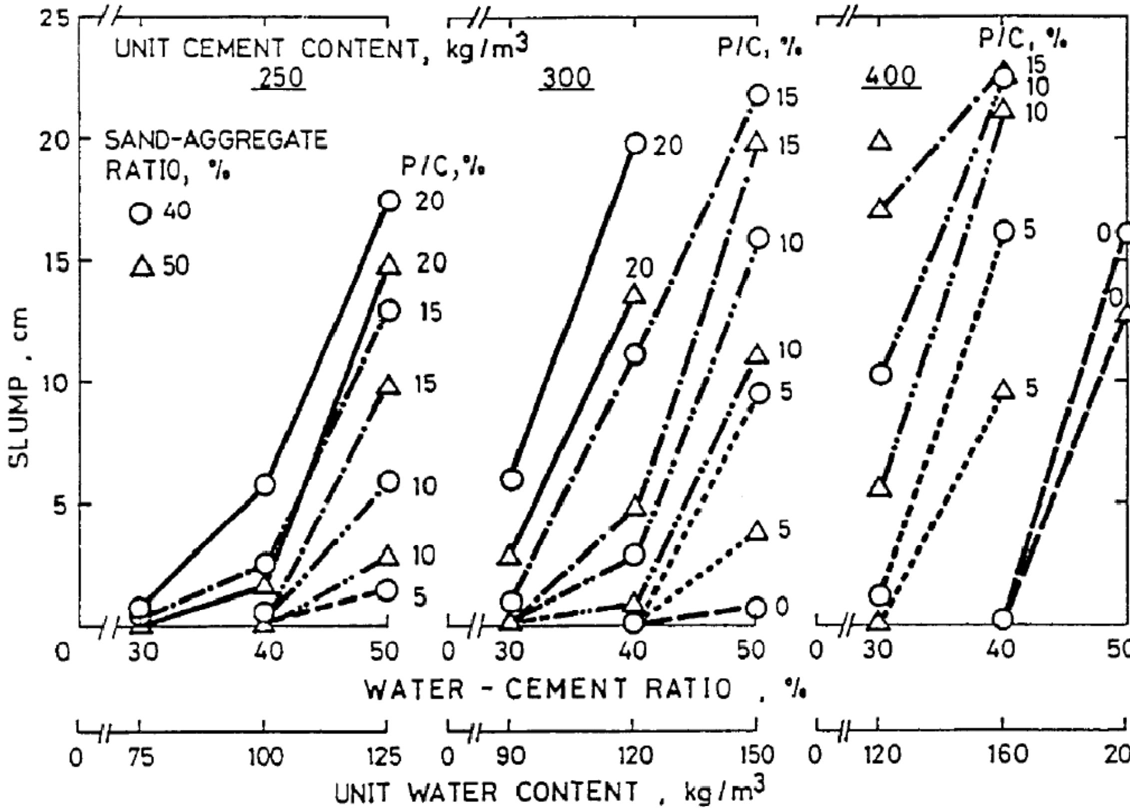

Figure 2-6. Effects of unit water content (water-cement ratio) and polymer-cement ratio on slump of SBR modified concrete (Ohama 1995a)

In most latex-modified mortars and concretes, a large quantity of air is entrained compared to that in ordinary cement mortar and concrete because of an action of the surfactants contained as emulsifiers and stabilizers in polymer latexes. An excessive amount of entrained air causes a reduction in strength and must be controlled by using proper antifoaming agents. Recent commercial latexes for cement modifiers usually contain proper antifoaming agents, and the air entrainment is considerably decreased. Consequently, the air content of most latex-modified mortars is in the range of 5 to 20%, and that of most latex-modified concretes is less than 2%, much the same as ordinary cement concrete. Such decreased air content of the latex-modified concretes over the latex-modified mortars is probably explained by the fact that air is hard to entrain in the concretes because of the larger size of aggregates used (Ohama 1995b).

Latex-modified mortar and concrete have markedly improved water retention over ordinary cement mortar and concrete. The water retention is dependent on the polymer-cement ratio. The reasons for this can probably be explained in terms of the hydrophilic colloidal properties of latexes themselves and the inhibited water evaporation due to the filling and sealing effects of impermeable polymer films formed. Accordingly, a sufficient amount of water required for cement hydration is held in the mortar and concrete and, for most latex-modified systems, dry cure is preferable to wet or water cure (ACI 2005; Ohama 1995a).

In contrast to ordinary cement mortar and concrete, which are apt to cause bleeding and segregation, the resistance of latex-modified mortar and concrete to bleeding and segregation is excellent in spite of their larger flowability characteristics. This is due to the hydrophilic colloidal properties of latexes themselves and the air-entraining and water-reducing effects of the surfactants contained in the latexes. Accordingly, in the latex modified systems, some disadvantages such as reductions in strengths and water loss caused by bleeding and segregation do not exist. Al-Zaharani et. al. (2003) assessed various types of commercial polymer based repair materials. In their study, they have noted that those polymer mortars which exhibited low flowability exhibited no bleeding in comparison to plain cementitious mortars which had similar flow characteristics.

2.3.5 Hardened Polymer Repair Concrete Properties

To ensure durability of structures repaired with polymer modified mortars/concretes it is necessary to ensure that the properties of the substrate concrete match with those of the repair material intended for use. In this section, hardened properties of polymer modified mortars are discussed.

In a study comparing four commercial polymer based repair materials with cement based repair materials, Al-Zahrani et al. (2003) report that polymer based repair mortars exhibit an increase in compressive strength between 2700 psi to 8700 psi. The polymer based repair mortars did not exhibit any higher strength gains in comparison to the cement and water based mortars. Studies also indicate that the strength gain is clearly dependent upon many factors such as type of polymer and polymer cement ratio adopted in the repair mortar, curing methods and testing methods (Mirza et al. 2002). The strength properties of the latex modified mortars and concretes are influenced by these factors and they tend to interact with each other. In their study of 25 polymer modified mortars, Mirza et al. (2002) have shown that the compressive strength of acrylic based polymer modified mortars increases as the polymer-cement ratio increases, however the type of curing has a moderate effect on the compressive strength and is slightly reduced when the samples are wet cured.

In general, latex-modified mortar and concrete show a noticeable increase in tensile and flexural strengths but no improvement in the compressive strength as compared to ordinary cement and mortar concrete. The increase in tensile strength is related to the high tensile strength of the polymer in itself and improved cement aggregate bond (Ohama 1995b). Researchers report tensile strengths in the range of $1/10^{th}$ of the compressive strength for polymer modified mortars using styrene butadiene or acrylic polymers whereas mortars prepared using epoxy based polymers exhibit tensile strengths in the range of $1/5^{th}$ of compressive strength (Hassan et al. 2000; Mirza et al. 2002).

The bond strength characteristics are vastly improved by using polymer modified cement based repair mortars (Lavelle 1988; Mirza et al. 2002; Ohama 1995b). Studies have shown that mortars containing styrene butadiene rubber based polymer modified cementitious systems exhibit approximately 20 % higher bond strengths in comparison to the bond strengths of mortars modified by acrylic based polymers (Lavelle 1988; Mirza et al. 2002). The type of curing does not affect the bond strength of polymer modified repair mortars. It has been reported that the bond strength of mortars containing styrene butadiene rubber polymer modifiers decreases over time when subjected to freezing and thawing cycles but stabilizes over a period of five years. Surface preparation and adhesion play an important role in the long-term bond strength of polymer based mortars to concrete substrate.

Elastic modulus plays an important role in maintaining the dimensional stability of the repaired structure. Polymer modified mortar and concretes contain polymers with considerably smaller modulus of elasticity compared to cement hydrates. Consequently the deformation of polymer modified mortars and their ductility can differ greatly than ordinary cement mortars and concretes. Generally, the maximum compressive strain at failure increases with increasing polymer-cement ratio though the elastic modulus in compression remains somewhat constant. Researchers have shown that the type of polymer modifier used has a significant effect on the elastic modulus of the repair mortar (Hassan et al. 2000; Lavelle 1988; Mirza et al. 2002).

Polymer properties are sensitive to relatively small temperature changes and they are significantly time dependent. Hence, it is imperative that information on the coefficient of thermal expansion (CTE) for a selected polymer modified mortar be assessed before using it in field. According to Ohama (1995a), the CTE of latex-modified mortar and concrete is directly influenced by that of the aggregates used, as in ordinary cement mortar and concrete. Latex modified mortars and concretes usually have coefficients of thermal expansion equal to or slightly higher than that of ordinary cement mortar or concretes.

Another important aspect of dimensional stability is the shrinkage properties of the individual repair material as well as of the complete structural system as a whole. The drying shrinkage of polymer modified mortars may be either large or small and is dependent upon polymer type and polymer-cement ratio. Researchers have shown that the drying shrinkage at 28 days for commercially available polymer modified repair mortars is typically between 150 µ to 1200 µ. The shrinkage strain development also depends on the ambient relative humidity and the restraint provided by the substrate. A polymer modified mortar exhibiting smaller drying shrinkage strains may not necessarily remain uncracked on the field. It is essential to understand the variation in development of tensile creep, tensile modulus of elasticity and drying shrinkage combined to predict the cracking tendency of polymer modified repair mortars (Pinelle 1995).

2.3.6 Durability Performance of Polymer Based Repair Concrete

The structure of latex modified concretes is such that the micropores and voids normally occurring in hardened portland-cement concrete are partially filled with the polymer film that forms during curing as explained in the section on polymerization (Section 2.3.1). This film is the reason for the mixture’s reduced permeability and water absorption. These properties have been measured by several tests, including water-vapor transmission, water absorption, carbonation resistance, and chloride permeability. There are indications that the permeability of latex modified mortars decreases significantly with age beyond 28 days (Kuhlmann and Foor 1984). The same study also indicated that amount of air (i.e. air content present in polymer based mortars) does not affect the chloride permeability. It was found that even at high amounts of air contents the air voids are small and well distributed and permeability does not increase. Researchers have conducted tests to ascertain affects of curing regime on chloride permeability by ponding specimens for 90 days in plain water and salt solution. It was observed that resistance to chloride ion penetration increased with increasing polymer content.

As reported in ACI 546 the resistance of LMC to damage from freezing and thawing has been demonstrated both in the laboratory (Ohama 1995a; Smutzer and Hockett 1981) and in the field (Bishara 1979). The frost resistance of SBR, PVA and EVA modified mortars is improved markedly at polymer cement ratios of 5% or more. It has been observed that as the degree of expansion by frost (calculated from the residual expansion of specimens from freezing and thawing) increases, the relative dynamic modulus of polymer modified mortars is reduced (Ohama 1995b). Increasing the polymer cement ratio does not necessarily cause an improvement in the frost resistance, and good frost resistance can be achieved by the composite effects of polymer modification and stable air content.

2.3.7 Gaps in Knowledge

During the literature review conducted for this study, it was noted that not many publications are available that deal with the fresh and hardened properties of commercially available proprietary materials. This gap in knowledge can be attributed to the fact that there are numerous types of polymer modified repair mortars and manufacturers develop products based on the needs of the region where it is being sold. Given this diversity in material components, two references that have been cited extensively in the earlier sections (ACI 2005; Ohama 1995b) appear to have a comprehensive collection of information on polymer modified mortars including different types polymers and its effects on properties. In order to approve a particular material for use in repair it is essential to evaluate its fresh and hardened properties. The durability of the repair material itself and the composite system consisting of the repaired concrete and the substrate concrete is an important parameter contributing to the long-term performance of the repaired structure. It is essential to adopt a holistic approach in repairing structures so that concurrent interaction of many factors such as shrinkage, permeability and absorptivity are considered.

2.4 SHEAR KEY MATERIALS

Section 5.14.4.3.2 of AASHTO Standard Specifications (2002) requires that the shear-key depth between the beams shall not be less than 7 inches. Longitudinal shear transfer joints are permitted to be modeled as hinges for analysis. The strength of the non-shrink grout material for the shear-key is required to be a minimum of 5 ksi at 24 hours. Section 5.14.1.2.8 of AASHTO LRFD (2004) specifies that the depth of shear key shall not be less than 5-in. and filled with non-shrink mortar attaining a compressive strength of 4 ksi within 24 hours. Section 708.3 of MDOT Standard Specifications for Construction (2003b) specifies Type R-2 grout to fill the longitudinal joints between beams. The transverse posttension is applied following 48 hours of curing of the grout. The mechanical properties of the Type R-2 grout will be given in Chapter 6.

2.4.1 Commercial Grout Materials

According to Gulyas et al. (1995), non-shrink grout (Set Grout) materials are not able to develop the specified minimum compressive strength within 24 hours. Comparative test results by Gulyas et al. (1995) showed that the magnesium ammonium phosphate ($Mg\text{-}NH_4\text{-}PO_4$) or so-called Set 45 grout samples develop a significantly higher strength than the non-shrink grout specimens. Issa et al. (2003) performed a total of 36 experiments for vertical shear, direct tension, and flexural capacity using four different grout materials. Polymer concrete was found to be the best material for transverse joints in terms of strength, bond, and mode of failure. However, the use of Set Grout was recommended for the transverse joints due to its ease of use and satisfactory performance. It was also recommended that polymer concrete may be used in critically stressed joints and for rapid replacement of bridge decks due to its rapid hardening properties (4500 psi in one hour) (Table 2-2).

Table 2-2. Grout Material Properties (Issa et al. 2003)

Age of Testing	Type of Test	Strength of Grout Materials, psi		
		Set 45 ($Mg-NH_4-PO_4$)	Set Grout (Non-shrink grout)	Polymer Concrete
3 hours	Compressive	-	-	9752
6 hours	Compressive	3718	-	10,169
1 day	Compressive	3775	2841	10,357
3 days	Compressive	4294	5109	10,460
	Tensile	574	548	988
7 days	Compressive	5516	6312	10,550
	Tensile	587	598	1130
28 days	Compressive	6122	10,031	10,756
	Tensile	605	703	1153

Compatibility of properties between parent material (box-beam material) and the joint material (shear key material) is an important parameter of structural and durability performance of box-beam bridge superstructure. The joint material is expected to transfer moment and shear while retaining the water tightness of the joints. Hence, the grout compressive, tensile, and bond strength, elasticity modulus, shrinkage, thermal expansion coefficient, permeability, and potential of joint sealing properties are of interest in this study. Further, cementitious materials/mixes that are used as grout are studied. Table 2-3 summarizes mechanical and durability properties of materials that are used or have a potential to be used for forming the joints between precast components. Data presented in Gulyas et al. (1995), Issa et al. (2003), Scholz et al. (2007), and Manufacturers' data sheets are the sources of information for developing Table 2-3. Scholz et al. (2007) performed the tests in accordance with the ASTM standards (ASTM C39, ASTM C 496, ASTM C 882, ASTM C 157, and ASTM C 1202). A ponding test was performed evaluating the potential for leakage at the shear key.

AASHTO Standard (2002) Section 5.14.4.3.2 requires 5000 psi grout compressive strength in 24 hours, while LRFD (2004) Section 5.14.1.2.8 requires 4000 psi. According to the data presented in Table 2-3, only a few materials are capable of satisfying the AASHTO strength requirements. According to Michigan practice, posttension is applied 48 hours (2 days) after grouting the shear keys (MDOT 2003b). This two-day lag time will help grout materials develop adequate strength before posttension applications. AASHTO LRFD (2004) requires that transverse posttensioning generates a stress level 250 psi at the shear key. All the materials listed in Table 2-3 show sufficient strength such that 250 psi compressive stress can be applied with a factor of safety of at least three.

In addition to facilitating load transfer through the joints between precast beams, grout materials are expected to prevent moisture intrusion into the joint. The data presented in Table 2-3 contradicts the common perception. It is expected that grout materials with good bond strength and lower shrinkage prevent moisture intrusion through the grouted joints. According to the data presented in Table 2-3, water leaks through the interface when grout material has lower shrinkage but higher bond strength. This indicates that a focus should be placed on not only shrinkage and bond properties, but also many other grout properties such as thermal expansion coefficient, mechanical properties, and compatibility between grout and beam material properties. Scholz et al. (2007) evaluated the joint sealing performance using a ponding test. In the test, the interface was not subjected to any clamping force; whereas, in precast systems, the joint is expected to be under compressive stress of some uniformity. Posttension force magnitude, force application sequence, and number of posttension locations are functions of the material used for shear keys to achieve uniform stress distribution throughout the shear keys.

Table 2-3. Summary of Grout Material Properties

Grout Type	Compressive Strength (psi)		Tensile Strength (psi)	Bond Strength (psi)	Shrinkage (in.)	Leakage		Thermal Expansion Coefficient (10^{-6}/F)	Permeability (coulomb)	Elasticity Modulus (10^6 psi)
	1-Day	7-Day	7-Day		28-Day	1 month	6 months		28-Day	
ThoRoc®10-60	5210	6380	540	540	0.0076	No	No			
SikaQuick®2500	3540	4710	340	1400	0.0080	No	No			4.6
Five Star®Patch	5080	5820	530	1810	0.0029	No	Yes			
Set®45 HW	4930	4930	410	470	0.0034	No	Yes	7.15		5.25
ThoRoc®extended	3150	5040	510	1730	0.0064	No	No			
SikaQuick®extended	1900	2550	335	850	0.0089	No	No			
Five Star®extended	4490	5440	555	1680	0.0036	No	Yes			
Set®45 extended	2650	4180	415	950	0.0018	No	Yes	7.15		5.25
Set®45	3375	5516	587	>252				7.15	606	4.55
Set Grout	2841	6312	598	85					2544	
Polymer concrete	10357	10550	1130						22	

Source: Gulyas et al., 1995, Issa et al., 2003, Scholz et al., 2007, and Manufacturers' data sheet

2.4.2 Other Cementitious Materials

Other cementitious materials that may have a potential of being used as grout materials are reviewed. Ghrici et al. (2007) studied the mechanical properties and durability of mortar and concrete containing natural pozzolana and limestone blended cement. Figure 2-7 shows the variation of compressive strength of mortar cubes made of different proportions of limestone filler (LF) and natural pozzolana (NP). Early age strength can be controlled by varying limestone filler (LF) content from 0 - 14% and natural pozzolana (NP) content from 0-5% (Figure 2-7). This demonstrates the potential for developing customized mixes based on the strength requirements at a specific time upon placement.

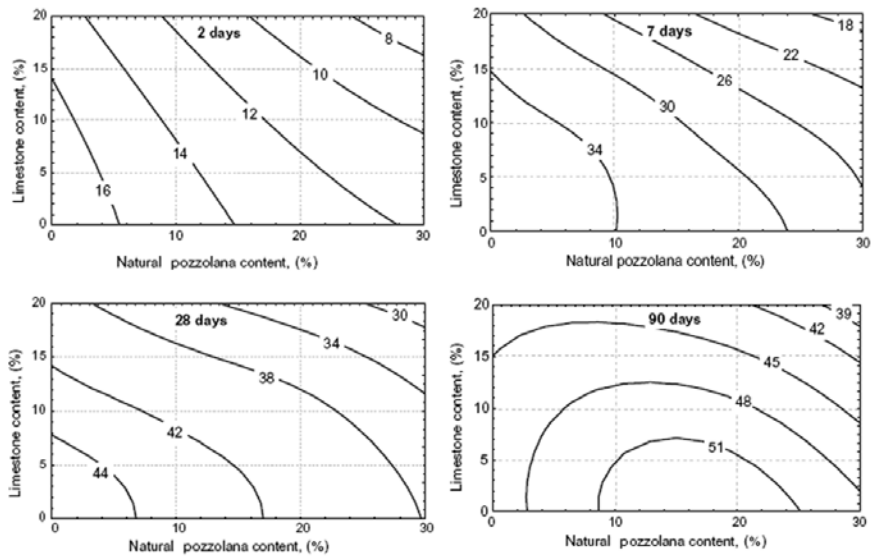

Note: 0.0069 MPa = 1 Psi

Figure 2-7. Compressive strength (in MPa) of mortar cubes at different ages (Ghrici et al. 2007)

Further, this study demonstrates that small percentage of natural pozzolana enhances the durability properties of concrete or mortar. The same ratio of blended mortar or concrete (OPC + 20% NP + 10% FL) mixture with a water/binder (w/b) ratio of 0.4 reduced the capillary sorption by 25%. The C-S-H is formed by the pozzolanic reaction in concrete and is instrumental in reducing the capillary sorption of concrete. Also, paste-aggregate interface quality is enhanced by this reaction.

The chloride penetration measured in terms of charge that passes through the specimens in unit time, in coulombs, is obtained at the age of 28 and 90 days. For 0.4 w/b ratio, concrete containing (OPC + 30% NP) exhibits greater resistance to chloride ion permeability (Figure 2-8).

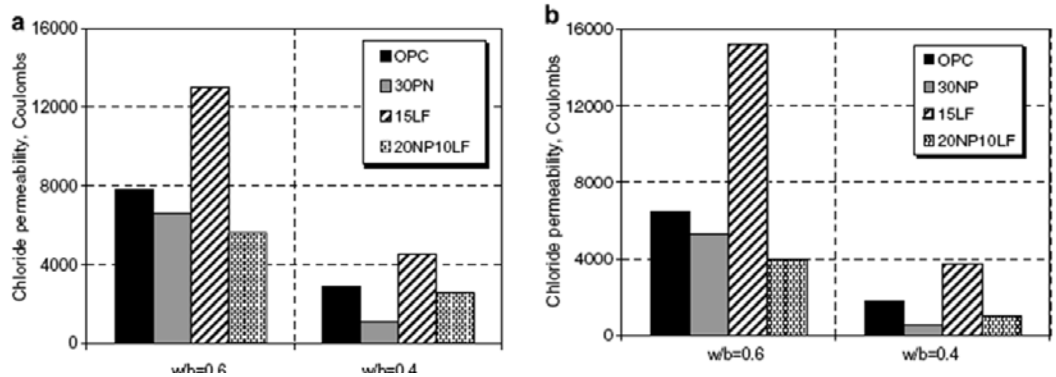

Figure 2-8. Chloride permeability of concrete at (a) 28 days and (b) 90 days (Ghrici et al. 2007)

Arandigoyen and Alvarez (2007) studied pore structure and mechanical properties of cement-lime mortar. According to experiments that were conducted on seven different proportions of cement-lime-calcite aggregate with three different binder/aggregate (B/Ag) ratios (by volume) such as 1:2, 1:3, and 1:4; it was observed that porosity is independent of the lime-cement ratio but depend on B/Ag ratio.

The study on influence of binder composition on mechanical strength of mortar showed that 0 to 40% of an increase in cement-in-lime rich mortar increases mechanical strength slightly. This is in contrast to a 25% increase in lime-in-cement rich mortar, in which mechanical strength diminishes considerably (Figure 2-9).

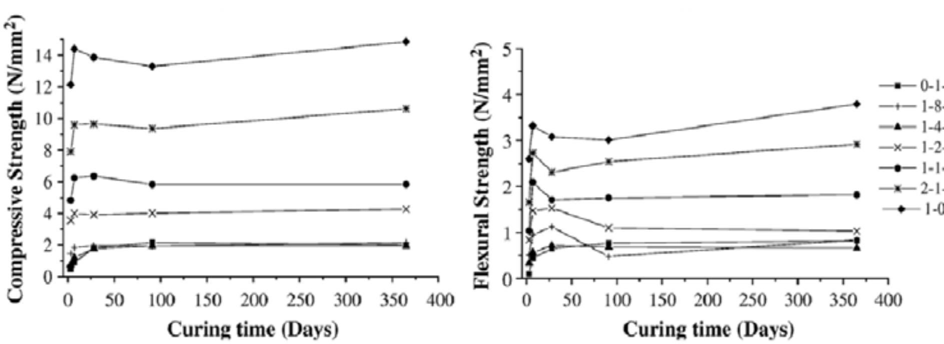

Note: 0-1-4 to 1-0-4 are the cement/lime/aggregate ratios by volume

Figure 2-9. Variation of compressive and flexural strength of mortar against time (Arandigoyen and Alvarez 2007)

Modulus of elasticity increases with the increase in cement percentage in the binder and with the increase in the B/Ag ratio. It was concluded that cement-rich mortar with high modulus may develop cracks and breakage after going through a phase of elastic deformation. On the other hand, lime-rich mortars (0-1-2 and 1-8-18) are able to absorb a high degree of deformation before the breakage. The presence of plastic zone for the lime – rich mortar is large along with higher flexibility.

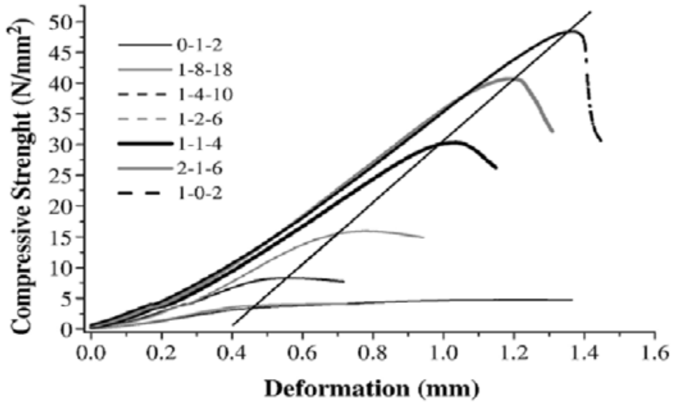

Note: From 0-1-2 to 1-0-2 are the cement/lime/aggregate ratios (by volume)

Figure 2-10. Changing mortar compressive strength (MPa) against deformation (mm) (Arandigoyen and Alvarez 2007)

Yurtdas et al. (2005) studied the influence of water/cement (w/c) ratio on mechanical properties of mortars that are submitted to drying. Mortar with two different w/c ratios of 0.5 and 0.8 were labeled as mortar05 and mortar08. Figure 2-11 describes the effect of drying on the uniaxial compressive strength of the Mortar05 and Mortar08. It is observed that the compressive strength of both the mortar samples remains almost constant with the increase in relative weight loss (RWL) which is defined in Eq. 2-1. For the mortar08 the strength increases by 32% at RWL value of 30%, and it decreases by same amount at 100% RWL. The strength of the mortar05 increases by 21% at 30% RWL and then remains constant.

$$RWL(t) = 100 \times \frac{\left(W_{(t)} - W_0\right)}{\left(W_{dry} - W_0\right)} \tag{2-1}$$

where;

W_{dry} = dry weight of the sample

W_o = initial sample weight

W_t = weight at time t

Two reasons are defined for the increase in the compressive strength:

1. Isotropic effect of capillary pressure, and
2. Confining of the sample core induced by moisture gradient.

It can also be concluded from Figure 2-11 that the mortar05 has higher compressive strength than the mortar08.

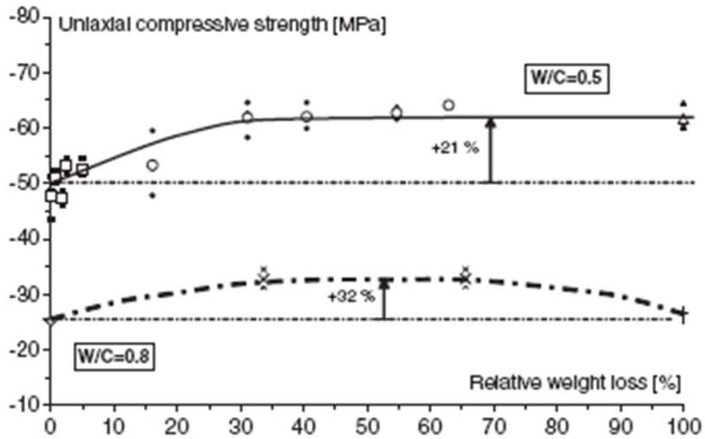

Figure 2-11. Variation of uniaxial compressive strength against relative weight loss of mortar (Yurtdas et al. 2005)

According to the data presented in Figure 2-12, Young's modulus for both samples remains constant up to an extent of relative weight loss (RWL), and then the modulus drops by 15% and 18% for mortar05 and mortar08, respectively. During the curing process capillary suction plays a dominant role due to higher content of water in the sample. This increases the apparent stiffness of the sample and reduces the effect of microcracking on the sample while maintaining the modulus of elasticity. After certain RWL the effect of capillary suction diminishes, and the effect of microcracking becomes dominant; hence, the reduction in the modulus of elasticity is observed.

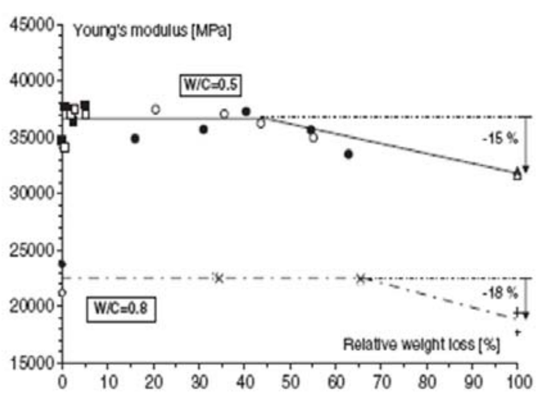

Figure 2-12. Variation of elasticity modulus against relative weight loss of mortar (Yurtdas et al. 2005)

2.4.3 The Bond between Girder and Shear Key Materials

Miller et al., (1999) studied the performance of shear-keys at locations along the girder depth considering non-shrink grout and epoxy as grout material. According to research findings, when epoxy is used substrate concrete cracks rather than the shear-key. This failure mode was defined as undesirable. Gulyas et al. (1995) showed that the failure mode for the non-shrink grout specimens tend to be at the bond line while the failure mode for the Mg-NH_4-PO_4 grout (Set 45) was usually at least partially through the substrate. In the study conducted by Issa et al. (2003), polymer concrete showed failure through the substrate. According to Gulyas et al. (1995) and ACI 503.1 Appendix Testing (1992), preliminary consideration should be given to grout materials that have inherent bond strength high enough to fail in the substrate material.

The composite direct tension test performed by Gulyas et al. (1995) showed that the bond failure occurs at a tensile load of 1940 lbs corresponding to a stress value of about 85 psi for non-shrink grout. The tensile strength of the non-shrink grout was 390 psi. Considering this tensile strength and the three-day tensile strength given by Issa et al. (2003) shown in Table 2-2, the bond between shear key grout and the beam fails before shear key grout tensile strength is reached.

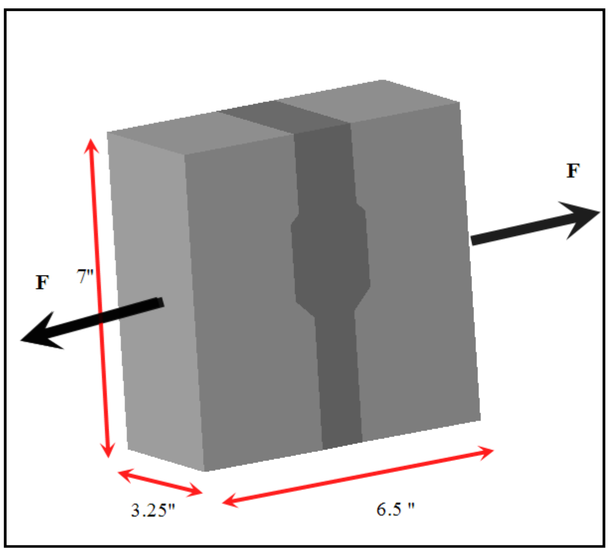

Figure 2-13. Composite direct tension test (Gulyas et al. 1995)

The literature on the side-by-side box beam modeling and analyses with transverse post-tensioning is limited. El-Remaily et al. (1996) modeled the assemblage as a grillage allowing the joint to transfer shear, bending, and torsion. Dong (2002) assumed a perfect bond between the grout and the beam surface throughout his analysis. Issa et al. (2003) simulated direct shear testing of a specimen modeling concrete crushing and cracking. Hawkins and Fuentes (2003) incorporated the link elements based on a beam-on-elastic foundation concept to define joint flexibility. According to this concept, connectivity stiffness controlling the relative vertical displacements of two adjacent beams is assumed proportional to shear force transmitted through the joint between the beams. The joint stiffness upon cracking and shear key fracture is then modeled by reducing the degree of shear force transferred between girders. It was concluded that cracking of the longitudinal joint had little effect on the stiffness of the bridge provided that the transverse tie rods were snug.

2.4.4 Load Bearing Capacity of Mortar joints

Barboza et al. (2006) studied the bearing capacity and compressive strength of mortar joints between precast elements. The bearing capacity is typically governed by the splitting stress of precast elements. Splitting stresses are developed due to flow of compressed grout to the border that develops frictional forces and “pulls” the precast element apart or the redistribution of stresses at the joint. The hypotheses for these behaviors are illustrated in Figure 2-14.

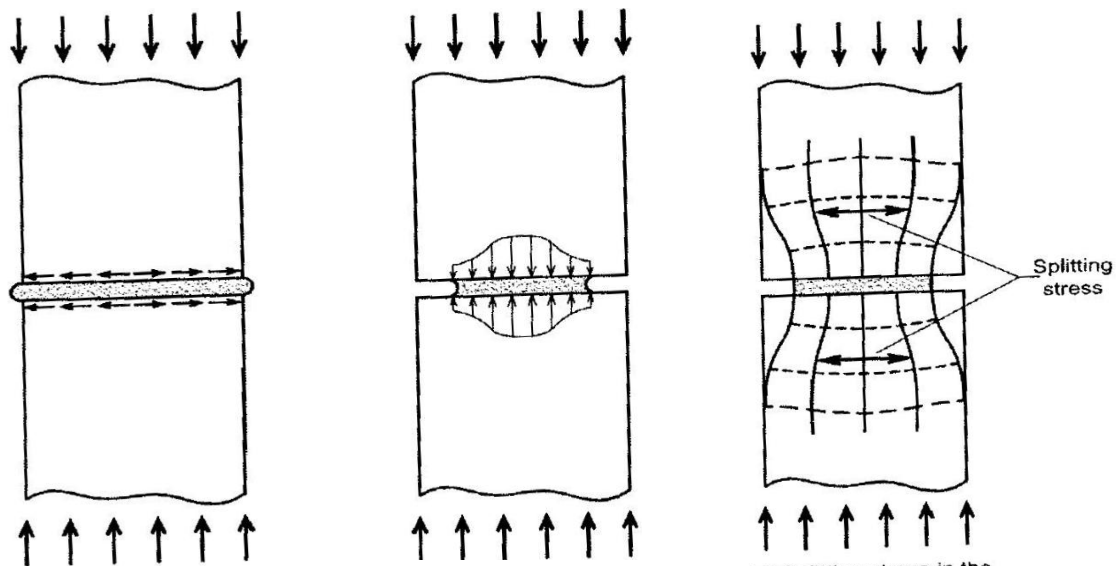

Frictional forces developed at the joints | Non-uniform stress distribution at the joint | Splitting stress developed in precast elements

Figure 2-14. Stresses developed at the joints and in the precast elements (Barboza et al. 2006)

Summarizing the work presented by Dragosavic (1978), Barboza et al. (2006) stated that the load-bearing capacity of a mortar grouted joint between precast elements under compressive loads can be determined based on the following conditions:

1. If the mortar compressive strength is greater than that of precast elements, the load-bearing capacity of the connection is equal to the compressive strength of the precast element.
2. If the compressive strengths of the mortar and precast elements are the same, the capacity of the connection will be equal to the compressive strength of the mortar, which equals the compressive strength of the precast elements.
3. If the compressive strength of the mortar is less than the compressive strength of the precast element, and the ratio of minor joint width and the joint thickness is small, the joint load-bearing capacity (f_j) can be calculated using the following equation:

$$f_j = \alpha f'_c \qquad (2\text{- }2)$$

where, $f_c^{'}$ is the compressive strength of concrete used in precast elements, and the factor α is determined from Figure 2-15. The factor α defines the joint efficiency.

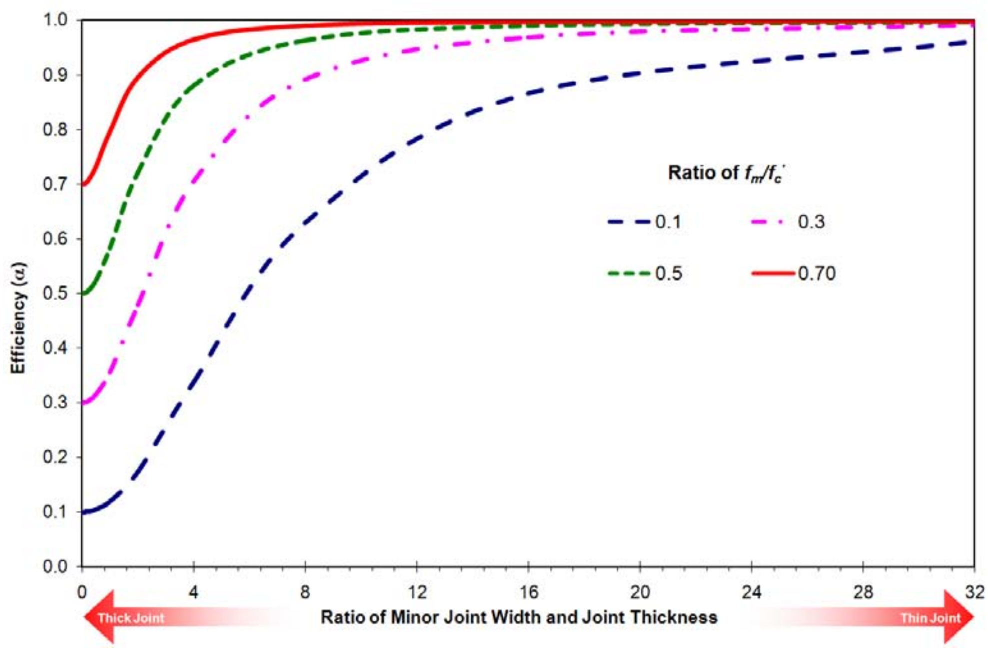

Figure 2-15. Variation of joint efficiency (α) against the ratio of minor joint width and joint thickness

In Figure 2-15, the ratio of minor joint width and the joint thickness is plotted along the x-axis and efficiency (α) along the y-axis. The family of curves, corresponding to the ratio of the compressive strength of the mortar (f_m) and precast element ($f_c^{'}$), is plotted against α.

Barboza et al. (2006) presented an equation proposed by Vambersky (1990) as an updated version of the original equation proposed by Dragosavic (1978) that incorporates the type of grout.

$$f_i = \eta \alpha f_c' \tag{2-3}$$

where, η

= 0.9 for fluid mortar placed in joint after assembly

= 0.7 for dry mortar placed in joint after assembly

= 0.3 for elements placed on mortar beds

Barboza et al. (2006) also conducted experiments to verify these equations by varying the joint thickness and the compressive strength of grout. The test configuration consisted of two axially loaded square columns with a 7 in. × 7 in. (175 mm × 175 mm) cross-section (Figure 2-16).

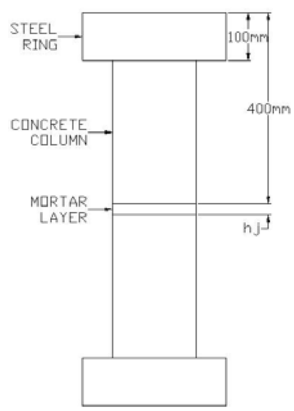

Figure 2-16. Test configuration used by Barboza et al. (2006)

The Barboza et al. (2006) study shows that the use of thin joints increases the joint load-bearing capacity when the grout material strength is lower than that of the precast elements. However, maintaining a uniform thickness of grout in thin joints is difficult but essential to generate uniform stress distribution.

2.5 THE INFLUENCE OF DIAPHRAGMS ON POSTTENSION STRESS DISTRIBUTION

The AASHTO LRFD (2004) Section 5.13.2.2 states that "diaphragms shall be provided at abutments, piers, and hinge joints to resist lateral forces and transmit loads to points of supports unless otherwise specified. Intermediate diaphragms may be used between beams in curved systems or where necessary to provide torsional resistance and to support the deck at points of discontinuity or at angle points in girders."

In side-by-side box beam bridges, the diaphragm function is more than what is specified in the AASHTO, such as in the transfer of post tensioning forces, distribution of clamping stress to keep shear keys under compression as well as forming a couple with the shear key for moment transfer between the girders. The AASHTO LRFD (2004) did not provide specific provisions for the side-by-side box beam bridge diaphragms. Several State Highway Departments have developed a criterion for the number of diaphragms and posttension locations and force magnitudes based on the depth of the girder and span length.

El-Remaily et al. (1996) proposed a design procedure for calculating posttension force magnitude from grillage analysis. According to the grillage procedure, the joints between the beams can transfer shear, bending, and torsion. The transverse connection between adjacent box-beams is through the diaphragms, so the shear key along the full length of the beam is not essential for the structural performance of the bridge. Thus, posttensioned diaphragms serve as the primary wheel load transfer mechanism between adjacent boxes. The number of diaphragms was calculated based on a parametric study that was carried out to limit differential displacements between the girders to 0.02 inches. According to the parametric study results, the posttension force magnitude is a function of beam depth and bridge width. The PCI Design Manual (2003), based on El-Remaily's analyses, recommends the use of three diaphragms for spans up to 60 ft (one @ each end, one @ mid-span) and five diaphragms for spans over 60 ft (1 @ each quarter point, 1 @ center of beam, and 1 @ each beam end).

2.5.1 Assessment of Load Distribution between Adjacent Girders

Posttensioned diaphragms serve as the primary wheel load transfer mechanism between adjacent boxes according to El-Remaily et al. (1996). Without posttensioned diaphragms each beam would have to carry the full wheel line load (Figure 2-17). El-Remaily's analysis was to assess the posttensioning effect on limiting differential displacement of the girders to 0.02 inches.

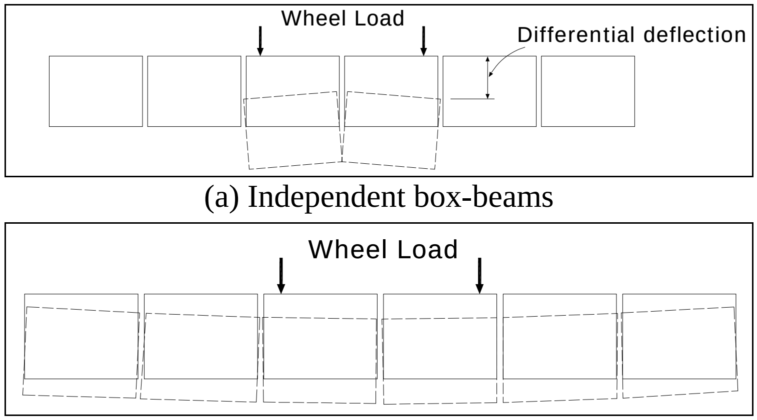

(a) Independent box-beams

(b) Fully connected box-beams

Figure 2-17. Deflection of a box-beam bridge (El-Remaily et al. 1996)

2.5.2 Bridge Width Effect on Posttension Stress Distribution

Section 5.14.1.2.8 of the AASHTO LRFD (2004) requires that transverse posttension stress, after all losses, shall not be less than 0.25 ksi along the shear key. However, the contact area between girders and the procedure for calculating transverse posttension force magnitude are not defined in the AASHTO LRFD (2004). This contact area can be regarded as the shear-key area, or the diaphragm-to-diaphragm contact area, or the entire side surface of the box-girder. El-Remaily et al. (1996) recommends considering the diaphragm-to-diaphragm contact area for the design.

The required posttension force also depends on bridge width (Figure 2-18). According to El-Remaily et al. (1996), the grillage analysis can be performed for calculating the force demand at the diaphragm locations.

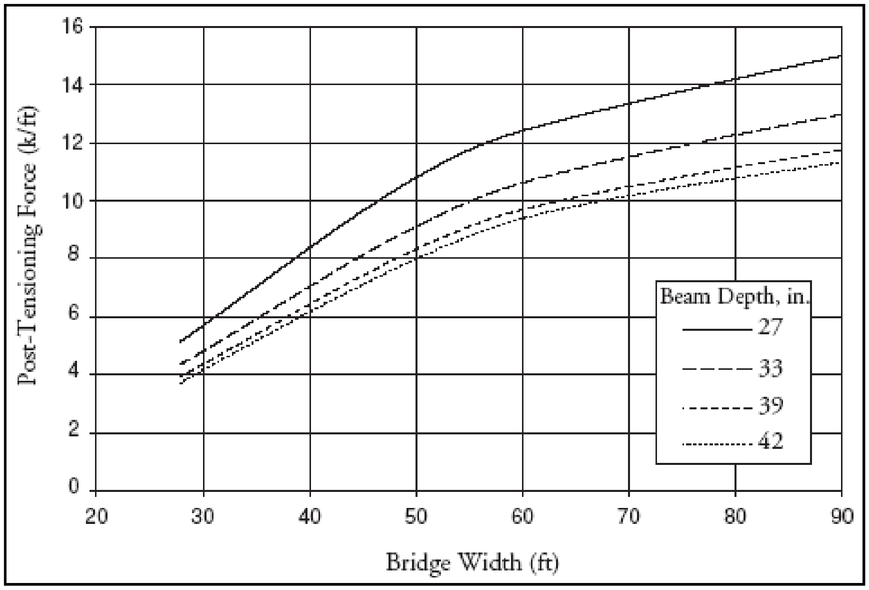

Figure 2-18. Posttension force variation with bridge width and beam height (El-Remaily et al. 1996)

2.6 SUMMARY AND CONCLUSIONS

This chapter summarized research related to capacity evaluation and load testing of distressed bridges/girders, materials used for shear keys, properties of cementitious materials and development of customized materials. The following list of conclusions is reemphasized in order of importance:

1. Fatigue is not an issue for uncracked beams. Fatigue may be an issue under frequent loading on bridges that creates bottom fiber stress in excess of $6(f_c^{'})^{1/2}$ psi or strand stress greater than $0.06f_{pu}$.
2. Distressed beam capacity can be accurately evaluated by analytical models.
3. Customized shear key grout mixes can be developed for specified strength requirements at a particular age of material.
4. Load transfer efficiency of the shear key joint increases as the thickness decreases. However, uniform thickness of the joint is vital to maintain uniform stress distribution.
5. Diaphragms generate rigid zones in the box-beam bridge superstructure and work as the primary load transfer mechanism.
6. The transverse posttension magnitude needs to be specified as a function of bridge width.

Intentionally left blank

3 LOAD TESTING OF DECOMMISIONED BOX-BEAM

3.1 OBJECTIVE AND APPROACH

The failure of a fascia girder of Lakeview Drive bridge in Pennsylvania on December 27, 2005 prompted the capacity evaluation of box beams with similar deterioration. The objective of the work discussed in this chapter is to remove a severely deteriorated fascia beam, instrument it, and perform load testing for evaluating the capacity of the beam. The remaining prestress was calculated from camber measurements and the strain gauge data. Beam capacity is calculated using strain data, and load rating is performed.

3.2 OVERVIEW

The four span side-by-side box beam bridge is located in Jackson County and carries traffic in north-south directions of Hawkins Road over the I-94 freeway (Photo 3-1). This bridge was built in 1957 and contains 11 double-cell box-beams on each span. The width of each beam is 36-inches. Spans two and three contain 21-inch deep beams over the I-94 freeway. The other two spans have nine 17-inch deep interior beams and two 21-inch deep fascia beams. The width of the bridge is 33' – 7½". The total length of the bridge is 164 ft. Each span over the freeway is 48'-6" long.

Photo 3-1. Bridge on Hawkins Road over I-94 (S11-38101)

Inspections revealed that the west fascia beam over westbound I-94 had a full-length crack with heavy leaching on the beam soffit (Photo 3-2).

Photo 3-2. West fascia beam with full-length crack

The bridge wearing surface showed multiple longitudinal cracks (Photo 3-3) reflecting from the girders. The transverse connection between the beams is provided by a shallow grouted shear key and a one-inch diameter tie-rod at 1/3rd locations along the second and third spans and at the center of the first and fourth spans (Photo 3-4).

Photo 3-3. Wearing surface with multiple longitudinal cracks

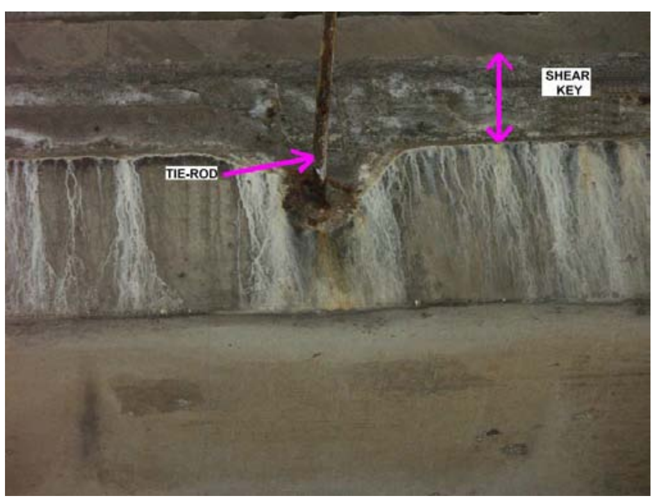

Photo 3-4. Shallow grouted shear key and tie-rod

The box-beams used in the 1950s were fabricated with open stirrups as shown in (Figure 3-1). The development of longitudinal full-length cracks and rust leaching out from the cracks raised safety concerns.

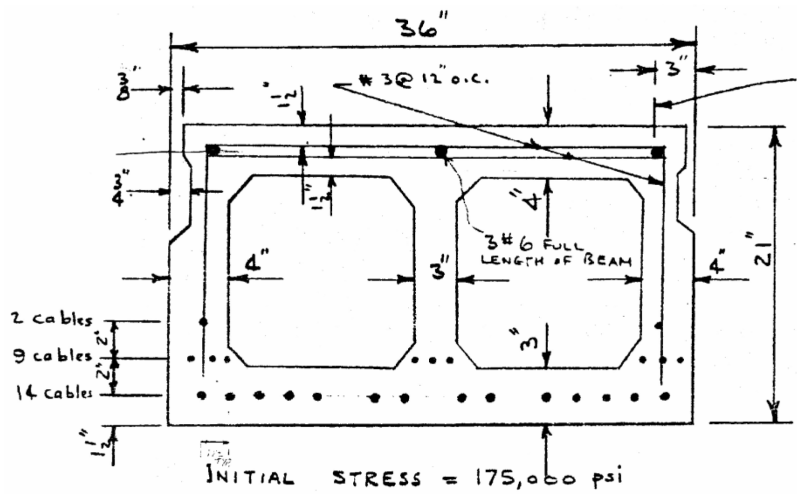

Figure 3-1. Typical box-beam section used in the 1950s

The beam was designed for the H-15-44 live load (Figure 3-2). Cross-section properties and the design parameters of the beam are given in Table 3-1. Concrete design strength was not specified on the plans. Michigan State Highway Department (MSHD) Specifications for Highway Bridges (1958) required 5000 psi ultimate concrete cylinder strength at 28 days for prestressed beams.

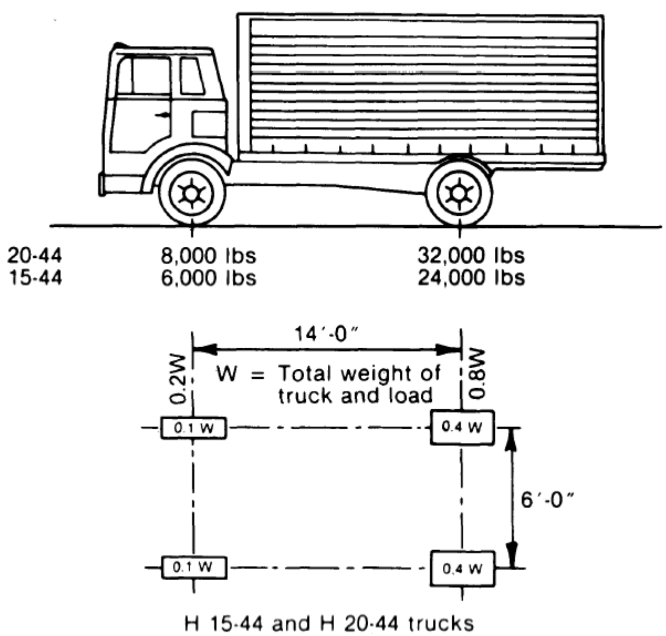

Figure 3-2. H-15-44 and H-20-44 vehicle configuration

Table 3-1. Beam Sectional Properties and Design Parameters used in 1957

Span length (in)	582
Beam length (in)	581.25
Beam span (distance between position dowels) (in)	568.25
Cross-sectional area, A (in^2)	407
Moment of inertia, I_c (in^4)	22,000
Weight of the beam (lb/ft)	424
Distance to top fiber, y_t (in)	10.21
Distance to bottom fiber, y_b (in)	10.79
Impact factor	0.291
Distribution factor	0.6×(wheel load)
Dead load moment M_{DL} (in-kip)	1,405
Live load moment M_{LL+I} (in-kip) (including impact factor and distribution factor)	1,450
Moment due to wearing surface M_{WS} (in-kips)	795
Total initial prestressing force P_i (kips)	350
Ultimate prestressing force, P_u (kips)	80% × (P_i)
Prestressing strand diameter (in)	3/8
Cross-sectional area of a strand, (in^2)	0.08
Center of gravity of strands, e (in)	8.15
Strand positions from bottom flange fiber (in)	14 @ 1.5 9 @ 3.5 2 @ 5.5

3.3 BEAM REMOVAL AND LOAD TESTING

On Monday September 25, 2006, I-94 west bound was closed at 9 p.m. for beam removal. E.C. Korneffel Co., of Trenton, Michigan was the contractor for beam removal and load testing. The Western Michigan University research team (at that time the research team was affiliated with Wayne State University) developed the load configuration and instrumentation layout. MDOT technicians installed the strain gauges, displacement transducers (DCDT), and cable actuated position sensors (CAPS) and also recorded the load test data.

3.3.1 Beam Removal Process

The contactor removed the bridge barriers of the fascia beam and saw cut the joint between the fascia and the interior beam (Photo 3-5). Lifting bracing was attached at the beam ends (Photo 3-6). Two cranes were used to lift the beam from its position. To avoid any possible damage to the beam during lifting, two hydraulic jacks were used to gently push the beam ends from the supports (Photo 3-7). The beam was lifted using two cranes, loaded onto a trailer, and transported to the test site (Photo 3-8 and Photo 3-9).

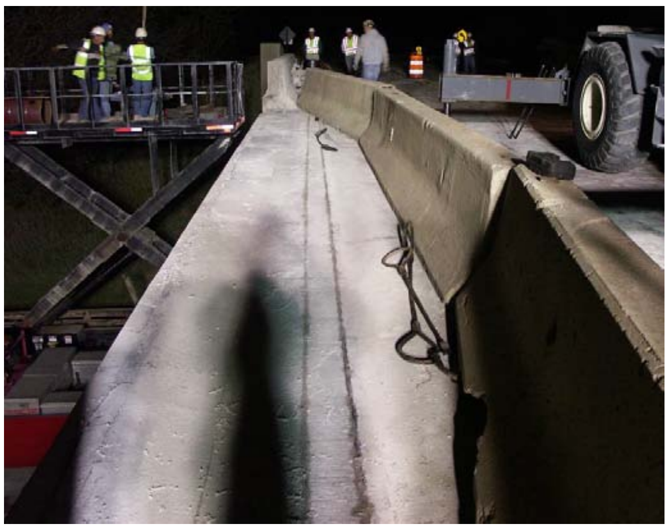

Photo 3-5. Saw cut at the exterior and interior beam joint

Photo 3-6. Lifting devices attached at the beam end

Photo 3-7. Force application using hydraulic jacks at both ends of the beam

Photo 3-8. Lifting of the beam using two cranes

Photo 3-9. Beam on the trailer before being transported to the test site

3.3.2 Instrumentation Layout

Shear strains within the end zones, flexural strains at the mid-span, vertical and horizontal deflections at the mid-span, and the support settlements were measured during load testing of the beam. Rosettes near the beam ends, uniaxial strain gauges at the mid-span, cable actuated position sensors at the mid-span, and displacement transducers (DCDT) next to the supports were mounted as shown in Figure 5-3 and Photo 3-10.

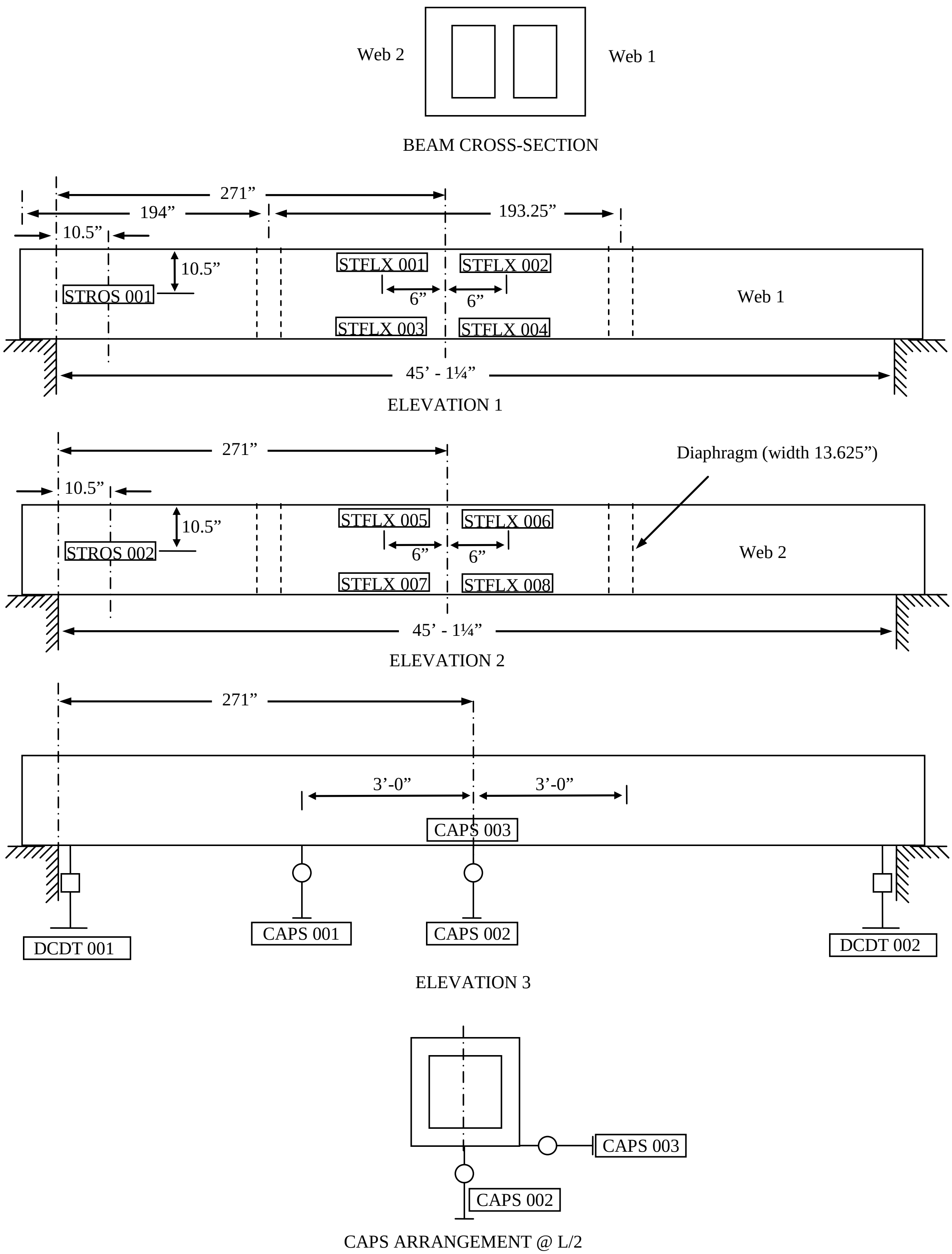

Figure 5-3. Instrumentation layout

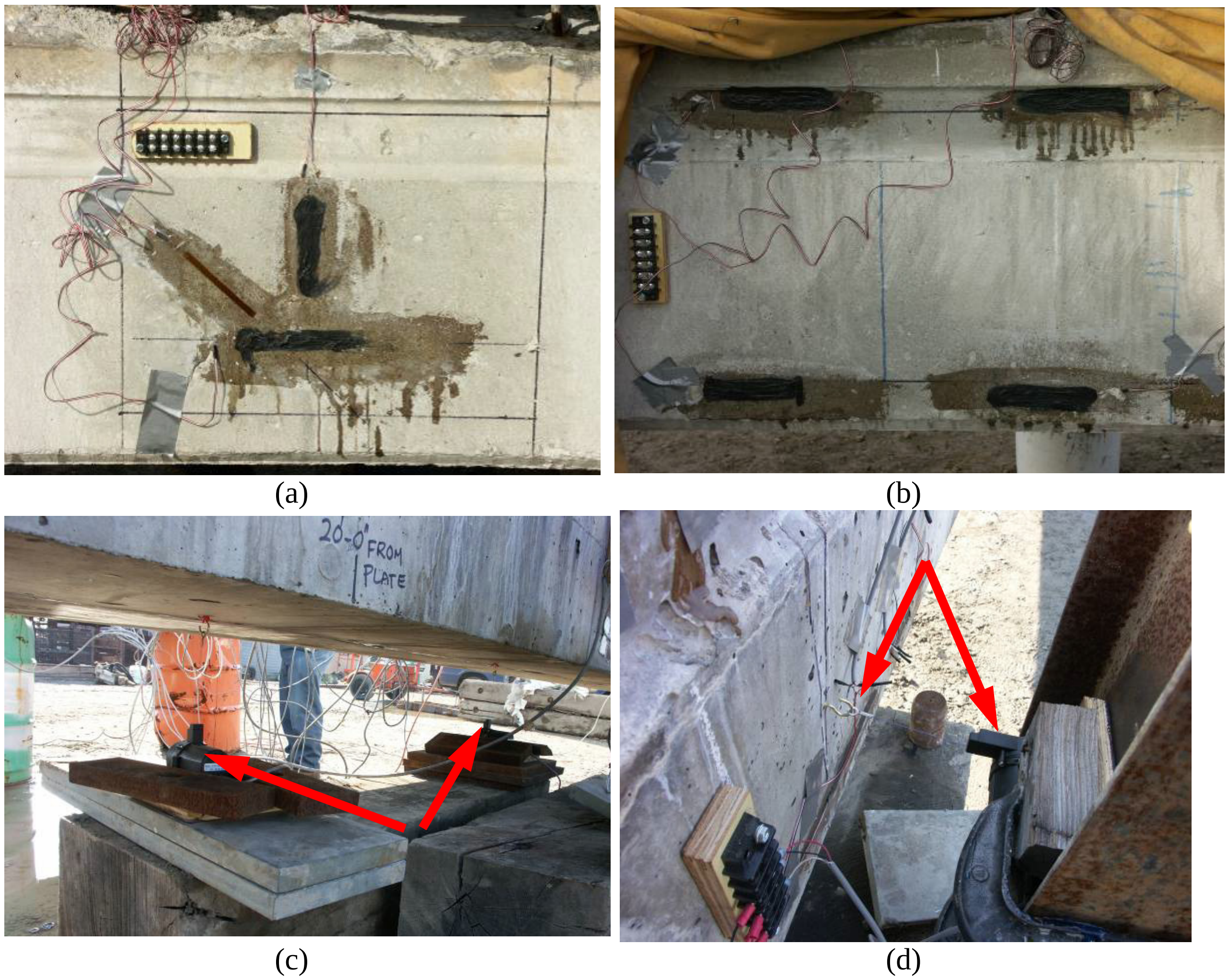

Photo 3-10. Strain gauges at (a) beam end and (b) mid-span and cable actuated position sensors at mid-span for (c) vertical and (d) horizontal displacement measurement.

3.3.3 Load Configuration

The cracking moment of the section was calculated as 399 k-ft using the concrete compressive strength of 5000 psi given in the MSHD (1958), and other data given in Table 3-1 and Table 3-2. Following Section 9.18.2 of the AASHTO Standard Specifications (2002) cracking moment was calculated.

A four-point bending test was performed (Figure 3-4). Because of the uncertainties involved in calculating flexural capacity of the distressed beam with unknown prestressing strand conditions and the observed distresses, it was decided to load the beam until flexural cracks initiation while closely monitoring the crack developments and recording loads, displacements, and strains. Once the flexural cracks developed and the moment on the beam exceeded the cracking moment capacity, the beam was loaded to failure without close monitoring. The load configuration was developed with the assumption that the flexural capacity of the beam should be 80% of the ultimate moment of the section. Section 9.17 of the AASHTO Standard Specifications (2002) was used for the ultimate moment capacity calculations.

Table 3-2. Moment Capacity of the Section

Concrete strength, (f_c'), psi	5000
Modulus of rupture, (f_r=7.5×(f_c')$^{1/2}$), psi	536
Section modulus, (S_c = I/y_b), in^3	2041
Effective prestress (i.e.,80% of initial prestress), ksi	140
Compressive stress of concrete due to effective prestress forces, (f_{pe}), psi	1810
Cracking moment, (M_{cr}), k-ft	399
Ultimate moment (M_u), k-ft	663

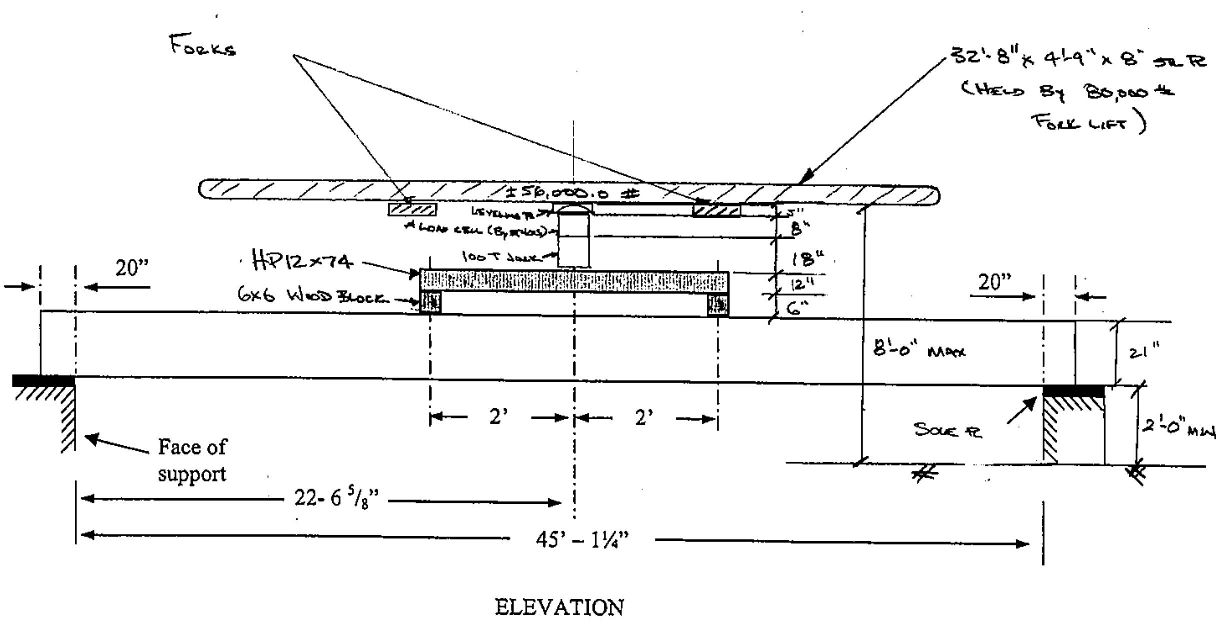

Figure 3-4. Load configuration developed by the contractor

Load testing was performed on November 13, 2006. Prior to conducting the load test, the beam camber was measured using a total station. During load testing the load was applied in 2 kips increments up to 20 kips; 1 kips increments from 20 to 30 kips; and 0.5 kips increments from 30 to 41 kips. After that the load was monotonically increased expecting to crush the beam. Due to limitations of the load application system, the maximum load applied to the beam was 51 kips. At 51 kips load, the resulting moment on the beam was about 80 percent of its ultimate capacity. Once the loads were removed, the beam deformations recovered. No signs of yielding in terms of permanent set were observed.

3.4 LOAD TESTING DATA ANALYSIS

3.4.1 Camber and Remaining Prestress

Camber measurement was performed using a total station, and the measurements are shown in Figure 3-5. Photo 3-11 shows the camber of the beam when it was placed at the test site.

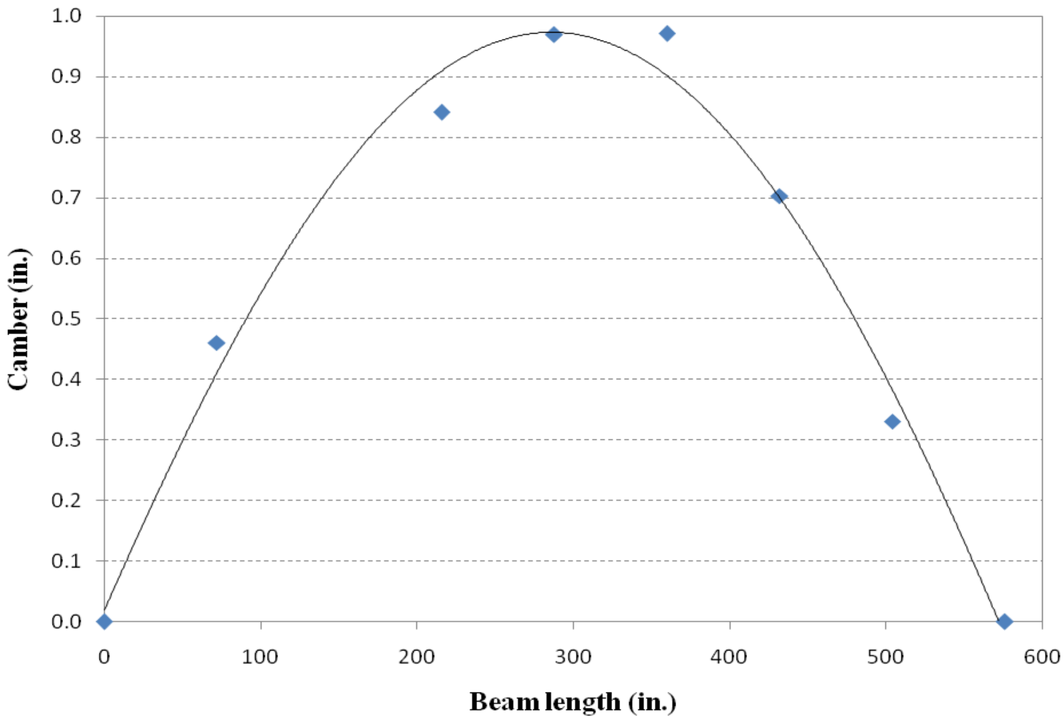

Figure 3-5. Variation of beam camber against length

Photo 3-11. Box-beam camber

Concrete material property tests were not performed. MSHD (1958) specifies the required concrete design strength as 5000 psi. According to Aktan et al. (2003), greater compressive strengths than 5000 psi were common in 1950s. Neglecting concrete material degradation, but not the strength development, a range of strength values was used for the calculations. The remaining prestress in the tendons are calculated as follows:

Concrete strength = 5000 – 7000 psi

Concrete modulus of elasticity = $57\sqrt{f_c'}$ ksi = 4030 – 4769 ksi

Beam camber (Δ_c) = 0.97 in.

Beam self weight deflection (Δ_d) = 0.64 – 0.54 in. (for f_c' = 5000 psi and 7000 psi)

Remaining prestress force = $[(\Delta_c + \Delta_d)\ 8EI/eL^2]$

= 413.7 – 459.3 kips (for f_c'= 5000 psi & 7000 psi)

Remaining stress = 206.8 – 229.7 ksi (25 strands -2.0 in^2.)

Initial prestress = 175 ksi

Prestress loss = 118 – 131 %

3.4.2 Cracking Moment and Remaining Prestress

As shown in Photo 3-12, two flexural strain gauges were attached to the bottom flange on each face of the beam at the mid-span. During load testing flexural cracks were documented as formed and marked on the beam faces near the mid-span bottom flange of the beam (Photo 3-12). Even though cracking sounds were heard during load application, the first flexural crack could not be noticed until the applied load reached 33 kips.

Photo 3-12. Flexural cracking at mid-span

Analysis of the data recorded by the strain gauges mounted near the bottom flange indicated that the first crack formed when the load was about 26.5 kips (Table 3-3). Based on the strain gauge data, the moment at mid-span due to applied load is 283 k-ft (Figure 3-6). The mid-span moment due to self weight of the beam was 125 k-ft. Thus the experimental cracking moment is calculated as 408 k-ft. As shown on Table 3-2, the analytical cracking moment of the section is 399 k-ft and correlates very well with the experimental data. The remaining prestress is calculated using Section 9.18.2 of AASHTO Standard Specifications (2002) as shown in Table 3-4. The remaining prestress for 5000 psi concrete corresponds to 82.6% of initial prestress.

Table 3-3. Load at Cracking – Strain Gauge Data

Strain Gauge	Load at Cracking (kips)
STFLX 003	26.5
STFLX 004	32.6
STFLX 007	30.9
STFLX 008	32.1

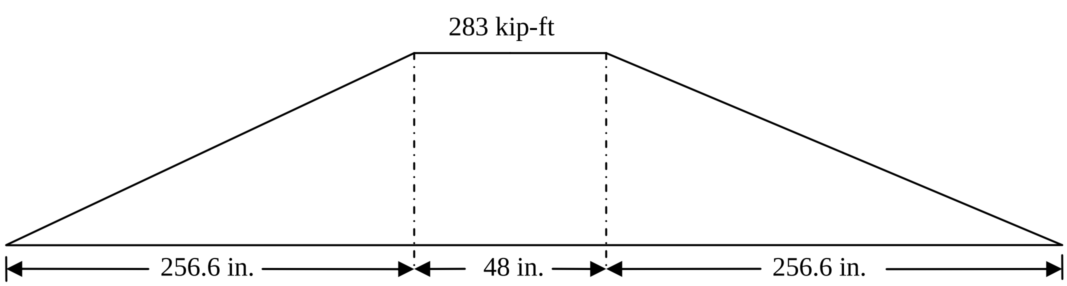

Figure 3-6. Moment due to applied load at cracking

Table 3-4. Remaining Prestress

Cracking Moment ft-kips	Effective Prestress Force P_{se}, kips		Remaining Prestress ksi	
	f_c' = 5000 psi	f_c' = 7000 psi	f_c' = 5000 psi	f_c' = 7000 psi
408	289	274	144.5 (82.6%)	137 (78.2 %)

The remaining prestress calculated using camber measurements ranges from 118 – 131 percent of initial prestress while the strain gauge readings yielded 78 – 83 percent. Prestress losses calculated using strain gauge data are in the order of 20 percent of initial prestress, which complies with the design assumptions. The use of camber measurements overestimates the remaining prestress by 40 – 50 percent.

3.4.3 Load Rating – Flexural Strength

Load rating was performed according to the MDOT Bridge Analysis Guide (2003). A concrete compressive strength of 5000 psi was used for the calculations. A live load distribution factor of 0.512 per wheel line load was calculated based on the AASHTO Standard (2002). It was also assumed that shear keys are functional and the tie rods are snug. Additional load rating was also performed assuming non-functional shear keys thus no load distribution between the beams (i.e., distribution factor = 1 per wheel line). Further, load rating was performed considering interior and exterior positions of the beam, assuming no load transfer. AASHTO Standard (2002) load distribution factors for interior and exterior beams are the same.

Table 3-5 summarizes the rating factors for interior/exterior beam with adequate load transfer as envisioned at the design stage. Table 3-6 and Table 3-7 summarize the rating results for an exterior and interior beam with no load distribution. When there is no load transfer, posting is required. The posting loads become considerably low when barrier loads are directly acting on the exterior beam with no load distribution. Table 3-8 summarizes the posting loads, recommended by MDOT in 1995, that were obtained from the bridge files.

Table 3-5. Bridge Load Rating (DF = 0.256 per lane; tons)

	Inventory Rating	Operating Rating			
		Federal Level	Michigan Legal Level		
			1 Unit	2 Unit	3 Unit
Flexural Strength	33.8	56.2	60	85	97

Table 3-6. Bridge Load Rating – Exterior Beam (DF = 0.5 per lane; tons)

	Inventory Rating	Operating Rating			
		Federal Level	Michigan Legal Level – Bridge should be Posted		
			1 Unit	2 Unit	3 Unit
Flexural Strength	10.6	17.6	15	16	22

Table 3-7. Bridge Load Rating – Interior Beam (DF = 0.5 per lane; tons)

	Inventory Rating	Operating Rating			
		Federal Level	Michigan Legal Level – Bridge should be Posted		
			1 Unit	2 Unit	3 Unit
Flexural Strength	18.4	30.5	25	28	38

Table 3-8. Bridge Posting Requirement in September 1995 (DF = 0.5 per lane; tons)

Michigan Legal Level – Bridge should be Posted		
1 Unit	2 Unit	3 Unit
33	42	47

3.4.4 Condition of Prestressing Strands

Corrosion stains were visible in the vicinity of the cracks at the bottom flange as seen in Photo 3-13a. Upon the completion of the load testing, the concrete was chipped away within the vicinity of cracks. There were no severed strands due to corrosion (Photo 3-13b).

(a)

(b)

Photo 3-13. Beam bottom flange condition (a) before and (b) after the testing was performed

3.4.5 Load Capacity of the Beam

Analysis results of the test data showed the longitudinal cracks on the bottom flange did not affect the flexural capacity of the beam. The beam was designed for H-15 loading following the guidelines given in MSHD (1958). The primary reason for rating and posting the bridge with similar beams would be due to non-functional shear keys. However, accurate assessment of load distribution is required to assure the safety of these bridges.

3.5 SUMMARY AND CONCLUSIONS

A 50-year old box-beam was removed from the bridge that carries Hawkins Road over I-94. This beam had severe longitudinal cracking at the beam soffit. After the Pennsylvania bridge beam collapsed in December 2005, there were concerns about the safety of similar bridges/beams. The beam was carefully removed, and load testing was performed. The following conclusions are drawn from the analysis results:

1. The bridge beam's experimental capacity was still in excess of its designed capacity. The beam, however, was designed for an H-15 which is lower than the current loads.
2. The use of camber measurements overestimates the remaining prestress by 40 – 50 percent.
3. A methodology needs to be developed for assessing load distribution of existing side-by-side box-beam bridges.
4. Concealed tendon corrosion evaluation and material characterization using nondestructive methods are essential for accurate safety assessment of distressed girders.

Intentionally left blank

4 EXPERIMENTAL PROCEDURE FOR DURABILITY STUDIES

4.1 INTRODUCTION

Task 4 of this study as outlined in Chapter 1 consists of experimental studies to determine the mechanical and durability properties of repair materials. Durability is a concern for design of new concrete structures as well as for repaired concrete structures. In order to design concrete repair for durability, different material parameters of the repair material as well as that of the concrete substrate need to be considered.

Vaysburd and Emmons (Beushausen and Alexander 2007) have stressed the importance of developing an integrated systems approach for concrete repair projects, including important design parameters such as environmental conditions, repair locations in the existing structure, its geometry, restraint, and nonuniformity, in connection with the specification of relevant material properties. Vaysburd (2006) also stresses the need for holistic approach to concrete repair since the repair process must successfully integrate new materials with old materials, forming a composite system capable of enduring exposure to service loads, exterior and interior (inside the structure) environments and time.

Figure 4-1 provides an overview of repair material characterization (based on Beushausen and Alexander 2007) required for ensuring long term performance of repaired structures. From a long term performance standpoint, a concrete repair must have adequate strength, resistance to freezing and thawing cycles, adequate transport properties and low susceptibility to cracking. It is important to relate individual material characteristics with the composite system as explained in Chapter 2.

A similar approach can be applied to shear key grout behavior. The literature review of Phase I of this project indicated that typically shear key grouts exhibit cracking at a very early age. It is essential to have a shear key grout that exhibits similar properties as those of the box beam to ensure a structurally stable composite element.

The overall goal of this task of this project was to analyze in detail commonly used polymer based repair materials commonly used for repair as well as evaluate shear key grouts used in construction of prestressed box beam bridges. The scope can be summarized as below:

1) Characterize individual material properties of common repair materials.
2) Establish key performance requirements for repair materials used for repair of prestressed concrete box beam bridges.
3) Determine the behavior of repair mortar in the fresh state
4) Determine the mechanical properties such as compressive strength and bond strength at various ages
5) Evaluate dimensional stability of repair mortars and shear key grouts by determining the shrinkage properties and cracking susceptibility of repair mortars and fatigue behavior of repair mortar and shear key grouts
6) Evaluation of long term durability of repair mortar and shear key grouts in terms of resistance to damage under freezing and thawing cycles, resistance to chloride ion penetration and rate of absorption of water
7) Evaluation of behavior of repair concrete under freezing and thawing cycles and fatigue by applying a 'systems approach'.

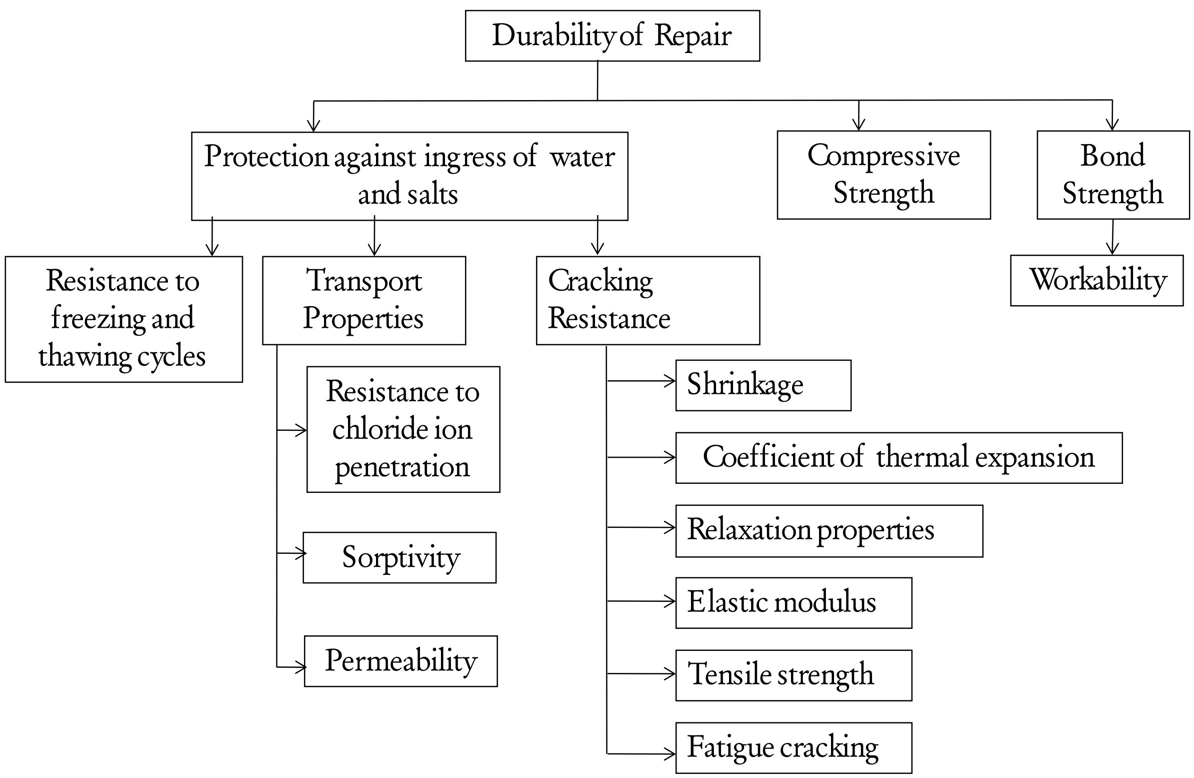

Figure 4-1. Characteristic material properties required for durable concrete repair

This chapter explains in detail the research plan adopted to study the durability and dimensional stability of selected repair materials and shear key grouts. Section 3.2 discusses the criteria adopted for the selection of available repair materials and shear key grouts. Information on the materials used in production of parent concrete is also provided in this section. Section 3.3 outlines the mixture proportions for the repair materials and the parent concrete whereas Section 3.4 provides information on test procedures adopted for this study. The testing regime included assessment of various fresh and hardened concrete properties such as slump or slump flow, setting time, rate of compressive strength development at various ages, drying shrinkage, cracking potential, freeze-thaw resistance and slant shear bond strength. The procedures adopted for preparation of combined specimens (repair material/parent concrete) are outlined in detail in Section 3.4.

4.2 MATERIALS

In this section, the materials used in the research program are described. Properties of the ingredients used in preparation of repair mortars, shear key grouts and the substrate concrete are specified below in Section 3.2.1 and 3.2.2, respectively.

4.2.1 Repair Materials and Shear Key Grouts

Based on the discussions held during the project progress meeting on May 4, 2007, four repair materials and three cements for shear key grouts were selected. There are many types of products and innumerable manufacturers of repair materials. Data sheets of various polymer based repair materials from different manufacturers were collected. An in-depth analysis of information provided by the manufacturer on the characteristics of the repair material was performed. To ensure a good sample size, the materials were chosen based on selection criteria involving:

- product approved by MDOT
- acceptable performance as indicated by a literature survey
- variability in manufacturer and chemical composition
- variability in elastic modulus of hardened repair concrete

The repair materials selected based on the above criteria include:

1) SikaRepair® SHA – According to the manufacturer, Sika®, SikaRepair® SHA is a fast-setting, one-component, cementitious based ready to use repair mortar. The repair material can be modified in to a polymer based repair mortar by addition of SikaLatex R instead of water. For this research, SikaLatex R will be used. SikaRepair® SHA is supplied in 50 lbs bags and the SikaLatex R is provided in 1 gallon plastic jug and provides a yield of 0.55 cu.ft/bag.
2) Sika Top®123*PLUS* - According to the manufacturer, Sika®, SikaTop ®123*PLUS*, is a two-component, polymer-modified, portland cement-based fast-setting, non-sag mortar. The cementitious component in addition to cement and small size aggregate also contains a penetrating corrosion inhibitor. The repair material is available in 44 lb bags while the liquid component is provided in a 1 gallon plastic jug; the two combined have a yield of 0.39 cu.ft/bag.
3) HB2 Repair Mortar – is a repair product manufactured by BASF. It is a two component polymer-modified high-build, lightweight repair mortar.
4) Conpatch V/O - Conpatch V/O is a single component, cement based, polymer modified repair mortar manufactured by Dayton Superior.

Material data sheets for the repair materials are included in Appendix A. Currently all shear keys are grouted using Type I Portland cement The cements selected for characterization of shear key materials were Type I Portland cement conforming to ASTM C 150, masonry cement Type M conforming to ASTM C 91 and SET 45. Type I cement is normally used by MDOT for shear key grouts in prestressed box beam bridges. Masonry cement and SET 45 were selected for evaluation so that these cements can be used as an alternative to Type I cement mortar currently used for shear key construction. SET 45 is magnesium phosphate based rapid-setting cement manufactured by BASF. The cement is supplied by the manufacturer in 50 lbs bags and is premixed with single size (~ 2mm diameter) siliceous aggregates.

4.2.2 Substrate Concrete

The substrate concrete necessary for preparing composite specimens was manufactured as per MDOT specifications. Information regarding materials and mixture proportion of concrete used for manufacturing box beam bridge components was obtained from local manufacturer of prefabricated prestressed box-beam elements. Type III Portland cement manufactured by

Lafarge Industries was used as the cementitious component of the mixture. The coarse and fine aggregate used in this study were conforming to MDOT 6A and 2NS, respectively. The physical properties of the aggregates are given in Table 3-1 whereas the gradation curve for coarse aggregate is shown in Figure 4-2 and for fine aggregate in Figure 4-3.

Table 4-1. Physical Properties of Aggregates used in Substrate Concrete

Physical Property	Coarse Aggregate	Fine Aggregate
Bulk Specific Gravity (Oven Dry)	2.69	2.62
Bulk Specific Gravity (Surface Saturated Dry (SSD))	2.69	2.63
Percent Absorption	1.2	1.8
Percent Moisture Content	1.8	1.9
Fineness Modulus	5.75	2.6

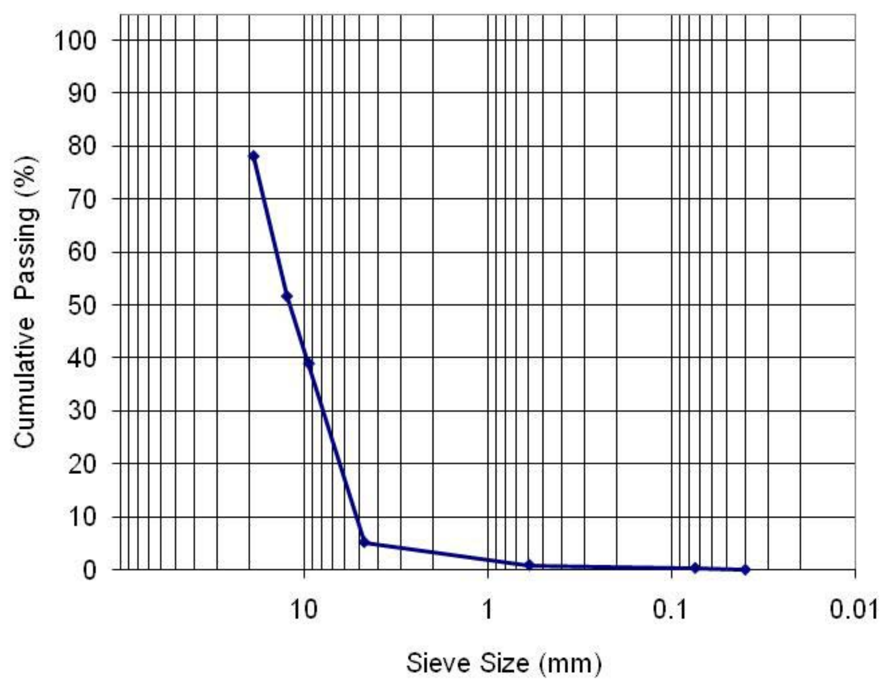

Figure 4-2. Gradation of coarse aggregates

Figure 4-3. Gradation of fine aggregates

4.3 MIXTURE PROPORTIONS AND MIXING

The mixture proportions for the repair materials and one shear key grout material selected as suggested by the manufacturer are given in Table 4-2. Mixing of the proportioned materials was carried out in a Hobart mixer as shown in Figure 4-4. The mixing process for this study was performed at the Benedict Laboratory of Michigan Technological University.

Figure 4-4. Hobart mixer used for mixing repair materials

Table 4-2. Mixture Proportions of Commercial Repair Products and Shear Key Materials

Product	Cementitious Component (A)	Liquid Component (B)	Quantity of (A) lb	Quantity of (B) Gallons
Sika Repair SHA	Sika Repair SHA	Sika Latex R	50	1
Sika Top 123 PLUS	Component A	Component B	44	1
HB 2 Mortar	HB 2 Mortar	Liquid	45	1
Conpatch V/O	Conpatch V/O	water	50	0.85
SET 45	SET 45	water	50	0.52

Repair mortar mixtures were prepared for evaluation in the laboratory without making any changes to the proportions suggested by the respective manufacturers. The amount of repair material mixed was governed by two factors - the mortar volume required to prepare specimens of a test as well as the time required for placing and consolidating the mortar in the molds. The time required for preparing the specimens was an important consideration because the selected repair materials have a very small window of time before the repair mortar starts to harden. Appendix B provides data on volume of material required for each test. Typically batch volumes of no more than 0.1 cu. ft was mixed at one time to ensure proper placing and consolidation before the repair mortar starts to harden. As a consequence the suggestion of all manufacturers about using one bag of repair material for mixing even if required volume is lower than the yield was not adopted in this study.

Three-fourths of the liquid was poured in the mixing container followed by the repair material. The mixture was then mixed continuously for three minutes with the mixer speed maintained at two. To ensure uniform consistency of mixing, the remaining liquid was added after two minutes of mixing.

The mixture proportion developed for shear key grout assessment using Type I cement and masonry cement is given in Table 4-3. The mixture proportions developed are as per MDOT R-2 mortar criteria (MDOT 2003). The fine aggregate used for these mixtures confirm to the MDOT gradation specified for Type 2 NS.

Table 4-3. Mixture Proportions for Shear Key Grout (R-2 mortar)

Ingredients	Specific gravity	Quantity (lb/cu.yd)
Cement (Type I/Masonry Cement)	3.15	930
Fine aggregate	2.63	1942
water	1.00	416
Air entraining admixture		1

Mixing was performed in a laboratory pan mixer as shown in Figure 4-5. Fine aggregate and air entraining agent were added initially to the mixer container and mixed for a minute. Cement and water were added next and mixed for five minutes.

Figure 4-5. Laboratory pan mixer

The mixture proportions for the substrate concrete to be used in testing the repair material's resistance to freezing and thawing cycles and fatigue specimens using Type III cement is outlined in Table 4-4. The mix design is representative of the mixture proportions approved by MDOT for construction of prestressed concrete box-beam girders.

Table 4-4. Mixture Proportions for Substrate Concrete

Ingredients	Specific gravity	Quantity (lb/cu.yd)
Cement (Type III)	3.15	600
Fine aggregate	2.63	1725
Coarse aggregate	2.69	1306
Water	1.00	230
Air entraining admixture		0.1
High-range water reducer		5.00

4.4 TEST METHODS AND REQUIREMENTS

Based on the literature review and evaluation of the data sheets of the selected repair materials, the following properties were selected as the key properties of the repair material that influence the long term performance of repair concrete:

1. Slump,
2. Air content,
3. Rate of strength gain,
4. Freeze-thaw durability,
5. Drying shrinkage,
6. Cracking potential,
7. Bond strength,
8. Chloride permeability,
9. Sorptivity, and
10. Coefficient of thermal expansion

Table 4-5 and Table 4-6 list the tests conducted to evaluate the above select material properties. The relevant standards adopted for conducting the test are also mentioned. In reviewing the data sheets of the selected repair materials (Appendix A) it was observed that none of them provided information on a performance criteria for material properties. All data sheets reviewed provide information on the test method and the performance of the material in a particular test. For this study, ASTM C 928 was adopted for comparing the performance of the repair materials for different properties.

Table 4-5. List of Tests for Repair Mortar and Shear Key Grout

Material Property	Type of Material	Test Method	Material Condition	# Specimens	# of Materials
Slump	RM	ASTM C 928	Fresh	1	4
	SK		Fresh	1	3
	Parent	ASTM C 143	Fresh	1	1
Air content	RM	ASTM C 928	Fresh	1	4
	SK		Fresh	1	3
	Parent	ASTM C 173	Fresh	1	1
Compressive Strength at the age of 24 h, 7 days and 28 days	RM	ASTM C 109	24 h, 7 days and 28 days	6	4
	SK		24 h and 28 days		3
	Parent		28 days		1
Slant Shear Bond Strength at 1 and 7 days	RM / Parent	ASTM C 882 and in-house	1 day/ 28 days	3	4
			7 days/ 28 days		
	SK / Parent		1 day/ 28 days		3
			7 days/28 days		
Resistance to freezing and thawing	RM	ASTM C 666 Procedure B	14 days	3	4
	RM / Parent		14/ 28 days		
	SK		14 days		3

Table 4-6. List of Tests for Repair Mortar and Shear Key Grout

Material Property	Type of Material	Test Method	Material Condition	# Specs.	# of Materials	% Complete
Free Shrinkage/ Length Change	RM	ASTM C 157	----	3	4	100
	SK				3	100
Chloride Permeability 28 days	RM	ASTM C 1202	28 days	2	4	50
Sorptivity[4]	RM	ASTM C 1585	28 days	2	4	100
Hardened concrete air content	RM	ASTM C 457	28 days	1	4	100
Restrained Ring Shrinkage Test	RM	AASHTO PP 34	----	3	4	50
Coefficient of thermal expansion	RM	AASHTO TP 60	7 days	2	4	50
	SK					50
	Parent					100
RM = repair material, SK = shear key grout, Parent = substrate concrete						

In this section the test procedures for measuring fresh and hardened concrete properties, deviation from approved test procedures if any, changes in curing regimes in comparison to those listed in relevant standards, requirements established for different tests, are specified in detail for the research program.

4.4.1 Slump

The workability of all repair materials and shear key grouts was measured in terms of slump of the concrete and the test was conducted as per ASTM C 143. The concrete/grout was poured in the slump cone in three layers. The material was rodded 25 times after each layer was poured.

4.4.2 Air Content

The air content of fresh concrete was measured as per ASTM C 231 for concrete/grout mixtures. Air content of hardened concrete was carried out as per ASTM C 457. One sample each was tested at the age of 28 days. Hardened concrete samples were sawed and polished before conducting the test. The procedure used here for the automatic characterization of the air-void system of hardened concrete works on the same principle of contrast enhancement and digital analysis first described in 1977 by Chatterji and Gudmundsson. The procedure used here can be broken into four basic steps:

A. Preparation of polished slabs
B. Black and white contrast enhancement procedure
C. Image collection
D. Automated ASTM C457

A) Each slab is trimmed to a width of 76 mm and a height of 100 mm to accommodate the dimensions of the retaining rings of the automated lapping equipment; a LapMaster with a 305 mm diameter grooved cast iron rotating lap with guide yokes. The slabs were ground flat using hand pressure on a water-cooled rotating wheel topped with a 60 grit metal-bonded diamond platen, followed by 24 minutes with an 800 grit SiC water slurry on the LapMaster. The flatness of the lap was monitored and maintained within ± 2.5 m. The surfaces were cleaned between steps with gentle pressurized water spray and a short ultrasonic water bath. The slabs were dried in a 50°C oven followed by the application of a 5:1 by volume solution of acetone and clear fingernail hardener, (New York Color brand 207A) (Roberts and Scali, 1984). The solution was brushed onto the lapped surfaces in two coats. After the hardener had set, the slabs were briefly polished using hand pressure on the water-cooled rotating iron wheel topped with 600 grit adhesive backed SiC paper, and cleaned as described previously.

B) Contrast enhancement was achieved by drawing slightly overlapping parallel lines with a wide tipped black permanent marker (Avery brand Marks-A-Lot). This was done in three coats, changing the orientation 90 between coats. After the ink dried, a few tablespoons of 2 m median size white powder (NYCO Minerals Inc. NYAD 1250 wollastonite) were worked into the samples using the flat face of a glass slide. A razor blade was used to scrape away excess powder, leaving behind powder pressed into voids. Residual powder was removed by wiping with a clean and lightly oiled fingertip. A fine tipped black marker (Sharpie brand) was used to darken voids in aggregates.

C) Each slab was scanned individually, and placed as near to the center of each flatbed scanners glass plate as possible. 8-bit grayscale, 3,175 dpi, (125 dpm, 8 x 8 m pixel) images were collected. A flat steel plate with applied black and white vinyl electrical tape was included at the top of each scan. The intensity distribution (histogram) of a population of 4 million pixels covering equal areas of the black and white tape was recorded for each scan in order to monitor variation in the gain of each scanners charged coupled device (CCD) array using Adobe Photoshop CS2 software enhanced with Reindeer Games Inc, Image Processing Toolkit 4.0 Plug In functions. To compensate for minor differences in gain between scans, a linear stretch was performed on the entirety of each scanned image.

D) A Visual Basic script developed at Michigan Technological University was used to compute paste volumes based on mix design information provided with the concrete samples according to the simple formula:

$$P=(100-A)[(Pm/Aggm)/(1-Pm/Aggm)] \tag{3-1}$$

where:

P = Vol. % paste in sample.

A = Vol. % air determined from automated procedure.

Pm = Paste volume computed from mix design.

Aggm = Aggregate volume computed from mix design.

Alternatively, the Visual Basic script also allows for paste content to be input directly for each sample. A third option available in the script allows for a manual point count to be performed on an image scanned from the polished sample before the black and white treatment. The script divides up the image into frames, and the operator answers either yes or no as to whether the cross-hairs fell on an aggregate particle or not. The paste volume is then computed according to the simple formula:

$$P = 100 - Agg - A \tag{3-2}$$

where:

Agg = Vol. % aggregate computed from point count data.

The script utilizes Adobe Photoshop CS2 to select the areas on the images to be analyzed, to extract the traverse lines, and to apply the threshold levels. The script also utilizes Microsoft Excel and Word to perform air-void calculations and to generate reports. The script has the option of whether or not to report an air-void chord length distribution.

4.4.3 Rate of Strength Gain

The compressive strength test for repair materials and shear key grouts was performed as per ASTM C 109 by casting samples in 2 x 2 in cubes. A total of 18 samples were cast for each repair material and shear key grout. The samples were prepared in two layers. The mortar was tamped in each cube compartment 32 times in about 10 s in 4 rounds, each round to be at right angles to the other and consisting of eight adjoining strokes over the surface of the specimen. Immediately after casting, the specimens were covered with a plastic sheet on the top to disallow moisture loss due to evaporation. The specimens were then demolded after 24 h after first addition of mixing liquid to the repair material. Six specimens were tested at age of 24 h. The other 12 specimens were placed in the moist room in Dillman Hall for curing. The specimens were removed from the moist room about 15 minutes prior to testing at ages 7 and 28 days. Specimens of SET 45 were not placed in the moist curing room since it is specified by the manufacturer that the material should not be moist cured.

The samples were subjected to compressive loading using the Tinius Olsen equipment located in Dillman Hall. The loading rate applied was between 250 to 300 lbs/s. The maximum failure load was recorded and the subsequently compressive strengths for the repair materials and shear key grouts were obtained.

The compressive strength test for substrate concrete was conducted as per ASTM C 39. Three 4 x 8 in. cylindrical specimens were cast in three layers of 2.5 in. each. The concrete was consolidated by tamping 25 times after placement of each layer. The specimens were covered with a lid on top after consolidation to avoid any water loss due to evaporation. The samples were demolded after 24 h after the first addition of water to the ingredients and placed in the moist cure room for curing purposes. The compressive strength test was performed at the age of 28 days.

The compressive strength test was performed on the Baldwin compressive strength testing equipment in Benedict Laboratory. The rate of loading for testing the substrate concrete specimen was 35 psi/s.

4.4.4 Slant Shear Bond Strength

The slant shear bond strength was performed as per ASTM C 882. The test set-up consists of repair mortar applied to substrate mortar to establish a 3 x 6” cylinder as shown in Figure 4-6.

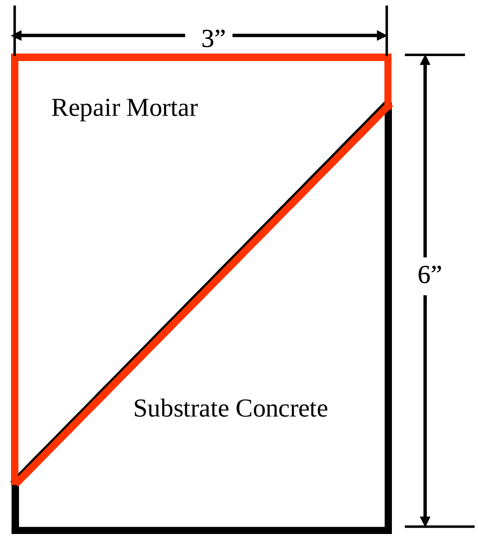

Figure 4-6. Cross-section of slant shear bond strength test set-up

To prepare the substrate concrete samples, initially a dummy sample was required. For this purpose an aluminum cylindrical rod was cut as per the dimension specified in ASTM C 882. The cut specimen was then placed in a 3 x 6” cylinder and this set-up was used as a mold to prepare the dummy samples. Five dummy samples were prepared using epoxy. Substrate concrete samples using Type III cement and mixture proportions as per ASTM C 882 were prepared by using the dummy samples in place of the repair mortar. The substrate concrete samples were cured for 28 days. The substrate concrete sample was then placed in a 3 x 6” cylinder and the repair concrete was cast against the substrate concrete. The combined specimen was demolded after 24 h.

The slant shear bond strength test was performed using the Tinius Olsen testing equipment. The rate of loading applied to the specimen was 200 lbs/s.

4.4.5 Resistance to Freezing and Thawing Cycles

The samples for evaluating the resistance of the selected repair materials and shear key grouts to freezing and thawing cycles was performed as per the ASTM C 666 *Procedure B.* Two types of samples of repair materials were prepared to ascertain the behavior of the selected materials.

One type of sample consisted of the repair material or the shear key grout only. The samples were cast in 3 x 3 x 16 in. molds in three layers and tamped 25 times after each layer was placed. The samples were demolded 24 h after the first addition of water and placed in moist curing room for 14 days. After 14 days the samples were removed from the moist curing room and the dynamic modulus was measured before placing each sample in the freeze thaw chamber. The samples were placed in the freeze-thaw machine for 300 cycles. Subsequently the samples were removed every 30 cycles to measure the dynamic modulus. Three samples of every repair material and shear key grout were tested under this regime.

The second type of sample was prepared as a combined specimen, one half of which was made of substrate concrete whereas the other half was made of the repair material. For the measurement of resistance to freezing and thawing of repair materials when cast on substrate concrete, initially specimens of the substrate concrete were prepared and cured for 14 days at temperature of 105-120°F to accelerate curing. The samples were split in the middle by applying a 3-point bending load as shown in Figure 4-7. The exposed surface of the sample was further prepared by using a chisel and hammer as shown in Figure 4-8 to simulate a roughened surface similar to that found in the field. The substrate sample was then placed in the mold and the repair concrete was placed in the remaining space. The final samples were demolded at 24 h after first addition of water to the repair material and cured for 14 days before being placed in the freeze-thaw chamber. Two samples of every repair material were tested under this regime.

Figure 4-7. Set-up used for splitting of the substrate concrete specimen for freeze-thaw testing

Figure 4-8. Surface preparation of the substrate concrete specimen

The dynamic modulus was measured in the same way as explained earlier. The samples were removed after every 30 cycles to measure the change in modulus.

4.4.6 Measurement of Free Shrinkage

The free shrinkage of repair materials was evaluated as per ASTM C 157. Six samples of each repair mortar and shear key grout of size 1 x 1 x 12 in. were cast. The samples were demolded 24 h after addition of water to the mortar. Two types of conditioning methods were adopted in this test. Three samples were cured in a humidity chamber having 100% humidity at 73°F whereas the other three samples were cured in an environmental chamber with 50% relative humidity (RH) at 73°F. The first measurement was taken 24 h after preparation of samples after which the samples were moved to different curing conditions as described earlier. Thereafter, measurements were taken every 24 h for 28 days from time of first addition of water.

4.4.7 Sorptivity

The measurement of rate absorption (sorptivity) of water by repair mortar and shear key grouts was conducted as per ASTM C 1585 by measuring the increase in the mass of a specimen resulting from absorption of water as a function time when only one surface of the specimen is exposed to water.

Cylinders of size 4 x 8 in. were cast as per ASTM C 192 and cured in moist curing room for 28 days. The cylinders were then removed from the curing room and cut using a water saw. The middle 2 in. of the cylinder was taken for the test as shown in Figure 4-9.

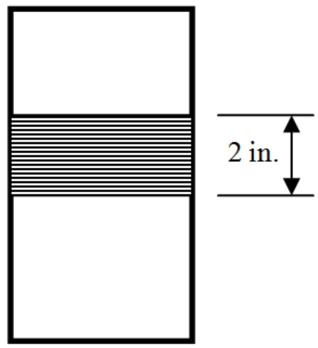

Figure 4-9. Diagrammatic sketch of sample location for sorptivity test

The two samples of size 2 x 4 in. were then placed in desiccators at a temperature of 122°F and RH of 80 $\pm$ 3% for three days. The desired relative humidity was achieved by placing a petri dish with potassium bromide solution in the bottom of the desiccator. The solution was maintained at a saturation point as stated in ASTM C 1585. The samples were removed from the desiccator after 3 days and placed in a sealable container. The containers were stored at 73°F for 15 days before performing the test. The samples were removed from the containers and the cylindrical part was coated with epoxy. The diameter of the surface exposed to water was measured and the sample then placed in a tub on two small supports so as to maintain the level of water 1 to 3 mm above the top of the support device. Change in mass of the specimen was observed for 9 days as per the standard.

4.4.8 Cracking Susceptibility

The cracking susceptibility of repair materials was evaluated as per AASHTO PP 34. The test set-up for measurement of cracking susceptibility through restrained shrinkage ring testing is elaborated in this section. A special environmental controlled chamber (50% RH and 73°F) was built for testing of the specimens. Steel rings as per AASHTO PP 34 were prepared and strain gages were mounted on the inside of the ring to monitor strains developed in the repair mortar. The strain gages with 120.0 $\pm$ 0.3% resistance and 2.08 nom gage factor were manufactured by Vishay Measurements Group. Figure 4-10 shows the test set up developed in the environmental controlled chamber.

Figure 4-10. Environmental control chamber with ring specimen

The Michigan Tech laboratory has a data logger MEGADAC 3451 AC manufactured by Optim Electronics as shown in Figure 4-11. The data is collected by the data acquisition system through TCS software which is supplied by Optim Electronics. The data logger had been procured about 10 years ago and had not previously set up for data collection for measuring the cracking susceptibility.

Figure 4-11. Data logger used for data collection from ring specimens

The rings were cast using six batches of repair mortar. Because the repair mortar tends to start setting quickly, tamping and consolidation was performed using a putty knife and pressing by hand. The rings were connected to the data logger within 20 minutes of mixing and placing. The outer mold ring was removed after 24 h. The ring was covered with plastic sheathing to avoid drying due to evaporation.

4.4.9 Coefficient of Thermal Expansion

Two 4 x 8 in. cylindrical samples of size of repair materials were cast and cured for 5 days. The coefficient of thermal expansion was measured as per AASHTO TP 60-00 (2004) using the PINE equipment in Benedict Laboratory. The top half-inch and bottom half- inch was then sawed using a kerosene saw to get the required test size of 4 x 7 in. The samples were then placed in water for 24 h so as to achieve constant weight.

The sample was then placed in the water bath of the equipment. One test cycle (one heating segment and one cooling segment) lasted approximately 24 hours. However, several specimens required longer to test to meet the AASHTO specification for successive CTE values (difference of no more than 0.5 micro strain/°F (0.3 micros strain/°C) between successive CTE values). Those samples which required longer testing time are listed in the chapter detailing the results and analysis of different tests

.

5 RESULTS AND ANALYSIS FROM DURABILITY STIDIES

5.1 FRESH AND HARDENED PROPERTIES OF REPAIR MATERIALS AND SHEAR KEY GROUTS

The fresh and hardened concrete properties evaluated for the different materials are listed in Table 5-1 through Table 5-7. The measured average value obtained in the lab for various material properties evaluated is compared with those listed in the data sheet of the relevant manufacturer if available. Coefficient of variation (COV) for test data is shown in brackets wherever applicable. Discussion of the different material properties is complied in the sections below.

5.2 SLUMP

The slump of the repair materials was zero due to extremely stiff mixtures and low workability. Among all repair materials, HB2 Repair Mortar was extremely stiff right after completion of mixing. The slump of the shear key grouts was between 7-8 in. and is provided in Table 5-5 through Table 5-7. No reference value was provided by the manufacturer of SET 45 and MDOT also does not have a minimum slump value for shear key grouts. The slump values of 8, 7 and 8 in. for SET 45, Type I cement grout and masonry cement grout, respectively, indicate that the grouts had sufficient workability and would lead to dense hardened mortar when properly consolidated.

5.3 AIR CONTENT

As explained in the note provided at the end of Table 5-7, the air content for repair materials and SET 45 was not measured due to its tendency to set rapidly (Refer Appendix A for manufacturer's data sheet for setting time values). It was observed that all commercial repair materials and shear key grouts used in this study lost workability and became stiff in about 10 minutes after the addition of water. The air content in the fresh state for Type I cement grout and masonry cement are within the MDOT requirements specified of 14+4.

Table 5-1. Test Results for SikaTop123® Plus

Test	Measured Value			Manufacturer's Data Sheet		
Slump (in.)	0			N/A		
Air content (%, fresh state)	N/A[1]			N/A		
Compressive Strength at the age of 1, 7 and 28 days (psi)	**1 day**	**7 days**	**28 days**	**1 day**	**7 days**	**28 days**
	3500 *(7.71)*	5381 *(7.91)*	6712 *(2.81)*	3500	6000	7000
Slant Shear Bond Strength at 1 and 7 days (psi)	**1 day**	**7 days**		**28 days**		
	1005 *(1.98)*	1298 *(1.85)*		2200		
Freeze/thaw Resistance @ 300 cycles (%, RDM)	96.5 %			98 %		
Free Shrinkage (micro strains) @ 90 days	100 % RH	50 % RH		N/A		
	450	1440				
Chloride permeability 28 days	504 Coulombs (100-1,000 very low)			500 Coulombs		
Sorptivity	Initial Absorption	Secondary Absorption		N/A		
	5.5×10^{-6}	8.0×10^{-7}				
Hardened concrete air content at 28 days	10.7 %			N/A		
Restrained Ring Shrinkage Test	First test specimen cracked in 8.7 days and second in 6.7 days			N/A		
Coefficient of thermal expansion (mm/mm/°C)[3]	18.88×10^{-6}			N/A		

Table 5-2. Test Results for SikaRepair®SHA

Test	Measured Value			Manufacturer's Data Sheet		
Slump (in.)	0[1]			N/A		
Air content (%, fresh state)	N/A[1]			N/A		
Compressive Strength at the age of 1, 7 and 28 days (psi)	**1 day**	**7 days**	**28 days**	**1 day**	**7 days**	**28 days**
	2530 *(6.06)*	4090 *(8.37)*	6205 *(6.88)*	2500	3500	5000
Slant Shear Bond Strength at 1 and 7 days (psi)	**1 day**	**7 days**		**28 days**		
	876 *(3.75)*	1166 *(2.7)*		1800		
Freeze/thaw Resistance @ 300 cycles (%, RDM)	86 %			N/A		
Free Shrinkage (micro strains) @ 90 days	100 % RH	50 % RH		N/A		
	86	1200				
Chloride permeability 28 days	800 Coulombs (100-1,000 very low)			N/A		
Sorptivity (mm/√s)	Initial Absorption	Secondary Absorption		N/A		
	3×10^{-6}	5.0×10^{-7}				
Hardened concrete air content at 28 days	12.43 %			N/A		
Restrained Ring Shrinkage Test	First specimen did not crack within 28 days			N/A		
Coefficient of thermal expansion (mm/mm/°C)[3]	14.80×10^{-5} *(5.13)*			N/A		

Table 5-3. Test Results for HB2 Repair Mortar

<table>
<tr><th>Test</th><th colspan="3">Measured Value</th><th colspan="3">Manufacturer's Data Sheet</th></tr>
<tr><td>Slump (in.)</td><td colspan="3">0[1]</td><td colspan="3">N/A</td></tr>
<tr><td>Air content (%, fresh state)</td><td colspan="3">N/A[1]</td><td colspan="3">N/A</td></tr>
<tr><td rowspan="2">Compressive Strength at the age of 1, 7 and 28 days (psi)</td><td>1 day</td><td>7 days</td><td>28 days</td><td>1 day</td><td>7 days</td><td>28 days</td></tr>
<tr><td>2535 (10.43)</td><td>4766 (3.32)</td><td>6538 (3.65)</td><td>2300</td><td>4500</td><td>5800</td></tr>
<tr><td rowspan="2">Slant Shear Bond Strength at 1 and 7 days (psi)</td><td colspan="2">1 day</td><td>7 days</td><td colspan="2">7 days</td><td>28 days</td></tr>
<tr><td colspan="2">336 (7.98)</td><td>1146 (6.67)</td><td colspan="2">2100</td><td>2700</td></tr>
<tr><td>Freeze/thaw Resistance @ 300 cycles (% RDM)</td><td colspan="3">See Note[4]</td><td colspan="3">N/A</td></tr>
<tr><td rowspan="2">Free Shrinkage (micro strains) @ 90 days</td><td colspan="2">100 % RH</td><td>50 % RH</td><td colspan="3" rowspan="2">350 (does not specify RH)</td></tr>
<tr><td colspan="2">1420</td><td>1360</td></tr>
<tr><td>Chloride permeability 28 days (Coulombs)</td><td colspan="3">1012
(100-1,000 very low)</td><td colspan="3">N/A</td></tr>
<tr><td rowspan="2">Sorptivity (mm/√s)</td><td colspan="2">Initial Absorption</td><td>Secondary Absorption</td><td colspan="3" rowspan="2">N/A</td></tr>
<tr><td colspan="2">6.0×10^{-7}</td><td>8.0×10^{-7}</td></tr>
<tr><td>Hardened concrete air content at 28 days</td><td colspan="3">33.5%</td><td colspan="3">N/A</td></tr>
<tr><td>Restrained Ring Shrinkage Test</td><td colspan="3">See Note[4]</td><td colspan="3">N/A</td></tr>
<tr><td>Coefficient of thermal expansion (mm/mm/°C)[3]</td><td colspan="3">10.88×10^{-6} (11.71)</td><td colspan="3">8.1×10^{-6}</td></tr>
</table>

Table 5-4. Test Results for Conpatch VO

Test	Measured Value			Manufacturer's Data Sheet		
Slump (in.)	0[1]			N/A		
Air content (%, fresh state)	N/A[1]			N/A		
Compressive Strength at the age of 1, 7 and 28 days (psi)	**1 day**	**7 days**	**28 days**	**1 day**	**7 days**	**28 days**
	4805 *(9.21)*	6145 *(1.99)*	9688 *(5.25)*	4500	7000	8000
Slant Shear Bond Strength at 1 and 7 days (psi)	**1 day**	**7 days**		NA		
	1067 *(0.31)*	1356 *(0.92)*				
Freeze/thaw Resistance @ 300 cycles (% RDM)	98.7			96		
Free Shrinkage (micro strains) @ 90 days	100 % RH	50 % RH		N/A		
	290	713				
Chloride permeability 28 days (Coulombs)	970 (100-1,000 very low)			430		
Sorptivity (mm/√s)	Initial Absorption	Secondary Absorption		N/A		
	7.5×10^{-6}	3.0×10^{-6}				
Hardened concrete air content at 28 days	7.6 %			N/A		
Restrained Ring Shrinkage Test	Rings cracked after 1.6 and 2.3 days of casting			N/A		
Coefficient of thermal expansion (mm/mm/°C)[3]	13.66×10^{-6} *(0.79)*			4.4×10^{-6}		

Table 5-5. Test Results for SET® 45

<table>
<tr><th>Test</th><th colspan="6">Measured Value</th><th colspan="6">Manufacturer’s Data Sheet</th></tr>
<tr><td>Slump (in.)</td><td colspan="6">8</td><td colspan="6">N/A</td></tr>
<tr><td>Air content (%, fresh state)</td><td colspan="6">N/A[1]</td><td colspan="6">N/A</td></tr>
<tr><td rowspan="2">Compressive Strength at the age of 1, 7 and 28 days (psi)</td><td colspan="2">1 day</td><td colspan="2">7 days</td><td colspan="2">28 days</td><td colspan="2">1 day</td><td colspan="2">7 days</td><td colspan="2">28 days</td></tr>
<tr><td colspan="2">4330 (7.85)</td><td colspan="2">5382 (7.91)</td><td colspan="2">6688 (4.62)</td><td colspan="2">6000</td><td colspan="2">7000</td><td colspan="2">8500</td></tr>
<tr><td rowspan="2">Slant Shear Bond Strength at 1 and 7 days (psi)</td><td colspan="3">7 days</td><td colspan="3">28 days</td><td colspan="6" rowspan="2">NA</td></tr>
<tr><td colspan="3">1513 (2.63)</td><td colspan="3">1900 (0.73)</td></tr>
<tr><td>Freeze/thaw Resistance @ 300 cycles (% RDM)</td><td colspan="6">82</td><td colspan="6">80</td></tr>
<tr><td rowspan="2">Free Shrinkage (micro strains) @ 90 days</td><td colspan="3">100 % RH</td><td colspan="3">50 % RH</td><td colspan="6" rowspan="2">N/A</td></tr>
<tr><td colspan="3">750</td><td colspan="3">128</td></tr>
<tr><td rowspan="2">Sorptivity (mm/√s)</td><td colspan="3">Initial Absorption</td><td colspan="3">Secondary Absorption</td><td colspan="6" rowspan="2">N/A</td></tr>
<tr><td colspan="3">3.0×10^{-5}</td><td colspan="3">3.0×10^{-6}</td></tr>
<tr><td>Hardened concrete air content</td><td colspan="6">11.13 %</td><td colspan="6">N/A</td></tr>
<tr><td>Coefficient of thermal expansion (mm/mm/°C)[3]</td><td colspan="6">12.48×10^{-6} (1.14)</td><td colspan="6">4.4×10^{-6}</td></tr>
</table>

Table 5-6. Test Results for Type I Cement Grout

<table>
<tr><th>Test</th><th colspan="6">Measured Value</th><th colspan="3">MDOT</th></tr>
<tr><td>Slump (in.)</td><td colspan="6">7</td><td colspan="3">N/A</td></tr>
<tr><td>Air content (%, fresh state)</td><td colspan="6">13.5</td><td colspan="3">14 ± 4</td></tr>
<tr><td rowspan="2">Compressive Strength at the age of 1, 7 and 28 days (psi)</td><td colspan="2">1 day</td><td colspan="2">7 days</td><td colspan="2">28 days</td><td>1 day</td><td>7 days</td><td>28 days</td></tr>
<tr><td colspan="2">4017 (5.44)</td><td colspan="2">4269 (8.53)</td><td colspan="2">4905 (2.59)</td><td>N/A</td><td>N/A</td><td>N/A</td></tr>
<tr><td rowspan="2">Slant Shear Bond Strength at 1 and 7 days (psi)</td><td colspan="3">7 day</td><td colspan="3">28 days</td><td colspan="3" rowspan="2">NA</td></tr>
<tr><td colspan="3">1043 (4.85)</td><td colspan="3">1402 (1.18)</td></tr>
<tr><td>Freeze/thaw Resistance @ 300 cycles (% RDM)</td><td colspan="6">99 %</td><td colspan="3">NA</td></tr>
<tr><td rowspan="2">Free Shrinkage (micro strains) @ 90 days</td><td colspan="3">100 % RH</td><td colspan="3">50 % RH</td><td colspan="3" rowspan="2">N/A</td></tr>
<tr><td colspan="3">150</td><td colspan="3">720</td></tr>
<tr><td rowspan="2">Sorptivity (mm/√s)</td><td colspan="3">Initial Absorption</td><td colspan="3">Secondary Absorption</td><td colspan="3" rowspan="2">N/A</td></tr>
<tr><td colspan="3">2.5×10^{-5}</td><td colspan="3">8.0×10^{-6}</td></tr>
<tr><td>Hardened concrete air content</td><td colspan="6">11.25 %</td><td colspan="3">N/A</td></tr>
<tr><td>Coefficient of thermal expansion (mm/mm/°C)[3]</td><td colspan="6">10.32×10^{-6} (6.23)</td><td colspan="3">N/A</td></tr>
</table>

Table 5-7. Test Results for Masonry Cement Grout

Test	Measured Value			MDOT		
Slump (in.)	8			N/A		
Air content (%, fresh state)	10.5			14 $\pm$ 4		
Compressive Strength at the age of 1, 7 and 28 days (psi)	**1 day**	**7 days**	**28 days**	**1 day**	**7 days**	**28 days**
	2441 *(12.86)*	3450 *(1.87)*	4500 *(0.89)*	NA	NA	NA
Slant Shear Bond Strength at 1 and 7 days (psi)	**7 day**	**28 days**		NA		
	924 *(2.30)*	1146 *(2.09)*				
Freeze/thaw Resistance @ 300 cycles (% RDM)	98 %			N/A		
Free Shrinkage (micro strains) @ 90 days	100 % RH	50 % RH		N/A		
	350	610				
Sorptivity (mm/√s)	Initial Absorption	Secondary Absorption		N/A		
	3.0×10^{-5}	3.0×10^{-6}				
Hardened concrete air content	8.432			N/A		
Coefficient of thermal expansion (mm/mm/°C)[3]	9.57×10^{-6} *(2.38)*			N/A		

Notes:

1. *The measurement of air content in the fresh state was not performed for repair mortars due to its rapid hardening characteristic which hindered the testing process.*
2. *Test values for two samples tested at 7 and 9 days are provided. Detailed explanation provided in Section 4.8.*
3. *HB2 Repair Mortar samples were not cast for this test.*

5.4 COMPRESSIVE STRENGTH

The rate of compressive strength gain was measured for repair materials as well as shear key grouts at the ages of 1, 7 and 28 days. Six samples were tested for each age for each repair material and shear key grout. Individual results are supplied in Appendix C, whereas the analysis of mean compressive strengths is provided in this section. The mean compressive strength was calculated as per ASTM C 109 whereas the acceptance criteria adopted was as per ASTM C 109. Figure 5-1 shows a comparison of the compressive strength results at various ages for all repair materials with respect to the manufacturer's data sheet as well as ASTM C 928 minimum.

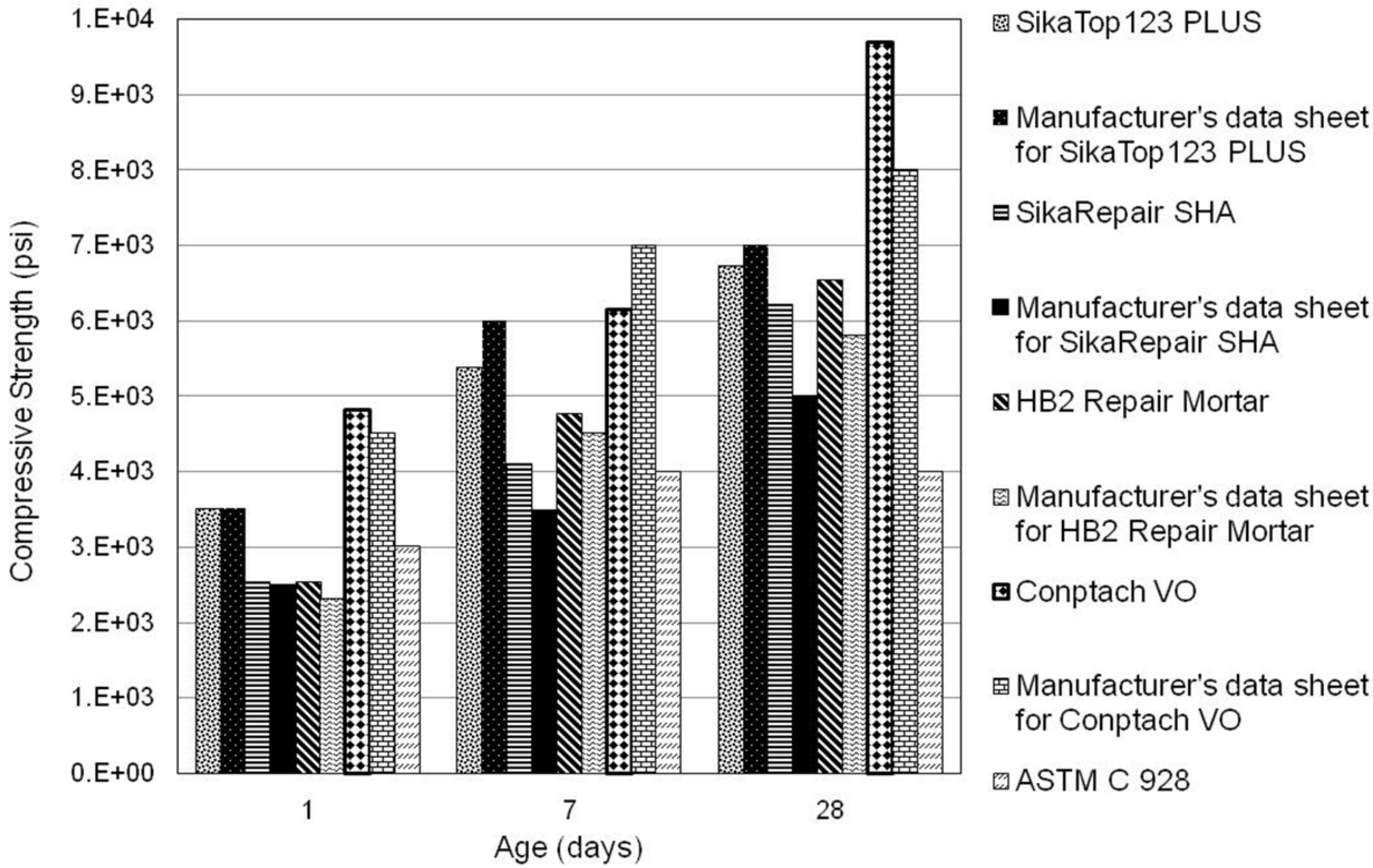

Figure 5-1. Compressive strength at various ages for repair materials

As shown in Figure 5-1, the compressive strength at 1 day was less than that specified by ASTM C 928. The coefficient of variation for all ages was between 6 to 8.5 % for Sika Repair® SHA. In case of HB2 Repair Mortar, the 1-day strength was lower than that stipulated by ASTM C 928. The COV for 1-day strength was also high (10.43). Amongst all repair materials evaluated, Conptach VO exhibited the highest compressive strength results at all ages. The 7 days strength of Conpatch VO as measured in this study was lower than that stipulated in the manufacturer's data sheet. From Figure 5-1 it can be observed that SikaTop 123®PLUS exhibited lower compressive strengths at 7 and 28 days in comparison to that stated by the manufacturer. The coefficient of variation (COV) of strengths at 7 days is higher (7.91) compared to that at 28 days (2.81). Compressive strengths at all ages for SikaTop 123®PLUS were above those required as per ASTM C 928. Sika Repair® SHA exhibited lowest compressive strength values amongst all the repair materials evaluated in this study.

Table 5-8 provides information on the percent increase of compressive strengths at ages 7 days and 28 day relative to the 1-day strength of the repair material. It can be observed that the highest increase in strength values is observed for HB2 Repair Mortar followed by Sika Repair SHA and Sika Top 123 PLUS. In the literature review it was discussed that the compressive strength of repair concrete/ mortar should be greater than or equal to the compressive strength of the substrate concrete. Based on the analysis in Figure 5-1 and Table 5-8, it can be concluded that for repair purposes of substrate concrete with compressive strength of 6000 psi or more, any of the repair materials evaluated in this study can be used based on the 28 day strength. Early age strengths are an important factor for rehabilitation projects because it is essential to open the bridge to traffic as soon as possible. If downtime is a factor in the decision of using a particular repair material, this study indicates that Sika Repair SHA and HB2 Repair Mortar have lower early age strengths but gain a higher percentage of strength at later ages.

Table 5-8. Percent Increase in Compressive Strength over Different Ages

Material	Percent Increase over 1 –day Compressive Strength	
	7–day (%)	28–day (%)
SikaTop 123® PLUS	35	48
Sika Repair® SHA	38	59
Conpatch VO	22	52
HB2 Repair Mortar	47	61

Figure 5-2 shows the graphical presentation of development of compressive strength at various ages for the shear key grouts. Among the three grouts, masonry cement grout exhibited the lowest compressive strength whereas SET 45 exhibited the highest compressive strengths for all ages. It has to be noted that though SET 45 exhibited high strength, the measured strengths are lower than those stipulated by the manufacturer in the data sheet.

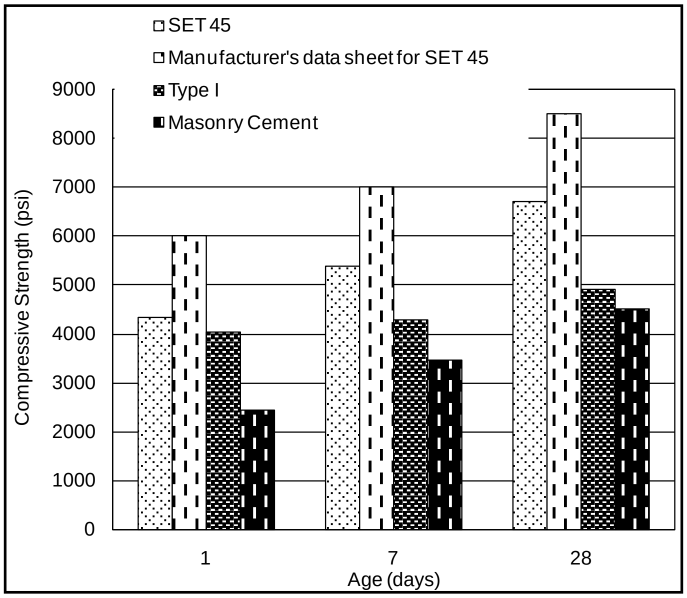

Figure 5-2. Development of compressive strength of shear key grouts

5.5 SLANT SHEAR BOND STRENGTH

In this section the analysis of mean slant shear bond strength at ages 1 and 7 days is discussed. Three samples for each age for each repair material and shear key grout were tested. Figure 5-3 shows the mean slant shear strength at ages 1 and 7 days for the repair materials tested.

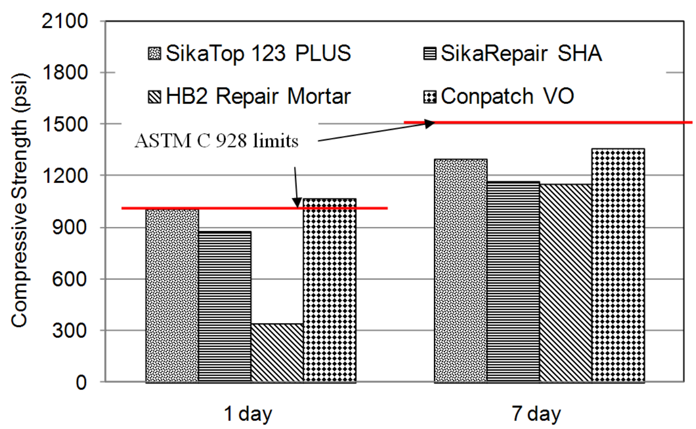

Figure 5-3. Development of slant shear bond strength at various ages for repair materials

ASTM C 928 prescribes performance requirements for slant shear bond strength testing for ages 1 and 7 days as 1000 psi and 1500 psi respectively (shown as bold lines). Figure 5-3 indicates that none of the selected materials exhibited the required strength at the age of 7 days. The slant shear compressive strength is the lowest for HB2 Repair Mortar at all ages. The COV for all of the repair materials is below 5% except for HB2 Repair Mortar (refer to Table 5-1through Table 5-4). Some of the samples failed along the cylindrical cut surface of the specimen (slant shear) whereas some samples sheared along the middle (compressive failure) as shown in Figure 5-4. Information on sample failure is provided in Appendix D.

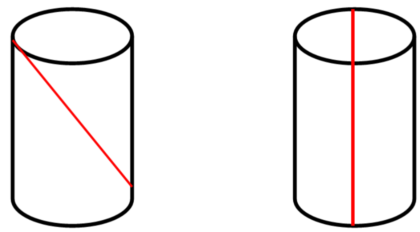

Figure 5-4. Failures of slant shear bond test specimens

One of the reasons for low strengths of HB2 Repair Mortar may be due to the early stiffening of the repair mortar in the fresh state. Due to rapid loss of workability of HB2 Repair Mortar, it was difficult to consolidate the mortar after placing it in the mold. This resulted in the presence of extensive voids in the sample as shown in Figure 5-5. A large part of the curved portion of the sample was not filled with repair mortar (area around the curve shown in Figure 5-5). Samples which exhibited large size voids as shown in Figure 5-5 due to improper consolidation were rejected but among those eventually selected for testing had small size voids (~0.2 in. in width).

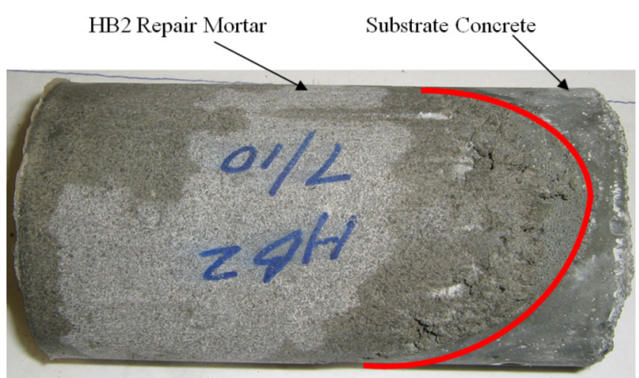

Figure 5-5. Voids in HB2 repair mortar specimen for slant shear bond strength test

Figure 5-6 is a graphical presentation of development of slant shear bond strength at 7 and 28 days for shear key grouts. SET 45 exhibited the highest slant shear bond strength among all shear key grouts. Since the shear key grouts were workable and could be consolidated easily in to the molds, the overall appearance of the test samples was smooth. No voids were observed in the specimens but this did not necessarily result in higher bond strengths. This indicates that the slant shear bond strength is dependent upon the material properties as well as the finish of the specimen.

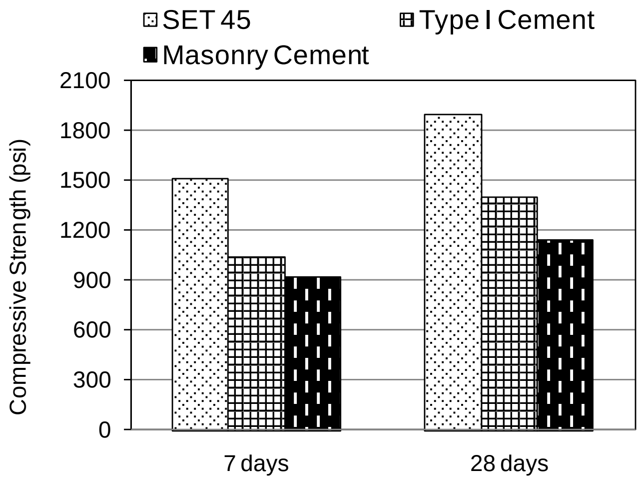

Figure 5-6. Development of slant shear bond strength at various ages for shear key grouts

5.6 SHRINKAGE BEHAVIOR

Similar to concrete, repair mortars too have a tendency to shrink on drying. A repair mortar patch is unable to shrink freely due to the restraint provided by the substrate concrete at the bottom interface of the patch, as well as the periphery in the case of an enclosed patch. If the repair mortar develops high shrinkage strains, the restraint prohibits it from shrinking leading to development of cracks in the patch. Presence of cracks not only reduces the dimensional stability of the repair patch, but also increases the chances of deterioration of the repaired structure due to exposure of internal concrete to penetration of de-icier salts and water through the cracks. In this study, free shrinkage and the cracking susceptibility of repair materials was studied whereas only free shrinkage was evaluated for shear key grouts (Appendix E). For the evaluation of cracking susceptibility, the crack width after appearance of the first crack was measured over a period of six days so as to ascertain the long term serviceability of the repair material.

Figure 5-7 represents the development of average free shrinkage strains in selected repair mortars. The specimens were stored in 100% RH at 73°F for a period of 95 days.

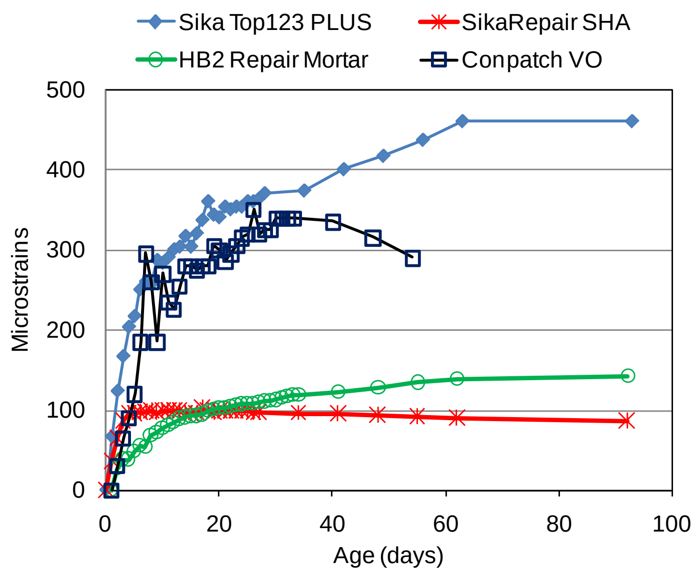

Figure 5-7. Free shrinkage strains in repair materials for samples at 100% RH and 73°F

The free shrinkage strains of specimens stored at 100% RH increased very rapidly at early ages for all the repair mortars. Sika Repair® SHA and Conpatch VO exhibited an initial expansion followed by a drop in the shrinkage strain after about 30 days indicating that some amount of relaxation had taken place. Overall, Sika Repair® SHA exhibited lowest shrinkage strains among all materials tested whereas Sika Top®123 PLUS exhibited the highest shrinkage strain values for specimens stored at 100% RH.

Free shrinkage strains of Sika Top®123 PLUS at 100% RH were measured over 150 days (refer to Figure E-1, Appendix E). The shrinkage strains progressively increased over time and exhibited extremely high average value of 483 microstrains. Typically, the shrinkage of repair material should be less than that of the substrate concrete. Such high strains even in 100% RH can be cause of concern but would also strongly depend upon the restraint provided by the substrate concrete.

Free shrinkage strain of Conptach VO samples in 100% RH does not exhibit a smooth linear progression like other repair mortars (refer to Figure 5-7 and E-7 in Appendix E). This behavior is consistently observed in all the specimens. Due to proprietary nature of repair mortars exact information about the ingredients are not known making it difficult to analyze the reasons for such behavior.

Figure 5-8 shows the graphical representation of free shrinkage strains developed in repair materials stored at 50% RH and 73°F. The overall behavior of the repair materials under lower humidity conditions is similar but reversed to that when placed in 100% RH, i.e., Sika Top®123 PLUS exhibited highest free shrinkage strains and Sika Repair® SHA and HB2 Repair Mortar exhibited lowest free shrinkage strains. Free shrinkage strains developed rapidly in the early ages for Sika Top®123 PLUS and Conpatch VO. Conpatch VO and Sika Repair® SHA did not exhibit a drop in free shrinkage strains for specimens stored at lower relative humidity unlike the drop in shrinkage strains over time observed in specimens stored at 100% RH (refer Figure 5-7 and Figure 5-8).

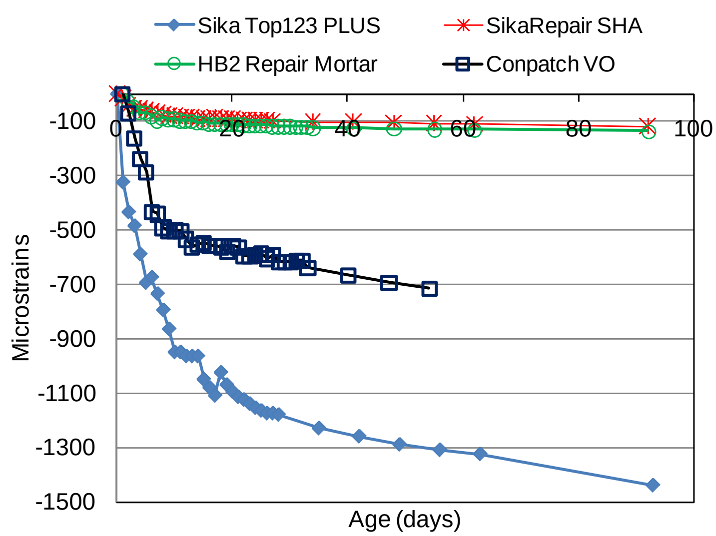

Figure 5-8. Shrinkage strains in repair materials for samples at 50% RH and 73°F

The main phenomena that are believed to contribute to the shrinkage of cement paste are the capillary stress, disjoining pressure, and changes occurring in the calcium silicate hydrate. At lower humidity, the capillary volume reduces leading to a quick rise in stresses. Literature suggests that polymer modification of repair mortar aids in reducing development of shrinkage strains. The reduction in strains is related to the low free water content and a well developed microstructure with fewer capillary pores in a polymer modified mortar. Thus, the development of high shrinkage strains in Conpatch VO can be explained by the lack of polymer modification. At the same time the high strain values in Sika Top®123 PLUS cannot be explained due to lack of information on the ingredients of this repair material or its specific microstructure.

The term ‘‘crack’’ in this report refers to a macrocrack that can be visually detected wherein the smallest measureable crack width would be 0.004 in. and above. Two ring specimens were prepared as per AASHTO PP 34. The average strains reported is the average of strains recorded using four strain gages per ring. Figure 5-9 shows the cracking susceptibility of Sika Top®123 PLUS. The ambient conditions were maintained at 50 % RH and 73°F. The induced tensile strain increases rapidly in the first six hours after addition of water to about -40 με for both specimens. The first ring cracked at 8.75 days beyond the addition of water to the repair mortar, whereas the second ring cracked at 6.20 days. The maximum strain reached by both specimens was comparable with each other at -105 με for Ring 1 and -95 με for Ring 2.

The variability in the age of cracking for the two specimens can be related to the batch variation and consolidation of the repair mortar in the specimen mold. Due to the large volume of mortar required, the mold was filled with 7 batches of mortar of 0.1 cu. ft each. The rapid-setting nature of the repair mortar at times made the process of consolidation slightly difficult leading to presence of voids in the specimen.

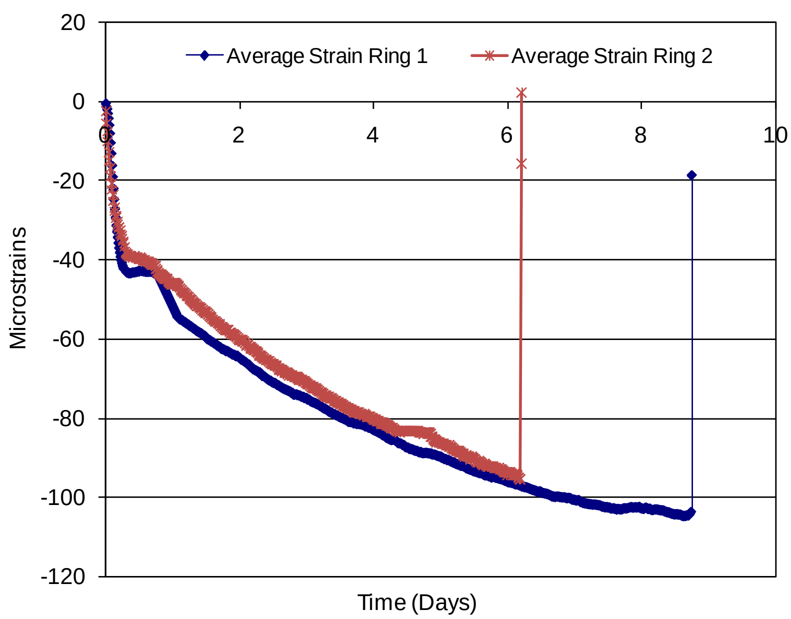

Figure 5-9. Cracking susceptibility of Sika Top®123 PLUS

Figure 5-10 shows the cracking susceptibility of Sika Repair SHA. Two specimens were cast to study the cracking susceptibility. The behavior exhibited by both the specimens was vastly different. Ring 1 specimen as seen in Figure 5-10 exhibited an initial expansion within the first few hours after addition of water to the mortar followed by steady rise in tensile strains. The specimen did not crack within 28 days from the time of addition of water to the mortar. Ring 2 did not exhibit any early expansion and the specimen cracked at the age of 3 days from addition of water to the repair mortar. These vast differences in behavior could be a result of - a) the two specimens were cast at different dates (Ring 1 was prepared on June 23, 2008 whereas Ring 2 was prepared on Aug 8, 2008) and b) a large number of voids were observed in Ring 2 due to insufficient consolidation. As noted in an earlier paragraph, the volume of repair mortar required for one specimen is very large and typically 1.5 bags containing about 45 lbs of repair mortar were used for casting one specimen.

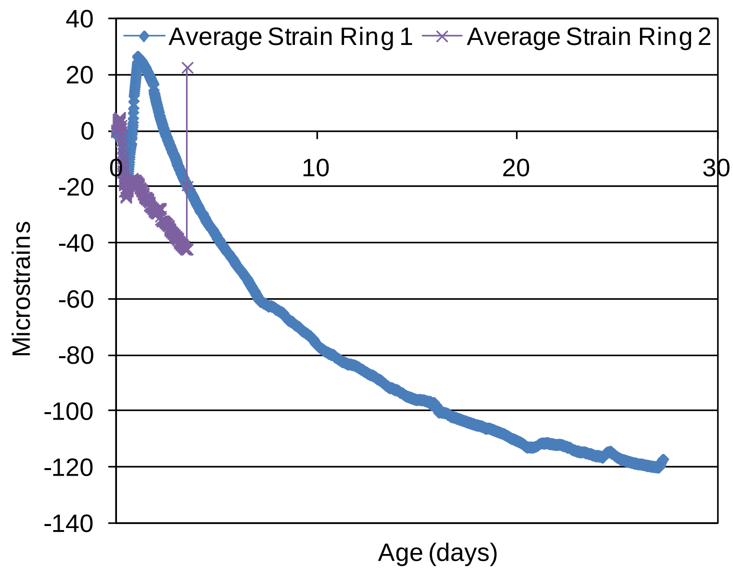

Figure 5-10. Cracking susceptibility of Sika Repair SHA

Figure 5-11 represents the development of tensile strains in ring specimens for Conpatch VO. The first ring developed a crack at the about 1.6 day since the addition of water whereas the second ring cracked at about 2.3 days since addition of water. Both rings exhibited a rapid rise in strains within the first two hours of casting the specimens followed by a drop in strains immediately after a time period of two hours. This behavior was not observed in any of the other repair materials. At the same time it has to be noted that this behavior was also observed at a later age (about 0.3 days) for free shrinkage specimens of Conpatch VO stored at 100 % RH (refer Figure 5-8). As mentioned earlier the mixing liquid used for mixing of Conpatch VO is water unlike the other repair materials. The initial increase in the strain values could be related to the increase in stress in capillary pores which eventually was reduced as the cement hydrated.

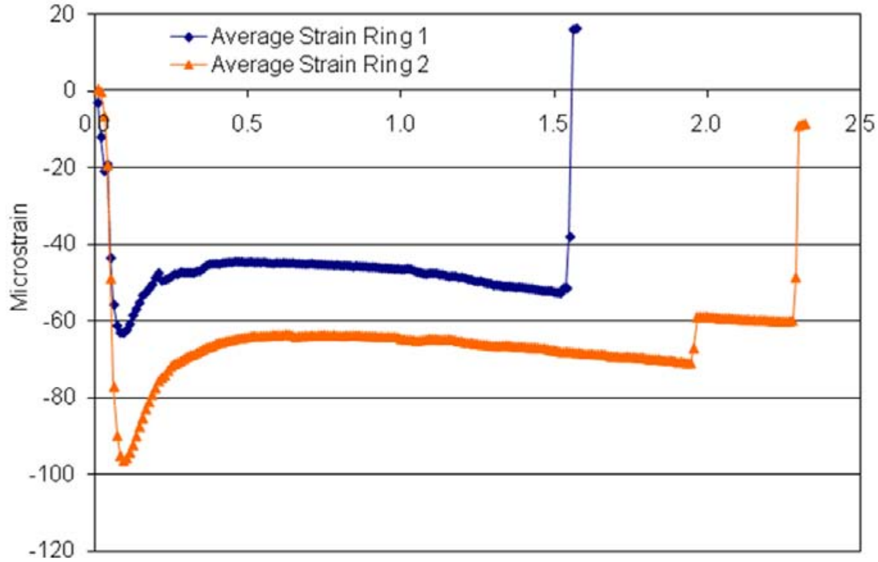

Figure 5-11. Cracking susceptibility of Conpatch VO

The potential of a material to crack under restrained conditions is related to its elastic modulus, tensile strength and relaxation stresses. The 'risk of cracking' of a repair material, based on the assumption of a rigid concrete substrate, is defined as $\varepsilon_{sh}E/f_t$ where f_t is the tensile strength, E is the modulus of elasticity, and ε_{sh} is the drying shrinkage strain (Al-Zahrani et al. 2003). The risk of cracking factor for the repair materials evaluated in this research is presented in Table 5-9. A high number indicates higher risk of cracking. In this analysis, the elastic modulus and flexural strength at 28 days of repair material as published in manufacturer data sheets was used (refer Appendix A). The 28-day mean free shrinkage strain developed in specimens stored in 50% RH and 73°F was used (refer Figure 5-7) was assumed for ε_{sh} value. This condition was selected because it is closer to the average humidity conditions in the field.

Based on the analysis of risk of cracking, it was observed that Sika Top®123 PLUS and Conpatch VO have the highest values of risk of cracking. These results correspond to the behavior of these materials in the restrained shrinkage test mentioned earlier. Both these materials experienced cracking at very early ages. Thus, the risk of cracking factor provides valuable information on the cracking tendency of repair materials.

Table 5-9. Risk of Cracking of Repair Materials

Repair Material	Elastic Modulus, E (psi)	Flexural Strength, f_t (psi)	Free Shrinkage Strain at 28 days	E/f_t	Risk of Cracking
Sika Top® 123 PLUS	3500000	2000	1.18	1.8E+03	20.65
Sika Repair® SHA	3200000	1100	0.101	2.9E+03	2.94
HB2 Repair Mortar	2000000	1000	0.118	2.0E+03	2.36
Conpatch VO	3900000	1200	0.616	3.3E+03	20.02

The average crack width developed over six days from the first day when cracking was observed in the ring specimens for the repair mortars is given Table 5-10. The average crack width was measured using a crack comparator at six points across the length of the crack and is reported in Table 5-10 as the average crack width. For Sika Repair® SHA, the first ring did not crack at the end of 28 days and hence it is reported such. The crack width for other rings increases over age. The restraint provided by the rings induced high restraint shrinkage strains leading to an increase in crack width.

Table 5-10. Average Crack Width over Six Days

Repair Material	Crack Width in Specimen 1 (in.)						Crack Width in Specimen 2 (in.)					
	1 day	2 day	3 day	4 day	5 day	6 day	1 day	2 day	3 day	4 day	5 day	6 day
Sika Top® 123 PLUS	0.007	0.009	0.01	0.013	0.016	0.020	0.007	0.009	0.010	0.020	0.020	0.035
Sika Repair® SHA	Specimen did not crack						0.005	0.005	0.007	0.007	0.007	0.010
Conpatch VO	0.005	0.005	0.007	0.013	0.016	0.020	0.013	0.013	0.016	0.016	0.020	0.025

The crack width is an important parameter from the perspective of durability of the repaired concrete. Cracking provides passage for water and harmful salts to penetrate the concrete leading to steel corrosion and loss of service life of the structure. Figure 5-13 is a pictorial presentation of the probable future effects of different crack widths in a structure and the allowable crack width from a serviceability perspective as outlined in ACI 318.

Comparing Table 5-10 and Figure 5-12 it can be seen that for specimens under the restraint provided by the steel rings, the average crack width at the end of six days is typically in the range that can cause controllable leakage. If no stress relaxation occurs during this time, the crack widths can continue to increase over time leading to a path for corrosion of embedded reinforcement.

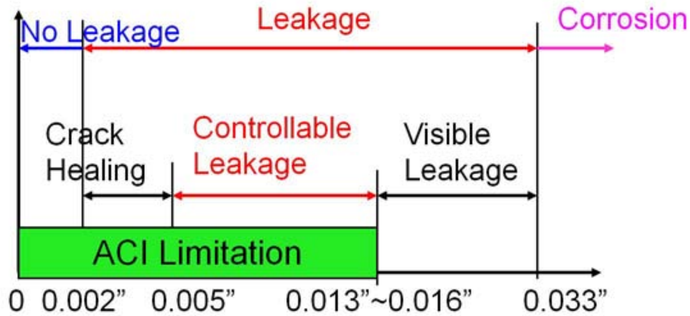

Figure 5-12. Pictorial presentation of crack width and effect on serviceability

It is pertinent to note that these cracks widths are in response to the restrain proivded by the steel rings, whereas in the actual structure the restraint provided by the substrate concrete would be of different value. The steel rings provide a equally proportioned restrained stress on the concrete while the substrate concrete can potentially provide unequal restraint. Hence the increase in crack width over age in such cases might differ from this experimental study. In an actual structure, aspects, such as the amount of stress developed at the bottom layers, creep and stress relaxation would also play an important role in the actual shrinkage strains developed in the element. When repair concrete is under stress (tensile or compressive), early age creep serves as a "relief valve" permitting restrained shrinkage to occur with a lower resultant stress.

Figure 5-13 presents the development of free shrinkage strains in three shear key grouts stored in 100% RH. The manufacturer of SET 45 clearly states in the data sheet that SET 45 should not be water cured. In order to maintain an identical environment for all specimens, the SET 45 free shrinkage specimens were also stored at 100% RH. The evidently different behavior of SET 45 under these environmental conditions can be noted in Figure 5-12. Set 45 samples exhibited contraction rather than expansion as observed in the Type I cement grout and Masonry cement grout specimens. Overall, masonry cement grout exhibited minimal expansion at the end of 150 days.

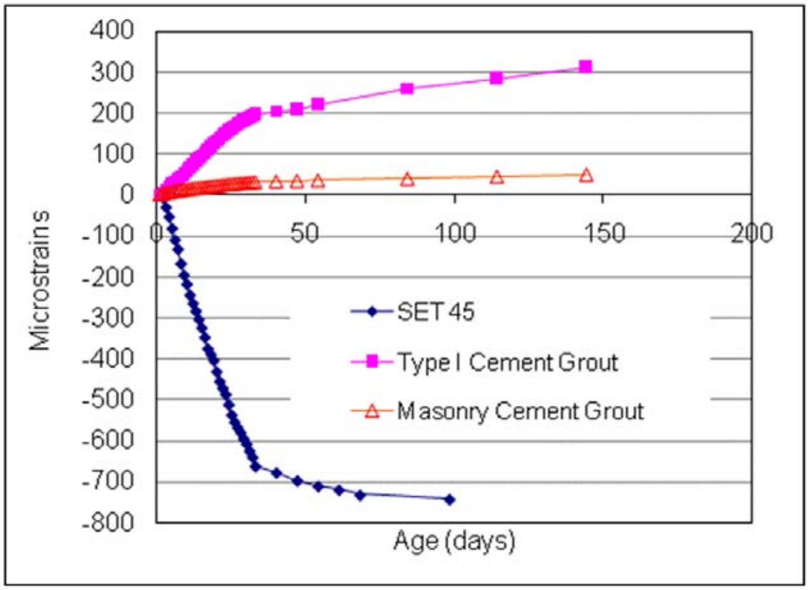

Figure 5-13. Free shrinkage strains in shear key grouts for samples at 100% RH

When free shrinkage specimens were stored in 50% RH it was observed that SET 45 exhibited the least contraction and the lowest development of free shrinkage strains as shown in Figure 5-14. The free shrinkage strains in both grouts are high (~ 525με at the end of 150 days). Due to the low humidity and high water to cement ratio of both cement grouts, the rate of diffusion of water from the specimen to the surrounding environment is high, leading to high negative strain value. In cement based system, between the relative humidity of say about 95% to 85%, typically water is lost predominantly from large capillary pores or commonly referred as macropores. As the humidity lowers (between 85% to 50%) water is lost concomitantly from both the mesopores and micropores, i.e. from fine capillary pores as well as from the calcium silicate hydrate. The grout mixtures examined in this study have high water to cement ratios as well as intrinsic high porosity leading to a higher tendency for water loss from the different sized pores, resulting in high strain values.

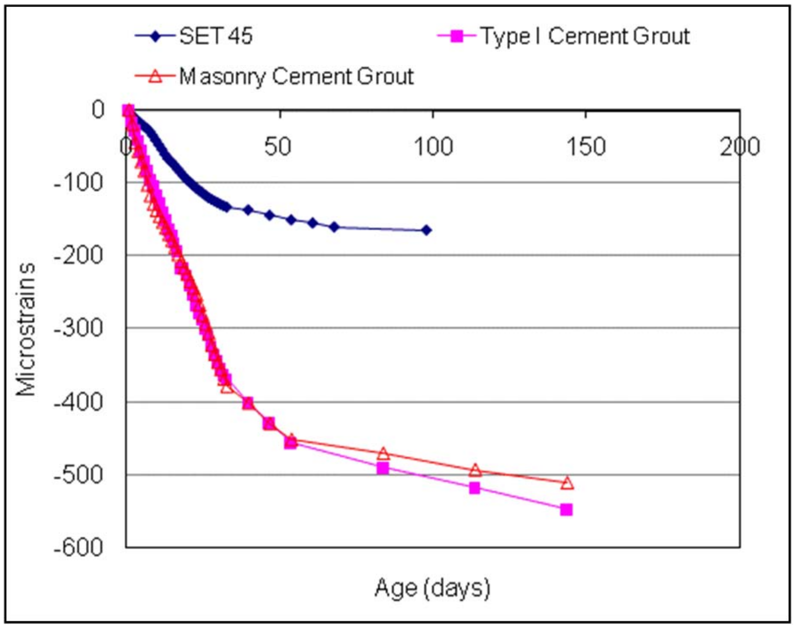

Figure 5-14. Free shrinkage strains in shear key grouts for samples at 50% RH and 73°F

5.7 RESISTANCE TO FREEZING AND THAWING

The long-term durability of repaired concrete is an important aspect in increasing the service life of a structure. In this study, an extensive evaluation of the durability of selected repair materials in freezing and thawing cycles was performed.

Figure 5-15 represents the mean change in relative modulus of different repair materials over 300 cycles of freezing and thawing. The relative dynamic modulus in this test is calculated by measuring the frequency of a wave in the specimen. In this experiment it was observed that the highest frequency was registered for Conpatch VO (~1745 to 1862 Hz at the start of the experiment). Sika Top123 PLUS and Sika Repair SHA had comparable frequencies in the range of 1550 to 1650 Hz at the start of the experiment. The measured frequencies are typically slightly lower than those measured in normal concrete (~1900 to 2100 Hz).

As per ASTM C 666, the relative dynamic modulus at the end of 300 cycles should not be below 60% for a material to be considered to have good resistance to freezing and thawing. All the repair materials evaluated exhibited good resistance to freezing and thawing cycles. Sika Repair® SHA exhibited the highest loss in relative dynamic modulus of 86.5% at 300 cycles. Sika Top123 PLUS and Conpatch VO have excellent resistance to freezing and thawing cycles and exhibit a very low loss in relative dynamic modulus at the end of 300 cycles.

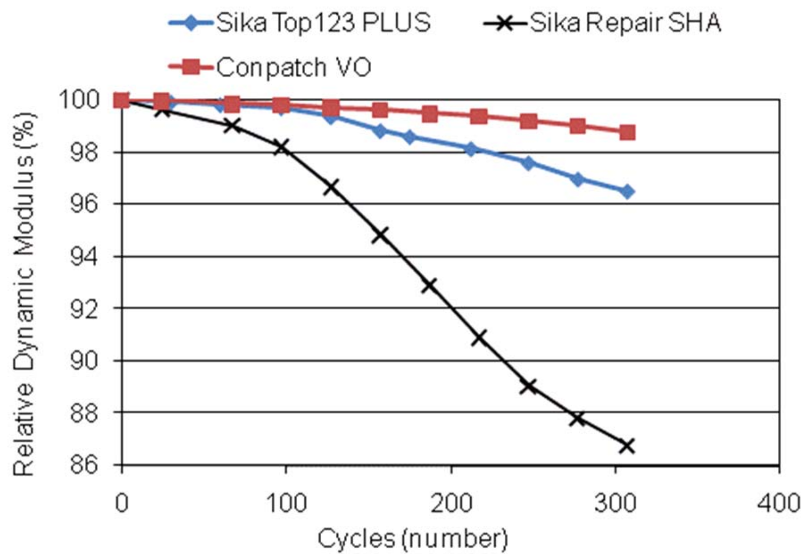

Figure 5-15. Relative dynamic modulus of repair materials over 300 cycles of freezing and thawing

Figure 5-16 shows the average change in length of the specimen for three specimens over 300 cycles of freezing and thawing. A very large change in length was not observed for Sika Top 123 PLUS and Sika Repair SHA specimens whereas Conpatch VO exhibited a high increase in length within the first 30 cycles. Conpatch VO subsequently exhibits a slight drop in its change in length measurements indicating contraction of the specimen. This behavior may be attributed to probable continued hydration of the specimens leading to healing of any cracks that might have formed during the first 30 cycles of the experiment.

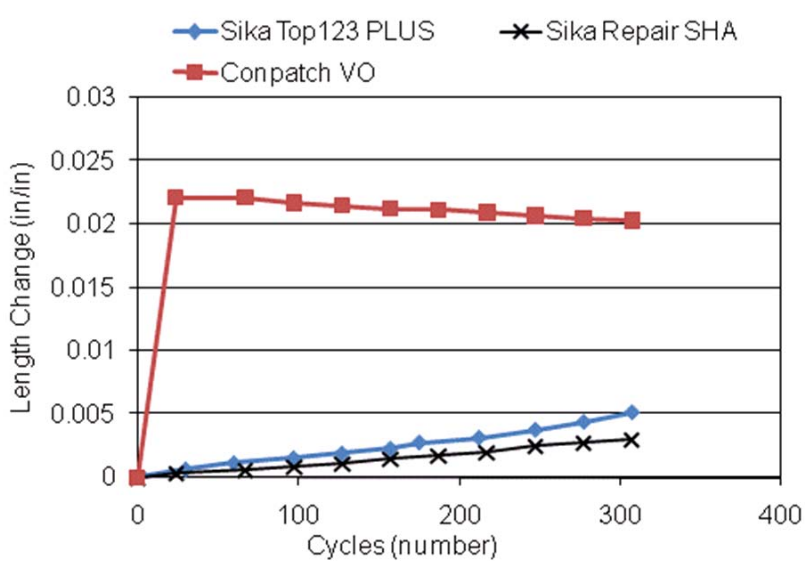

Figure 5-16. Change of repair materials over 300 cycles of freezing and thawing

Appendix F contains graphical presentation of the change in relative dynamic modulus and change in length over 300 cycles of freezing and thawing for all samples tested in this study. Photographs of specimens of repair materials are presented in Appendix F. All repair mortars tested exhibit intact surface on all sides of the specimen at the end of 300 cycles. Specimens of Sika Top123 PLUS and Sika Repair SHA exhibited some circular voids as can be seen in Figures F-13 and F-14 of Appendix F. It should be noted that the occurrence of these voids was very less and overall it did not reduce the relative dynamic modulus of the specimens.

HB2 Repair Mortar samples were not subjected to freezing and thawing cycles because of the presence of large amounts of voids as shown in Figure F-16. Due to the sample size required by ASTM C 666 (3 x 3 x 16 in.) a large volume of the repair mortar is required for preparing the sample. On account of the rapid setting nature of HB2 Repair Mortar, the consolidation of the repair mortar in the molds was very difficult. The mortar was consolidated by vibrating as well as by pressing with fingers and a putty knife in to the mold. Even though different consolidation techniques were adopted, it was observed that a large number of voids (about ½”~1” long) existed in the specimen after the mortar had hardened (refer Figure F-16).

Figure 5-17 is a graphical presentation of the mean change in relative dynamic modulus of shear key grouts subjected to 300 cycles of freezing and thawing. SET 45 had the highest change in relative dynamic modulus in comparison to the traditional cement grouts, but at 82% it is within the requirement of ASTM C 666. Similarly, the change in length of SET 45 samples is also the highest among all the shear key grouts tested (refer Figure 5-18). Type I cement grout, as well as Masonry cement grout, show almost identical changes in relative dynamic modulus and length change over 300 cycles.

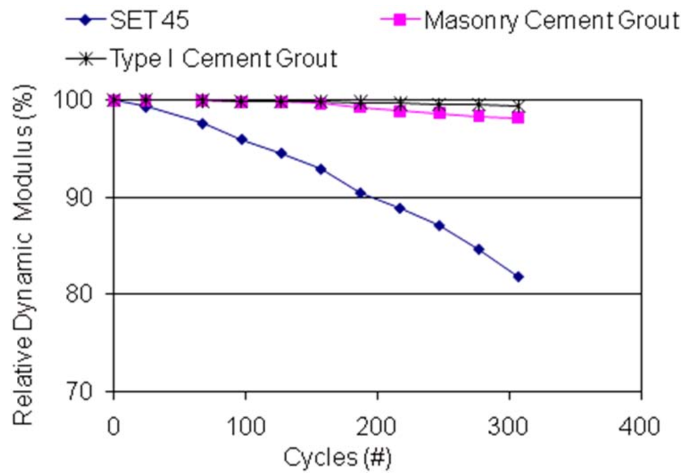

Figure 5-17. Change in relative dynamic modulus of shear key grouts over 300 cycles of freezing and thawing

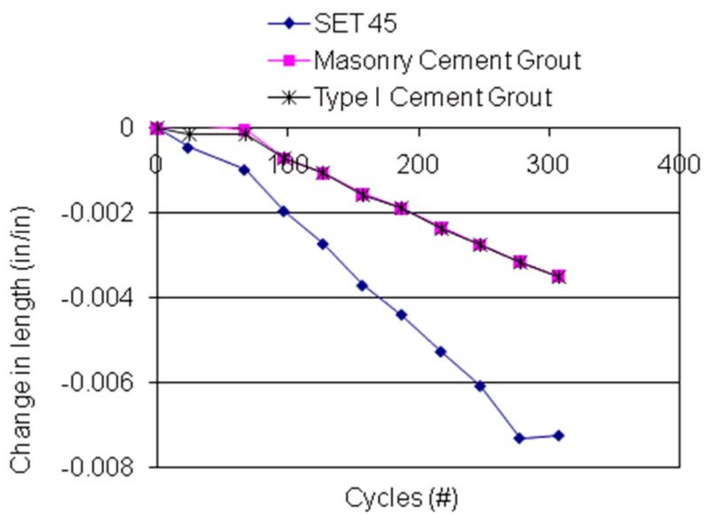

Figure 5-18. Change in length of shear key grouts over 300 cycles of freezing and thawing

Composite specimens of substrate concrete and repair materials were tested for durability of the composite system in freezing and thawing cycles. The composite specimens exhibited excellent resistance to freezing and thawing cycles as shown by the minimal reduction in relative dynamic modulus (see Figure 5-19). As seen in Figure 5.20 Sika Repair® SHA showed a slightly larger drop in relative dynamic modulus over 300 cycles in comparison to Sika Top123 PLUS and Conpatch VO. It is necessary to note that Sika Repair® SHA exhibits higher durability factor for combined specimens as compared to those specimens of the repair material only (refer to Figure 5-15 and Figure 5-20), whereas the other repair materials exhibited relative dynamic values similar to their composite counterparts.

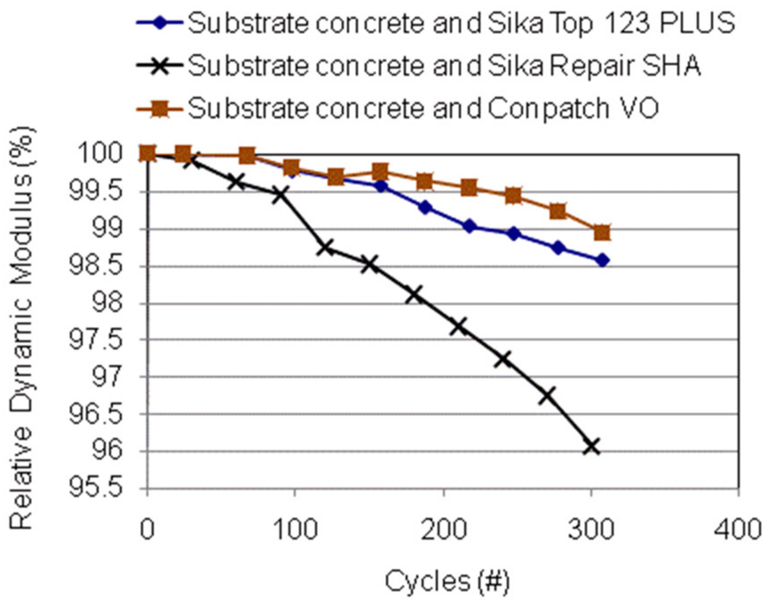

Figure 5-19. Change in relative dynamic modulus of composite specimens of substrate concrete and repair material over 300 cycles of freezing and thawing

5.8 AIR CONTENT

The air void system is critical for the satisfactory performance of the repair mortar and shear key grouts under freezing and thawing conditions. The critical parameters defining a satisfactory air void system are the percentage of air voids, spacing factor, specific area, and bubble frequency. Figure 5-20 shows the amount of air in hardened repair mortar and shear key grouts evaluated in this study. For a durable system, the optimum percentage of air entrainment is about 5 to 6.5%. All the materials evaluated in this study have a higher percentage of entrained air than the prescribed value. HB2 Repair Mortar has the highest amount of air entrainment at 33.5% while the remaining materials ranged from 7.6% to 12.43%.

Figure G-3 in Appendix G shows a stereo image of HB2 Repair Mortar. The image shows the highly porous nature of HB2 Repair Mortar in comparison to other repair mortars (refer Figure G-1 through G-4). Figure G-4 also gives an indication of the high amount of voids formed due to insufficient consolidation given the rapid setting nature of the mortar.

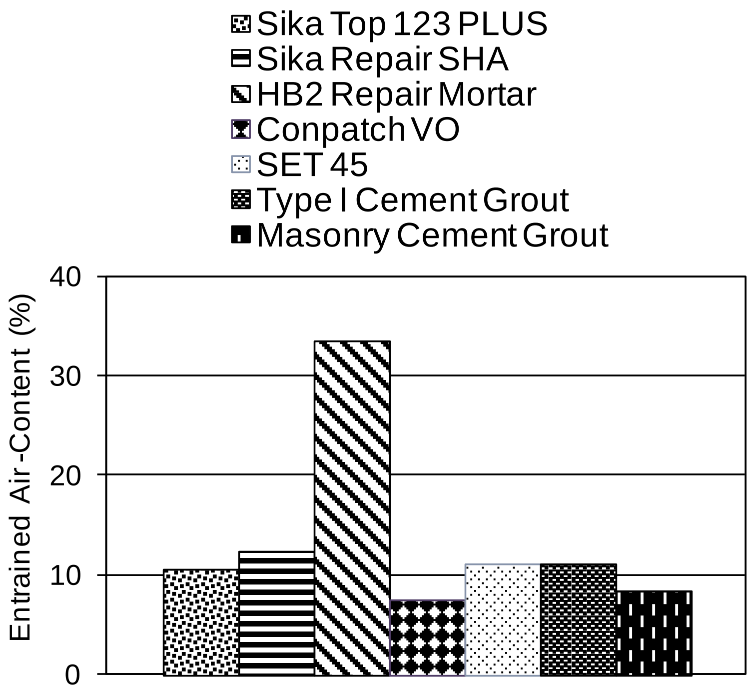

Figure 5-20. Air content in hardened repair mortar and shear key grouts

Specific surface area and void frequency are inter-related and reflect the mean size of the air bubbles. For a protective air void system, the specific surface area should not be less than 25 mm^2/mm^3. As seen in Figure 5-21, all materials evaluated except for Sika Top®123 PLUS have a lower specific surface area than 25 mm. Table 5-11 presents the void frequencies and spacing factors of repair mortars and shear key grouts. For a protective air void system the void frequency should be within 0.3 – 0.6 /mm. Only one repair mortar and two shear key grouts fall within this range. The spacing factor is defined as the average distance between any point in the paste to the edge of the nearest void and typically should not exceed 0.2 mm for adequate resistance to freezing and thawing.

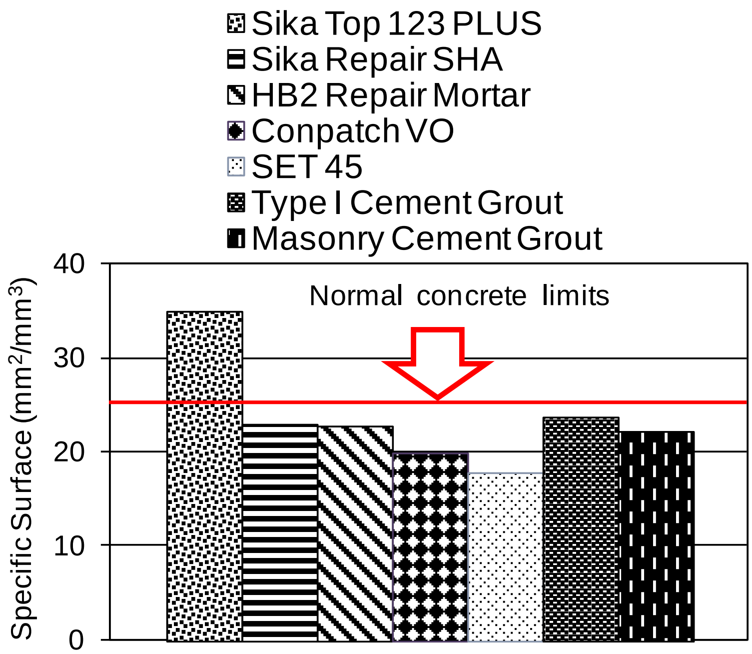

Figure 5-21. Specific surface area of repair mortars and shear key grouts

Table 5-11. Void Frequencies and Spacing Factors for Repair Mortars and Shear Key Grouts

Material	Void Frequency (/mm)	Within Criteria	Spacing Factor (mm)	Within Criteria
Sika Top 123 PLUS	0.939	N	0.144	Y
Sika Repair SHA	0.712	N	0.169	Y
HB2 Repair Mortar	2.039	N	0.055	Y
Conpatch VO	0.381	Y	0.268	N
SET 45	0.496	Y	0.262	N
Type I Cement Grout	0.664	N	0.167	Y
Masonry Cement Grout	0.466	Y	0.218	N

Comparing the air void system data with the results of the freeze-thaw test, it can be observed that although polymer modified repair mortars do not reveal numbers close to the requirement for stable air void system as specified for normal concretes, they do exhibit a desirable performance in the freeze-thaw test.

5.9 COEFFICIENT OF THERMAL EXPANSION (CTE)

Differential thermal strains due to varying CTE values between the substrate concrete and repair mortar can result in an increase in strains in the repaired concrete, leading to cracking and reduced serviceability. Figure 5-22 shows the average CTE values for repair mortars and shear key grouts. It should be noted that although average values have been used for the graphical presentation, the age difference between any two companion samples varied by up to three days due to equipment scheduling. In Appendix I complete information for each sample is provided.

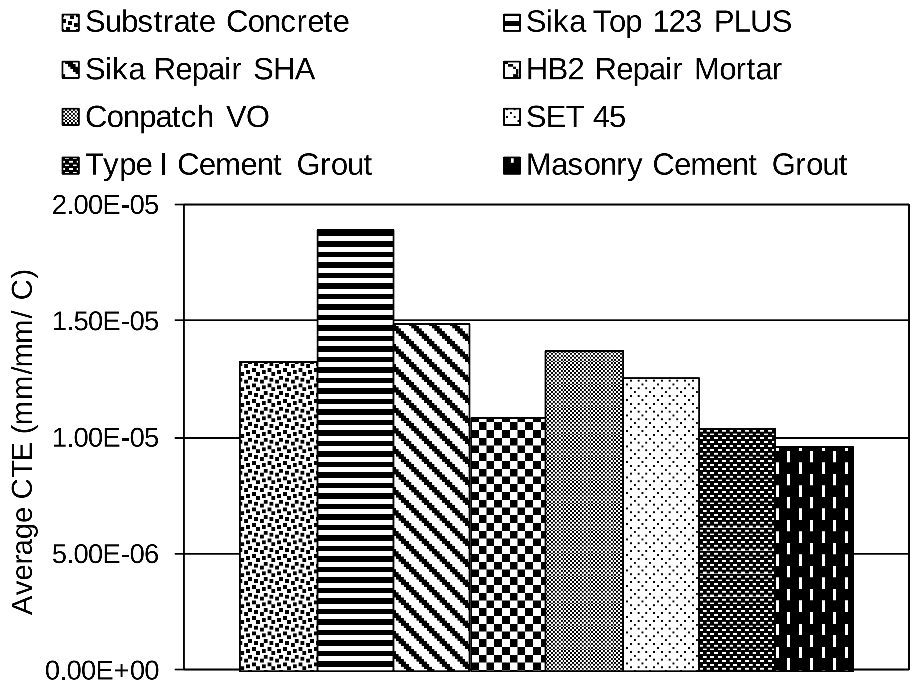

Figure 5-22. Average coefficient of thermal expansion of repair mortars and shear key grouts

In comparison to the substrate concrete, Sika Top 123 PLUS and Sika Repair SHA have higher CTE values whereas cement based grouts have lower CTE values. HB2 Repair Mortar exhibited a high variation in values between the two samples (refer to Appendix H). This variation could be attributed to improper consolidation of the material leading to the presence of voids within the test cylinder. Presence of air in the voids varies the values of change in length with larger difference due to discontinuity in material.

To understand the effects of using repair materials with CTE values different from the substrate concrete, numerical calculations are presented in Table 5-12. If a composite 1 ft long beam is subjected to a temperature variation from 73°F to 113°F, then

Change in length (Δl) = length of element (l) x CTE (∝) x change in temperature (Δt)

Table 5-12. Change in Length Observed

Material	Change in length (in)	Change in comparison to substrate concrete
Substrate Concrete	0.011	--
Sika Top 123 PLUS	0.016	0.005
Sika Repair SHA	0.013	0.002
HB2 Repair Mortar	0.009	-0.002
Conpatch VO	0.012	0.001
SET 45	0.011	0
Type I Cement Grout	0.009	-0.002
Masonry Cement Grout	0.008	-0.003

A repair mortar having a higher CTE value than the substrate concrete can cause undesirable tensile strain development in the substrate concrete. Sika Top 123 PLUS and Sika Repair SHA exhibit slightly higher length change values in comparison to other repair mortars. Conversely, lower CTE values can cause undesirable compressive strain development.

5.10 SORPTIVITY

The rate of water absorption of repair mortars is an important property because it determines the ability of the material to protect the substrate concrete and reinforcement.

Figure 5-23 and Figure 5-24 compares the values of rate of initial absorption and secondary absorption, respectively, for repair mortars and shear key grouts. ASTM C 1581 states that rate of absorption for a material is accepted only if the regression coefficient for a plot of initial absorption versus time is more than 0.98. It was observed that all repair mortars except Sika Top 123 PLUS has lower regression coefficients (refer Table I-1 in Appendix I).

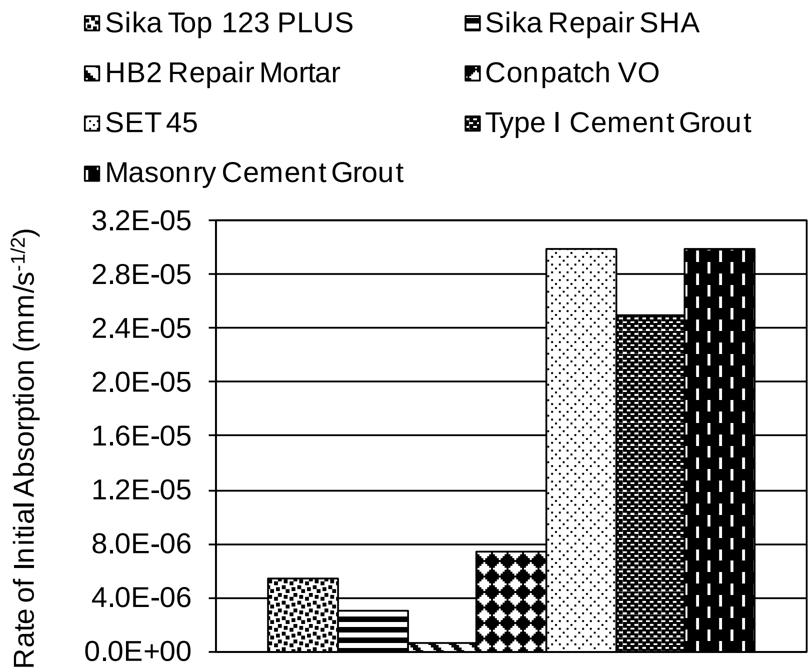

Figure 5-23. Comparison of rate of initial absorption of repair mortars and shear key grouts

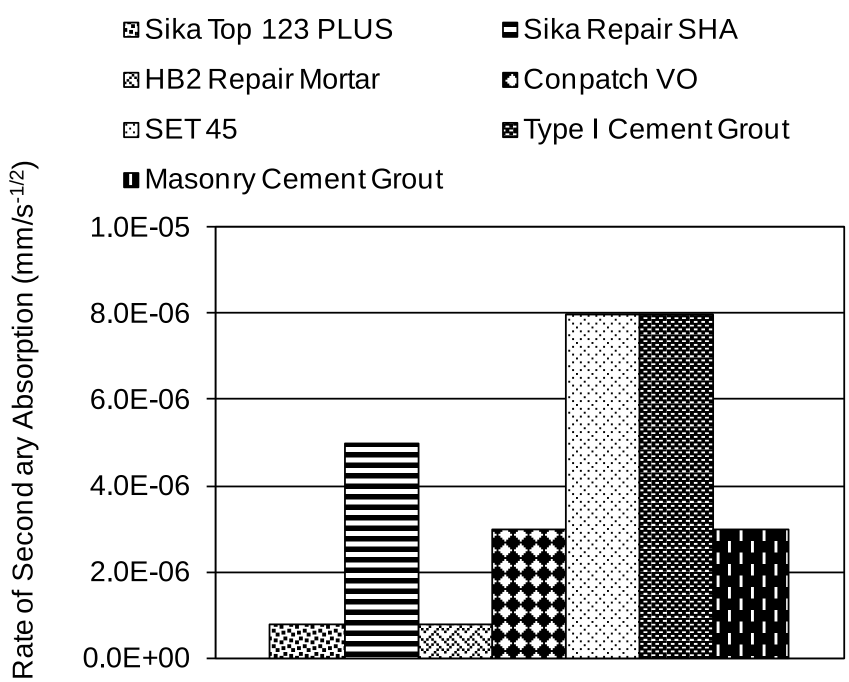

Figure 5-24. Comparison of rate of secondary absorption of repair mortars and shear key grouts

The average data points provided in Figure 5-23 are presented to give a perspective to the absorption behavior of different repair mortars and the values cannot be accepted as absolute values as per ASTM C 1581. The secondary rate of absorption exhibited a more definitive behavior and all repair mortars had a regression coefficient greater than 0.98. Based on the absorption values, it can be inferred that the repair mortars selected in this study exhibit a lower tendency to absorb water or harmful ions in comparison to the shear key grouts. The absorption values reduce over time thus indicating that as the humidity within the sample increases due to exposure to water, the absorption capacity of the repair mortar is reduced.

In the earlier sections on shrinkage and CTE, the difficulty in measuring a particular property for HB2 Repair mortar has been mentioned. The primary reason for it was related to the difficulty in consolidating HB2 Repair Mortar specimens leading to voids in the hardened mortar. The sorptivity results indicate that the presence of voids inside the specimen did not affect the rate of absorption. In fact, the lowest absorption rate was observed for HB2 Repair Mortar.

5.11 CHLORIDE PERMEABILITY

The ability of repair material to resist chloride ion migration was determined by performing the ASTM C 1202 test. Figure 5-25 shows the average values of charge passed through two test specimens for different repair mortars. Material data sheets of two repair materials (i.e. Sika Top 123 PLUS and Conpatch VO) provide information on chloride permeability. As per ASTM 1202 specifications, a low permeability concrete should pass a charge of 100-1000 Coulombs at the end of the test. Based on this criterion, it was observed that all repair materials evaluated exhibited low permeability. Conpatch VO exhibited higher values than those prescribed as per the manufacturer but the measured value (930 Coulombs) was still in the low permeability range as prescribed by ASTM C 1202.

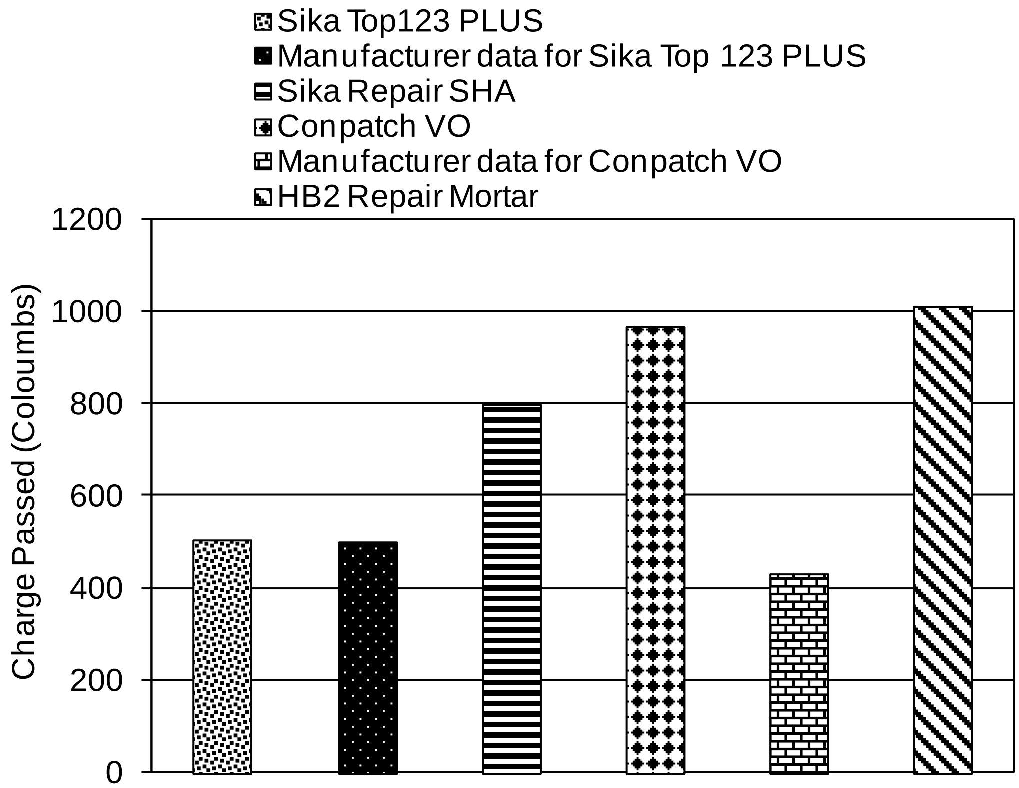

Figure 5-25. Comparison of chloride permeability for repair materials

5.12 SUMMARY OF DURABILITY STUDIES

The basic tenet of this research component was to investigate the durability characteristics of repair materials used for box-beam bridges so as to improve its life expectancy. Phase I of this project identified several levels of deterioration found through inspection of MDOT-owned adjacent box beam bridges. The major concerns observed in Phase I were: 1) the longitudinal reflective cracking and apparent failure of the grouted shear keys between beams, 2) corrosion of concrete especially along the bottom side of the box beams of the bridge. Onset of corrosion is caused due to moisture penetration from existing cracks and application of deicer salts on the bridge deck.

One objective of this project component was to determine the causes of the longitudinal cracking in shear keys by evaluating the mechanical properties of the currently used shear key grouts. Analysis of the design methods and material properties will provide insight in the interaction between the shear keys and the box beams. To evaluate the mechanical properties and its effect on the structural stability of the bridge, three types shear key grouts were selected. Two of these were cement based grouts whose mixture proportion was based on MDOT specifications. The third shear key grout selected was SET 45, a commercially available rapid setting phosphate cement based grout.

Another objective of the research component was to analyze the dimensional stability and the durability properties of repair materials commonly used by MDOT. Durability is not only the concern for the design of new concrete structures but also needs to be taken into account in concrete repair. Literature review conducted for this study clearly indicated that though repair is performed to increase serviceability and durability of bridges, sufficient research on the repair material parameters governing this behavior has received little attention. One of the main results of the literature review was the development of design parameters from the perspective of durability of repaired structures as shown previously in Figure 4-1. To this end, four commercially available repair materials typically used for bridge repairs were selected to evaluate their performance in terms of dimensional stability and durability. The properties evaluated were slump, air content, rate of gain of compressive strength, bond strength, shrinkage and cracking susceptibility, resistance to freezing and thawing cycles, coefficient of thermal expansion, chloride permeability and sorptivity.

It was observed that the repair materials and shear key grouts investigated in this study have a wide range of values for all the properties for which the materials were evaluated and the results are discussed in the preceding sections of this chapter. A summary of all the test results is provided below:

1) All repair materials exhibited zero slump and had very low workability. The most unworkable repair mortar was the HB2 Repair Mortar. The mortar was extremely stiff after mixing and would typically require an excessive amount of consolidation. The shear key grouts, including SET 45, exhibited good workability with slump values in the range of 8 in.
2) Compressive strength of commercial polymer modified mortars varies for each material. Amongst all repair materials evaluated in this study Sika Top 123 PLUS exhibited slightly lower strengths in comparison to those listed in the manufacturer's data sheet and Conpatch VO exhibited the highest strength at all ages. All repair materials exhibit strengths in the range of 6000 psi or more at the end of 28 days. Sika Repair SHA and HB2 Repair Mortar exhibited lower early age strengths but gain

a higher percentage of strength at later ages. The compressive strength of cement based shear key grouts was below 5000 psi whereas SET 45 exhibited slightly higher strength at 28 days.

3) Slant shear strength results were compared with the stipulation provided in ASTM C 928. Specimens of polymer repair material tested at the age of 1 day exhibited lower strengths than those stipulated in ASTM C 928 except for Conpatch VO. None of the polymer based repair materials nor the cement based shear key grouts exhibited strengths as per the requirements of ASTM C 928 at 7 days. SET 45 exhibited good bond strength and the average values were above those stipulated by ASTM C 928.
4) The effect of shrinkage on volumetric stability was evaluated by conducting tests to determine the free shrinkage as well as the cracking susceptibility under different curing regimes. It was observed that HB2 Repair Mortar and Sika Repair SHA exhibited low free shrinkage strains under both curing regimes (100% RH and 50% RH). The highest free shrinkage or expansion was observed for Sika Top123 PLUS irrespective of the curing regime. The shear key grouts exhibited opposing behavior when free shrinkage specimens were cured at 100% RH. Cement based shear key grouts exhibited expansion when specimens were stored at 100% RH whereas SET 45 experienced large amount shrinkage (~700 $\mu\varepsilon$) under the same environment. Specimens of cement based shear key grouts stored at 50 % RH exhibited high values of free shrinkage strains in comparison to SET 45.
5) Cracking susceptibility was measured for polymer repair materials by performing the restrained ring shrinkage test. Two samples were cast for all materials except HB2 Repair Mortar. It was observed that the cracking susceptibility for the materials varied. All materials cracked within 10 days from the start of the test except for one sample of Sika Repair SHA. The *risk of cracking factor* was determined for the polymer repair materials based free shrinkage strains and elastic modulus. Sika Top 123 PLUS and Conpatch VO exhibited highest risk of cracking factor.
6) Durability of construction materials under freezing and thawing cycles is an important property and was evaluated for both polymer repair materials as well as shear key grouts except for HB2 Repair Mortar. All materials exhibited excellent resistance to freezing and thawing cycles. The resistance to freezing and thawing

cycles is related to the amount and spacing of air content in the mortar. It was observed that though the polymer repair materials exhibit a high air content, the parameters that define stable air content for concretes cannot be directly applied. It was observed that the specific surface area of air bubbles and the void frequency of some of the polymer repair materials were not within the requirements as specified for normal concrete. Cement based shear key grouts also exhibited excellent resistance to freeze thaw cycles. SET 45 though exhibited adequate resistance to freezing and thawing cycles, the value of relative modulus at the end of 300 cycles was 80 % whereas the cement mortar based grouts exhibited had higher relative modulus values of 98% for the same cycles.

7) Resistance to freezing and thawing of composite specimens consisting of substrate concrete and polymer repair material was evaluated in this study. Composite specimens of Sika Repair SHA exhibited higher resistance to freezing and thawing cycles in comparison to only repair material samples.
8) Thermal coefficient of expansion of polymer repair materials evaluated in this study is approximately equal to the substrate concrete for mortars except for SikaTop 123 PLUS.
9) Permeability of chloride ions and water absorption capacity of all the repair mortars evaluated in this study is low. The polymer based repair materials exhibited extremely low values of charge passed through specimen indicating high resistance to chloride ion penetration. Water absorption in terms of sorptivity values for all repair mortars was extremely low in comparison to typical values of sorptivity for substrate concrete.

Table 5-13 and Table 5-14 summarize the results for all repair materials and shear key grouts, respectively. The values are compared with respect to requirements and volumetric stability of the whole system consisting of the substrate concrete and the repair concrete.

Table 5-13. Repair Material Test Results Summary

Property	Ideal Requirement	Repair Materials			
		Sika Top 123 PLUS	Sika Repair SHA	HB2 Repair Mortar	Conpatch VO
Workability	Good	Good	Good	Low	Good
Compressive Strength (psi)					
1 day	≥ 3000	> 3000	< 3000	< 3000	> 3000
7 day	≥ 3000	> 3000	> 3000	> 3000	> 3000
28 day	> substrate compressive strength	~ 6700	~ 6200	~ 5800	~ 9600
Slant Shear Bond Strength (psi)					
1 day	1000	> 1000	< 1000	< 1000	> 1000
7 days	1500	< 1000	< 1000	< 1000	< 1000
Free Shrinkage	low	high	high	low	low
Cracking Susceptibility	low	high	high	NA	low
Resistance to freeze-thaw damage	≥ 60 %	Good	Good	NA	Good
Coefficient of Thermal Expansion	~ substrate concrete	high	equal	equal	equal
Sorptivity	low	low	low	low	low
Chloride Permeability	low	low	low	low	low

Table 5-14. **Shear Key Grout Test Results Summary**

Property	Ideal Requirement	Shear Key Grouts		
		Type I Cement	Masonry Cement	SET 45
Workability	8 – 10 in.	8	7	8
Air content	14 $\pm$ 4	13.5	10.5	--
Compressive Strength (psi)				
1 day	≥ 2000	> 2000	< 2000	< 2000
7 day	≥ 3000	> 3000	> 3000	> 3000
28 day	> substrate compressive strength	~ 4500	~ 4500	~ 5500
Slant Shear Bond Strength (psi)				
7 day	1000	> 1000	< 1000	> 1000
28 days	1500	< 1500	< 1500	> 1500
Free Shrinkage	low	low	low	low
Resistance to freeze-thaw damage	≥ 60 %	Good (80%)	Good	Good
Coefficient of Thermal Expansion	~ substrate concrete	equal	equal	low
Sorptivity	low	low	low	low

6 MATERIAL TESTING

6.1 OBJECTIVE AND APPROACH

One of the project tasks deals with finite element (FE) simulation of box-beam bridge construction stages. Another task deals with developing FE models for load response assessment for the purposes of determining load capacity of the side-by-side box-beam bridges with distressed box-beams. Mechanical properties of materials used in the bridge are required as input parameters to the FE models. Concrete, steel, and prestressing strand properties are well documented in the literature. Mechanical properties of manufactured grout materials (e.g., set grout and set-45) and repair materials and are also documented in manufacturers' technical data sheets. Type R-2 grout is commonly used in Michigan box-beam bridges to form the shear-keys. Mechanical properties of R-2 grout have not been documented in literature.

This chapter summarizes mechanical properties of Type R-2 grout obtained from laboratory testing performed at Western Michigan University. Mechanical properties of repair materials and manufactured shear-key materials that were obtained from manufacturers' technical data sheets and published literature are included in Chapter 2. Mechanical properties of selected manufactured shear key grout materials and repair materials were evaluated for verification purposes and are summarized in this chapter.

6.2 TYPE R-2 GROUT

The mix ID and a brief description of the mixes are given in Table 6-1.

Table 6-1. Grout Mix ID and Description

Mix ID	Description
BB	Grout made of Type 1 Portland cement. Prepared by Consumer's Concrete and used in Oakland over I-94 bridge
BBA	Grout made of Type 1 Portland cement – Laboratory mix
BBM	Grout made of Type M masonry cement – Laboratory mix
BBN	Grout made of Type 1 Portland cement and Type N masonry cement – Laboratory mix
BBS	Grout made of Type 1 Portland cement and Type S hydrated lime – Laboratory mix

6.2.1 Plastic Properties of Type R-2 Grout

Table 6-2 includes slump and percent of air in the grout samples prepared in the laboratory. The mixes were prepared according to the proportions and guidelines given in the Table 702-1 of MDOT Standard Specification for Construction (2003b). Also, Standard Specification Section 708.3 requires approximately 5 in. slump for the grout.

Table 6-2. Slump and Air Content of Grout Mixes

Mix ID	Slump (in) (ASTM C 143)	Air (%) (ASTM C 231)
BBA	7.25	13.5
BBM	9.00	12.75
BBN	21.0*	10.0
BBS	7.75	13.75

*Diameter of the flow

6.2.2 Mechanical Properties of Type R-2 Grout

Ultrasonic pulse velocity (UPV) tests were performed evaluating the dynamic elasticity modulus and Poisson's ratio of the material. The UPV tests were performed in compliance with ASTM C597. In addition, compressive strength of grout was evaluated.

The dynamic modulus is generally greater than the static modulus determined in accordance with ASTM C469. However, for the type R-2 grout materials, the dynamic modulus was measured as lower than the static modulus determined following the procedure given in ASTM C469. The reasons for the disparity was investigated and discussed later in this chapter. Strength, Poisson's ratio, and dynamic modulus of grout materials are presented below:

Table 6-3. Mechanical Properties of R-2 Grout - Mix BB

Age (Days)	Strength (psi)	Poisson's Ratio	Dynamic Modulus (ASTM C597) (ksi)
3	3,730	-	-
7	3,651	0.31	2,985
14	4,385	-	-
28	4,859	0.31	3,163

Table 6-4. Mechanical Properties of R-2 Grout - Mix BBA

Age (Days)	Strength (psi)	Poisson's Ratio	Modulus (ksi)	
			Dynamic (ASTM C597)	Static (ASTM C469)
3	2,693	0.31	2,554	-
7	3,668	0.28	2,718	-
14	4,256	0.30	2,954	-
28	4,309	0.31	3,040	3251

Table 6-5. Mechanical Properties of R-2 Grout - Mix BBM

Age (Days)	Strength (psi)	Poisson's Ratio	Dynamic Modulus (ASTM C597) (ksi)
3	2,125	0.32	2,445
7	2,358	0.32	2,619
14	2,646	0.32	2,737
28	2,677	0.31	2,917

Table 6-6. Mechanical Properties of R-2 Grout - Mix BBN

Age (Days)	Strength (psi)	Poisson's Ratio	Dynamic Modulus (ASTM C597) (ksi)
3	1,916	0.31	2,349
7	2,693	0.32	2,593
14	3,377	0.33	2,734
28	3,680	0.32	2,888

Table 6-7. Mechanical Properties of R-2 Grout - Mix BBS

Age (Days)	Strength (psi)	Poisson's Ratio	Dynamic Modulus (ASTM C597) (ksi)
3	2,470	0.30	2,283
7	2,899	0.31	2,427
14	3,403	0.30	2,349
28	3,626	0.31	2,622

Figure 6-1, Figure 6-2, and Figure 6-3 give the early age changes in the mechanical properties. As seen in Figure 6-1, the compressive strength of grout material varies significantly depending on the cement type used in the mix. Mix BBM made from masonry cement (Type M) gives the lowest strength. The dynamic modulus and Poisson's ratio of the materials show a more limited difference across the mixes.

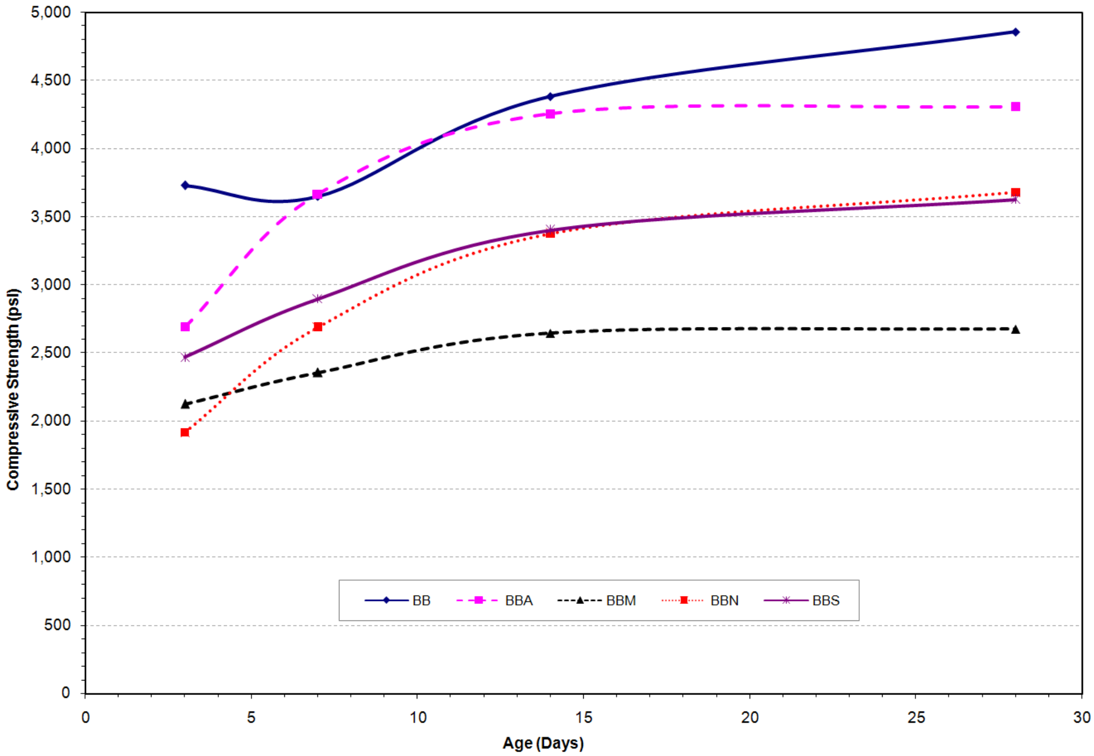

Figure 6-1. Compressive strength of grout material during early age

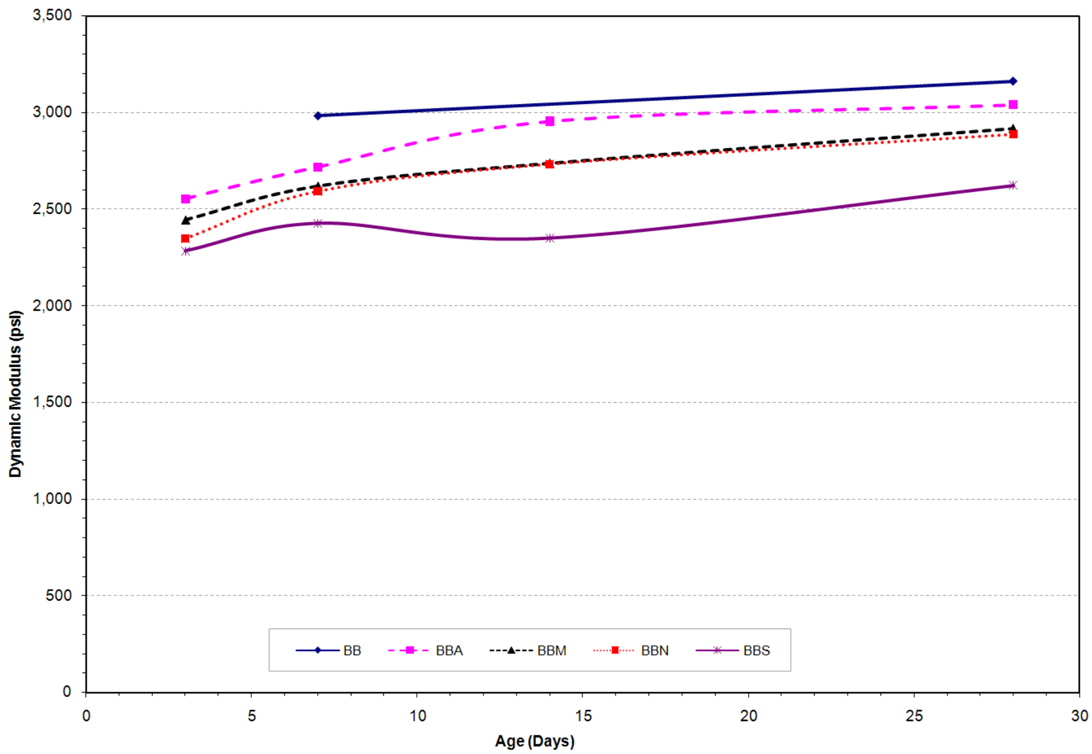

Figure 6-2. Dynamic modulus of grout material during early age

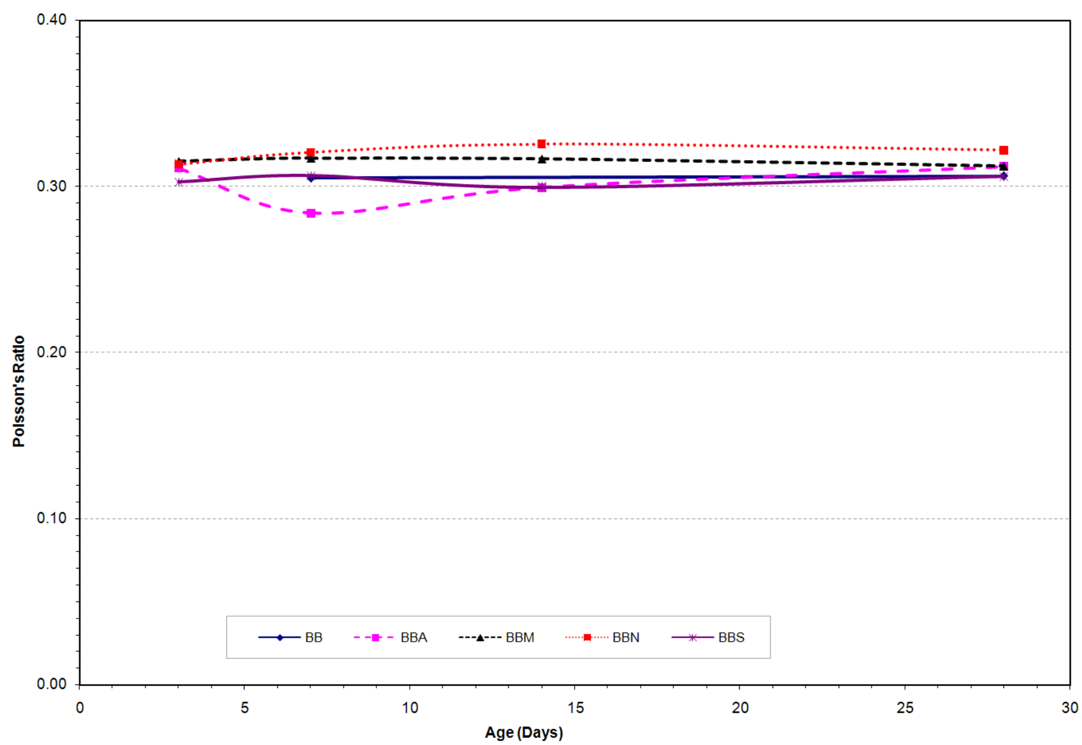

Figure 6-3. Poisson's ratio of grout material during early age

6.2.3 Type R-2 Grout Material Behavior under Axial Compression

The disagreement between the expected values of the static modulus and dynamic modulus of grout material is investigated by establishing the stress-strain relationship of a grout specimen. A cyclic axial compression test on a sample made from the mix BBS was conducted. The applied load reached about 40% of the 14-day compressive strength. The stress - strain plot of the specimen is shown in Figure 6-4. As seen in the figure, the grout specimen exhibits a pinched stress-strain curve with post yielding strain hardening behavior that is not typical of concrete. The second loading cycle falls over the initial loading curve indicating that there is no degradation due to internal cracking at a stress level that reaches only 40% of the compressive strength. Samples prepared using BBS mix contained 13.75% air. The shift in the unloading curve is an indication of energy dissipation due to internal friction. The elastic modulus dramatically changes in proportion to strain within the load cycle. The static modulus test (ASTM C469) is not able to capture this behavior and produces an average modulus value.

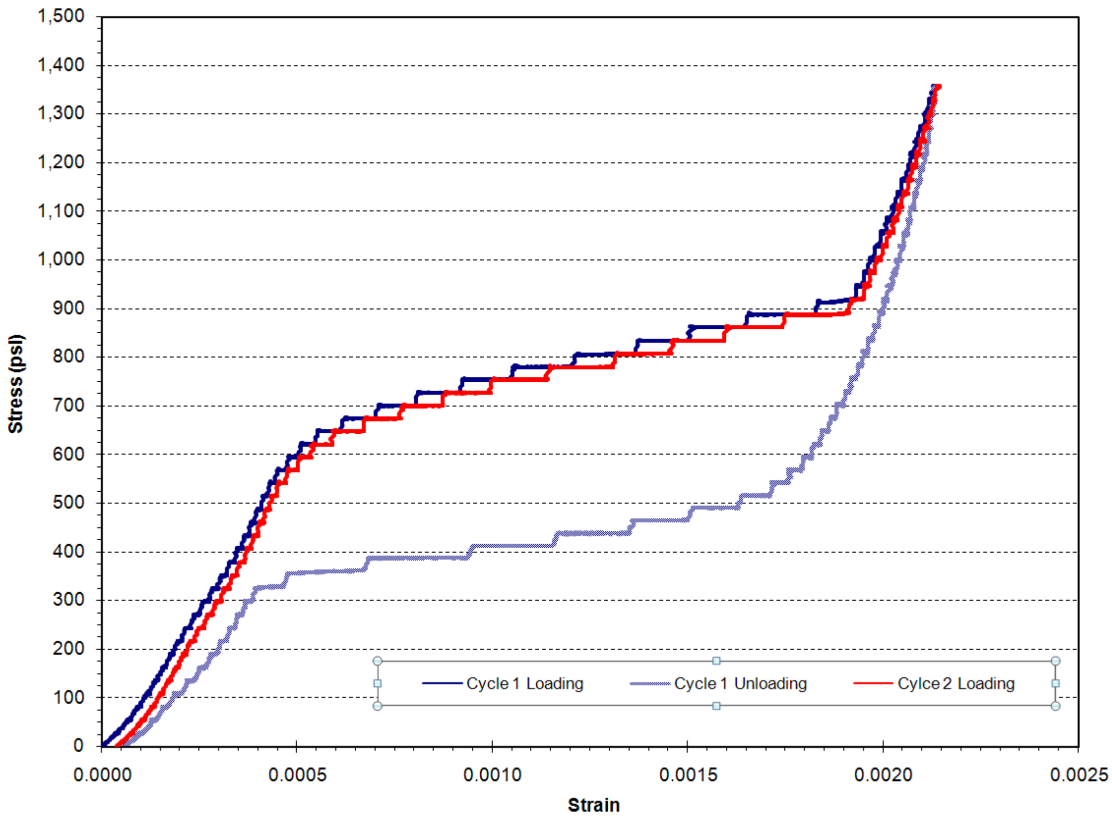

Figure 6-4. Stress-strain behavior of grout (mix BBS) under axial compression

AASHTO LRFD (2004) requires a posttension stress of 250 psi at the shear key. When the stress-strain behavior of the grout BBS is investigated under uniaxial compression, the effective modulus of the material at 250 psi stress level is about 1100 ksi (Figure 6-5). However, using a measured static modulus for this purpose (<3000 ksi), the grout strain would have been much smaller. The effective grout modulus at the time of posttension application is important as it governs the load distribution as well as providing a seal between the beams. Further investigation is required to formulate grout behavior under various load levels since the ASTM C469 procedure is not useful for capturing this elastic nonlinear behavior of the grout material.

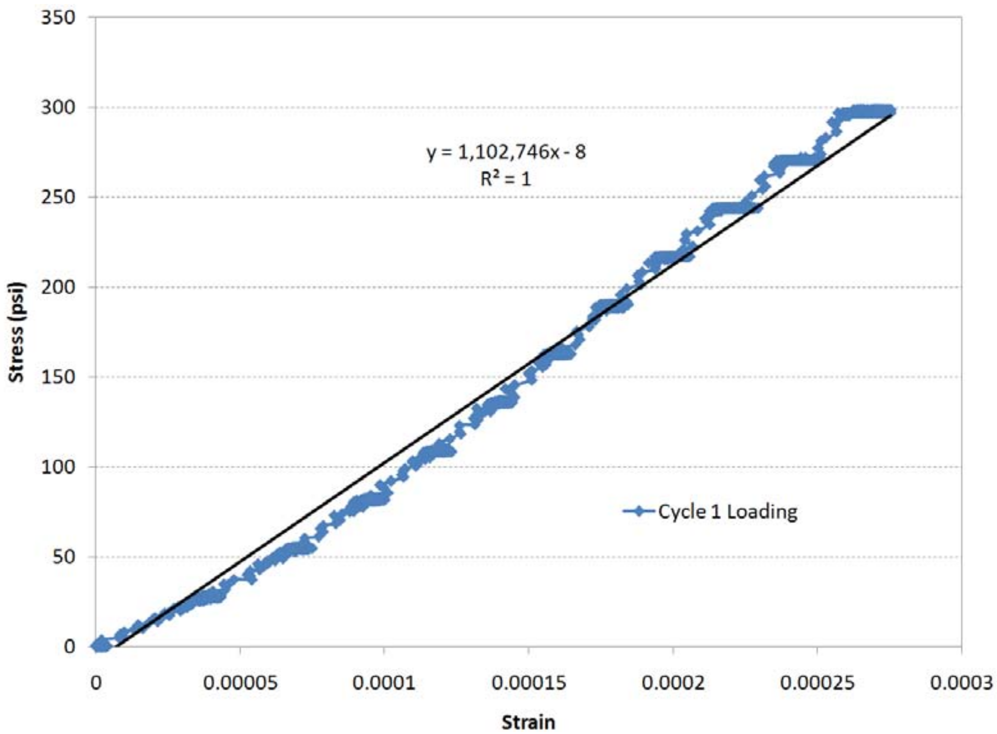

Figure 6-5. Stress-strain behavior of grout (mix BBS) under axial compression

6.3 SET 45 GROUT PROPERTIES

Set® 45 grout properties were tested in accordance with ASTM C109, ASTM C469, and ASTM C597. Strength was measured lower than that the manufacturer spec sheet. The static modulus calculated following ASTM C469 is similar to the dynamic modulus determined as per ASTM C597. As discussed in the previous section, the ASTM C469 procedure is not suitable of capturing the nonlinear elastic behavior of grout material.

Table 6-8. Mechanical Properties of Set® 45 Grout

Set® 45					
Age (days)	Strength (psi)	Poisson's Ratio		Modulus of Elasticity (ksi)	
		Dynamic	Static	Dynamic ASTM C597	Static ASTM C469
1	719	0.29	---	3,265	---
2	774	0.29	---	3,497	---
7	2,104	0.28	0.26	3,377	2,885
14	2,233	0.28	0.24	3,595	3,406
28	4,410	0.29	0.22	3,932	3,844

6.4 PROPERTIES OF REPAIR MATERIAL

Four repair material properties were tested in accordance with ASTM C109, ASTM C469, and ASTM C597. Strength values obtained are lower than those specified by the manufacturers. Similar to R2 grout, the nonlinear elastic behavior of the materials needs to be documented for proper evaluation of the repair application. This is because the repair performance will be a function of the stress or strain level at the location of the repair.

Table 6-9. Mechanical Properties of SikaRepair® SHA

SikaRepair® SHA					
Age (days)	Strength (psi)	Poisson's Ratio		Modulus of Elasticity (ksi)	
		Dynamic	Static	Dynamic ASTM C597	Static ASTM C469
1	1,041	0.31	---	2,623	---
2	1,367	0.31	---	2,738	---
7	3,719	0.31	N/A	2,858	3,032
14	4,132	0.29	0.24	3,126	3,209
28	4,552	0.31	0.22	3,072	3,400

Table 6-10. Mechanical Properties of Conpatch V/O

Conpatch V/O					
Age (days)	Strength (psi)	Poisson's Ratio		Modulus of Elasticity (ksi)	
		Dynamic	Static	Dynamic ASTM C597	Static ASTM C469
1	883	0.32	---	2,829	---
2	1,491	0.31	---	2,902	---
7	2,386	0.31	0.20	3,311	3,242
14	1,868	0.41	0.22	3,244	3,227
28	4,549	0.33	0.24	3,140	3,310

Table 6-11. Mechanical Properties of SikaTop® 123 PLUS

SikaTop® 123 PLUS					
Age (days)	Strength (psi)	Poisson's Ratio		Modulus of Elasticity (ksi)	
		Dynamic	Static	Dynamic ASTM C597	Static ASTM C469
1	3,075	0.31	---	2,357	---
2	3,579	0.31	---	2,480	---
7	4,338	0.30	0.24	2,653	2,281
14	4,484	0.30	0.23	2,706	2,431
28	4,425	0.30	0.24	2,760	2,571

Table 6-12. Mechanical Properties of HB2® Repair

HB2® Repair					
Age (days)	Strength (psi)	Poisson's Ratio		Modulus of Elasticity (ksi)	
		Dynamic	Static	Dynamic ASTM C597	Static ASTM C469
1	1,857	0.30	---	1,565	---
2	1,949	0.31	---	1,609	---
7	1,867	0.31	0.22	1,669	1,640
14	2,320	0.31	0.21	1,689	1,562
28	3,729	0.31	0.23	1,723	1,686

6.5 SUMMARY AND CONCLUSIONS

Mechanical properties of Type R-2 grout specified for Michigan bridges were tested and documented. Additional manufactured shear key grout materials and repair materials were also tested for mechanical properties. The AASHTO Standard (2002) Section 5.14.4.3.2 requires 5000 psi grout compressive strength in 24 hours, while the LRFD (2004) Section 5.14.1.2.8 requires 4000 psi. Grout specimens tested during the project could not satisfy the strength required by the AASHTO Standard or LRFD at the time of posttension. AASHTO LRFD (2004) requires that posttension generates a stress level 250 psi at the shear key. According to Michigan practice, posttension is applied 48 hours after grouting the shear keys (MDOT 2003b). All the grout mixes tested showed sufficient strength such that 250 psi compressive stress can be applied with a factor of safety of at least three.

The static modulus of R-2 grout as well as the commercial grout specimens were measured to be greater than the measured dynamic modulus. This is contrary to the expected properties of cementitious materials. Further experimental testing showed that grout exhibits nonlinear hysteretic elastic stress-strain relationship. Hardened grout properties given in Chapter 5 are also studied to identify the reasons for the nonlinear hysteretic behavior. Further study is recommended to characterize the grout materials since the elasticity modulus of grout at the time of posttension applications controls the stress distribution and the interface performance between the adjacent beams without separation or cracking in order to develop a watertight fit. The AASHTO LFRD (2004) grout strength requirements should also be investigated.